

Ethanol Chemical Vapor Deposition Process Design for Selective
Growth of Vertically-Aligned Single-Walled Carbon Nanotubes

A Dissertation Presented

by

Hatem Mansour Abuhimd

to

The Department of Mechanical and Industrial Engineering

in partial fulfillment of the requirements

for the degree of

Doctor of Philosophy

in the field of

Industrial Engineering

Northeastern University

Boston, Massachusetts

December 2011

Abstract

Science and engineering communities have given the synthesis of vertically aligned single walled carbon nanotubes (VA-SWNTs) considerable attention due to their attractive physical properties, unique morphology, and better potential for building advanced devices than those with asymmetric and entwined carbon nanotubes (CNTs). Chemical vapor deposition (CVD) is one of several viable methods for growing VA-SWNTs, which is well known for its economic viability and good yield of VA-SWNTs. Utilizing Co catalyst (0.5 ~ 1 nm thick) supported on an Al/SiO₂ multilayer substrate and a hydrocarbon feedstock, VA-SWNTs are grown in excess of a millimeter height.

To control the CVD process to selectively produce tall VA-SWNTs, one has to use the right combination of process inputs such as gas flow rate, chamber temperature, and chamber pressure. This dissertation investigates their main effects and interactions on VA-SWNT yield and length by conducting design of experiments and analysis on the metamodel of the CVD process. The artificial

neural network (ANN) based metamodel was constructed using the experimental data.

The interactions among control variables and response surface plots show that pressure and temperature are the most significant CVD process control variables to selectively produce VA-SWNTs. In addition, the analysis confirms that higher temperature and higher pressure will result in a better yield of VA-SWNTs. In contrast, the analysis points out that the flow rate and the pressure are the most statistically significant factors that influence the length of VA-SWNTs. The response surface graphs indicate that higher flow with lower pressure will consistently yield tall VA-SWNTs. We found that gas flow rate is the most significant of the control variables and only the optimum value of the gas flow rate can ensure the growth of tall VA-SWNTs. We also found that the interaction of gas flow rate with chamber temperature and pressure is extremely important to ensure the quality of VA-SWNTs. This observation indicates that dynamic pressure of the fluid in the chamber affects the quality of VA-SWNTs grown on the substrate. We have also found out that flow rate less than 150 sccm and a growth time of 20 minutes are suitable for the repeatability

of medium length VA-SWNTs. Outcomes of this investigation are beneficial for moving the CVD process closer to producing VA-SWNTs on large mass-produced scale.

Table of Contents

Abstract	ii
List of Figures	viii
List of Tables.....	xiii
1. Introduction	1
2. Literature Review	7
2.1 Vertically Aligned Single Walled Carbon Nanotubes	7
2.1.1 Experimental Methods	10
2.1.2 Growth Mechanism.....	16
2.1.3 Applications	20
2.2 Computational Methods.....	22
2.2.1 Multi-Layer Perceptron.....	23
2.2.2 Design of Experiments.....	24
2.3 Design of Experiments for CVD Grown Carbon Nanotubes.....	26
2.3.1 Experiments and Discussion	34
3. Experimental Setup	40

3.1 System Variables	42
3.2 Catalyst Preparation	45
3.3 CVD Process Setup.....	45
4. Process Design for Controllability	47
4.1 Metamodel and Design of Experiments.....	48
4.2 Comparison of Main Effects Plots	52
4.3 Pareto and General Response Surface Plots	54
5. Process Design for Length Assurance.....	56
5.1 Metamodel and Design of Experiments.....	57
5.2 Pareto Chart Analysis	65
5.3 Marginal Mean Plots.....	66
5.4 Comparison of Main Effects Plots.....	67
5.5 General Response Surface Plot.....	69
6. Process Design for CVD Flow	73
6.1 Pareto Chart Analysis	77
6.2 Comparison of Main Effects Plots.....	78

6.3 General Response Surface Plot.....	79
7. Scientific Formulation of the Process Input Variables.....	80
7.1 Ideal Gas Law	83
7.2 Dynamic Pressure	85
8. Conclusion and Future Work.....	88
References.....	90
Appendix A	99
Appendix B.....	102
Appendix C	139
Appendix D	155
Appendix E.....	159

List of Figures

Figure 1.1 CVD of VA-SWNTs input output diagram (Co: Cobalt, C: Carbon).....	2
Figure 1.2 Schematic of the modeling process framework	4
Figure 2.1 Homogenous MWNT samples in a network characterized by TEM done by Iijima in 1991 [6]	8
Figure 2.2 Schematic of the types of pure Carbon forms like Carbon Nanotubes, Graphite and Diamond [7].....	9
Figure 2.3 Schematic of the arc-discharge apparatus employed for CNT production [12]	11
Figure 2.4 Laser ablation schematic for growing CNTs [12]	12
Figure 2.5 Schematics of ethanol CVD systems and experimental procedures for the growth of VA-SWNTs.....	13
Figure 2.6 (a) An image of the 2.5-mm-height VA-SWNTS (b) & (c) SEM images of VA-SWNTs [6]	16

Figure 2.7 CVD grown VA-SWNTS base or tip growth mechanism schematic with catalyst as Cobalt.....	19
Figure 2.8 Scanning electron microscope image of a VA-CNTs membrane (scale bar = 10 μm) [18].....	20
Figure 2.9 Histogram of observed permeability in VA-CNTs [18].....	21
Figure 2.10 5 mm long TiO_2/CNT arrays [20]	22
Figure 2.11 Architecture of a Multilayer Perceptron	24
Figure 2.12 Most researchers utilize Full Factorial designs for their publications instead of other techniques like Fractional Factorial and Taguchi.....	32
Figure 2.13 Histogram of years 2004-2009 of papers related to Orthogonal Arrays	33
Figure 2.14 Schematic diagram of the CCVD setup for carbon nanotube synthesis	35
Figure 2.15 Schematic diagram of VCVD [50]	36

Figure 3.1 Schematics of ethanol CVD systems and experimental procedures for the growth of VASWMTs	41
Figure 3.2 Cause and effect matrix of input variables	44
Figure 3.3 Schematic of the cross section of the substrate.....	45
Figure 4.1 Classifications accuracy of process outcome.....	51
Figure 4.2 Interaction Plots between Temperature and Pressure for VA-SWNTS53	
Figure 4.3 Process Analysis Pareto Plot.....	55
Figure 4.4 Response Surface Plots of VA-SWNTs Length (Temperature VS Pressure)	55
Figure 5.1 Architecture of a multi-layer perceptron network	59
Figure 5.2 VA-SWNTs length (target) versus estimated VA-SWNTs length (output) regressions graph for the MLP 4-21-1 network	60
Figure 5.3 Histograms showing the distribution of control variables in the training data for neural networks.....	64

Figure 5.4 Process Pareto Analysis, (A) CVD Temperature (°C), (B) CVD Pressure (sccm), (C) Gas Flow Rate (Torr)	65
Figure 5.5 Marginal mean plots, (A) CVD Temperature (°C), (B) CVD Pressure (sccm), (C) Gas Flow Rate (Torr).....	66
Figure 5.6 Main effect plots for VA-SWNTs length of pressure and flow.....	68
Figure 5.7 Response surface plot of VA-SWNTs length VS flow rate VS pressure	70
Figure 5.8 Main effect plots for VA-SWNTs length of temperature and flow	71
Figure 5.9 Response surface plot of VA-SWNTs length VS flow rate VS temperature.....	72
Figure 6.1 VA-SWNTs length (target) versus estimated VA-SWNTs length (output) regressions graph for the MLP 2-12-1 network	74
Figure 6.2 Process Pareto analysis	77
Figure 6.3 Main effect plots for VA-SWNTs length of time and flow	78
Figure 6.4 Response surface plot of VA-SWNTs length VS flow rate VS time	79

Figure 7.1 First and second runs graphs to measure the stability of pressure sensor during VA-SWNTs growth time (average = 705.2 torr, 703.5 torr) 81

Figure 7.2 Matrix plots between flow, temperature and pressure for VA-SWNTS (101 = VA-SWNTs, 102 = MWNTs, 103 = MWNTs & SWNTs, 104 = None) 84

Figure 7.3 Interaction plots between temperature and pressure for VA-SWNTs 86

List of Tables

Table 2.1 Historical timeline of CNT growth methods [19].....	14
Table 2.2 Researchers used many substrate materials to produce the tubes [19].	17
Table 2.3 The feasible factorial design either for full or fractional factorial designs, which can be utilized to optimize processes	25
Table 2.4 Taguchi Designs orthogonal arrays.....	26
Table 2.5 Journals including nanotechnology papers utilizing DOE	27
Table 2.6 Publications using variable conventional processes and designs for the optimization of carbon nanotubes characteristic [23-26,31,32,34,38,45-49]	28
Table 2.7 Nano-manufacturing improvements techniques	31
Table 2.8 Summary of articles in the use of Orthogonal Arrays to optimize the processes and designs related to carbon nanotubes [30,39,41,44,51]	33

Table 2.9 CCVD and VCVD process for growing CNTs synthesis conditions, MRL: mean rectilinear length, C%: Carbon Deposit, QDN: quality descriptor number.....	37
Table 4.1 CVD three level-three variables full factorial design of experiment	52
Table 5.1 Experimental records of the CVD process input and output variables	64
Table 6.1 Experimental records of the CVD process input and output variables	77
Table 7.1 Process inputs combinations based on the desired output.....	87

Acknowledgment

I would like to extend a deep gratitude to my advisors, Prof. Kamarthi and Prof. Zeid, as they have been the driving force behind my academic and research success. In addition to their expertise in my research field, I appreciate their constant encouragement and guidance, which was critical to my dissertation. I would also like to thank the other member of my committee, Prof. Jung, for taking the time to understand my work and providing the feedback. In addition, I would like to acknowledge Prof. Jung's research group in general and specifically Dr. Hahm, and Mr. Sanghyun for performing the experiments. I want to show appreciation to everyone in Network/Nano Science and Engineering Laboratory and Mechanical and Industrial Engineering Department and for all their support. I would like to thank my parents and siblings for instilling in me the seeds of interest and determination that led me to this career choice, and my lovely wife and two wonderful daughters for being extremely patient and making the process worthwhile. Finally, I would like to take this opportunity, to personally, thank everyone who has assisted, in any way, me in getting my PhD degree.

Dedication

I dedicate this work to my parents, family, and friends.

1. Introduction

Materials at the nanoscale exhibit unparalleled physical and chemical characteristics in contrast to the macro scale because of the Quantum phenomena [1]. In addition, mass-producing those materials (nanomanufacturing) does not receive as much funding as dedicated to their science [2]. Chemical vapor deposition (CVD) is a common nanomanufacturing process for growing vertically aligned single walled carbon nanotubes (VA-SWNTs). It is expected to enable the scale-up of CNT production. However, the fact that CVD yields only a small fraction of VA-SWNTs makes it hard to scale up production [3]. To move nanoscience from labs to mass production, a multidisciplinary scientific approach is needed.

Our proposed approach aims to analyze experimental data from a CVD process, build neural network models, and perform an experimental design analysis with the goal of relating the CVD input parameters to the characteristics of the VA-SWNTs to gain better understanding of their properties. There are many variables influencing the CVD process; some of those variables include catalyst type, particle size, surface roughness, reactant

composition, etchant composition, reactant pretreatment, and gas flow rate.

Our objective is to evaluate all input variables statistically to find the significant ones. Figure 1.1 shows the input output diagram for VA-SWNTs growth using CVD process.

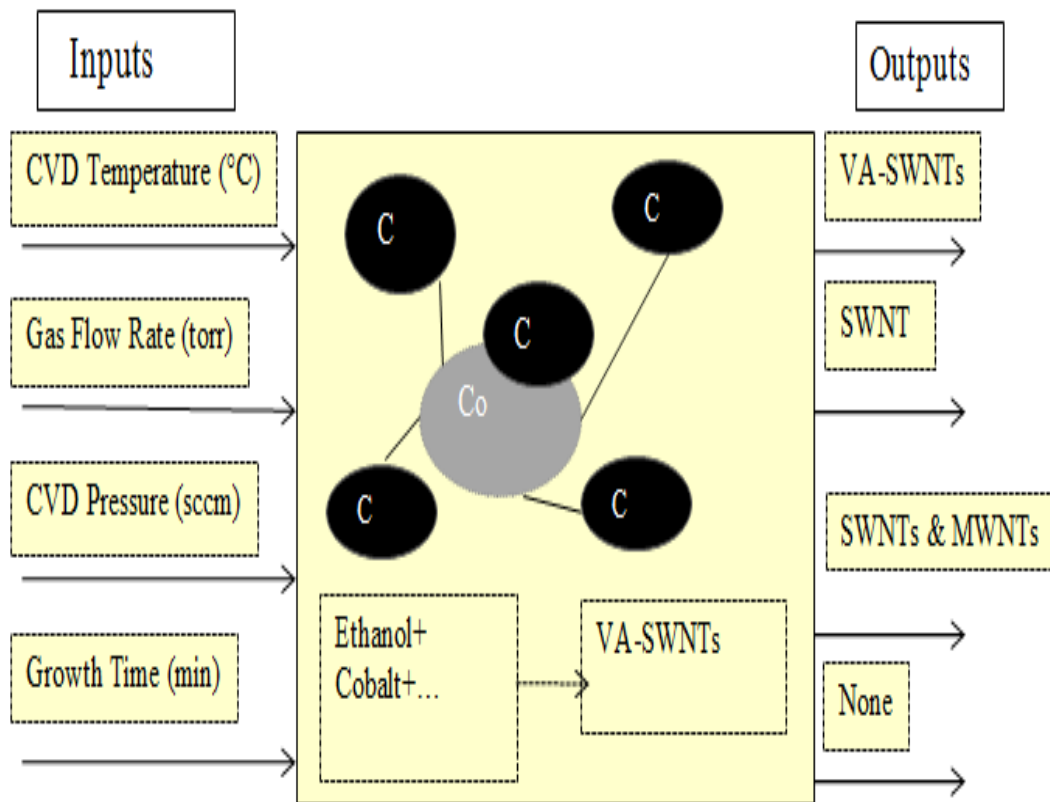


Figure 1.1 CVD of VA-SWNTs input output diagram (Co: Cobalt, C: Carbon)

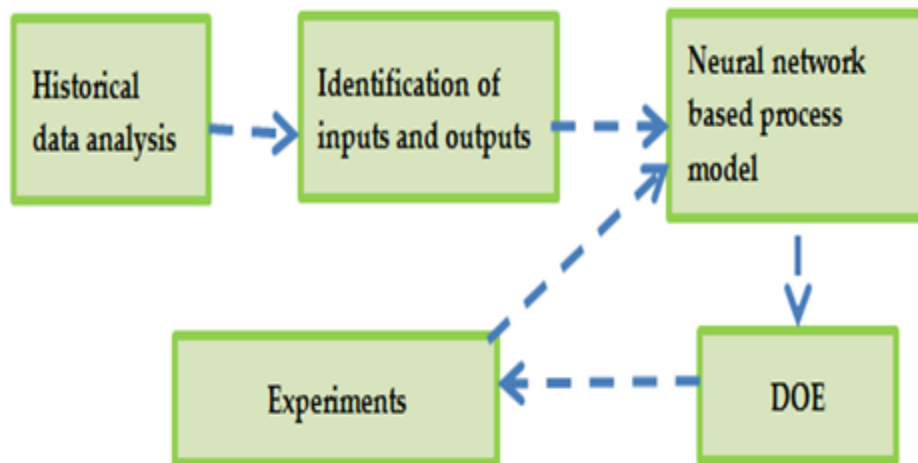
The figure shows the controllable variables (process inputs), and the key performance indicators (process outputs). Superior morphology and fascinating

physical features of VA-SWNTs can result in interesting applications.

Therefore, we need to address the control of their growth and length. Growing VA-SWNTs on a substrate surface is an important step toward manufacturing nanoscale devices [4]. Here are the main objectives of this dissertation

1. Build a deep understanding of CVD based VA-SWNTs growth processes
2. Screen available optimization methods to identify suitable designs
3. Employ the most suitable design
4. Analyze the design results and make recommendations

To achieve the above objectives we plan to analyze a data set from a CVD machine and perform statistical analysis. In order to relate the CVD input parameters to the characteristics of the VA-SWNTs, we correlate the input to the output to allow the optimization and control the CVD process to gain better VA-SWNTs properties. Figure 1.2 shows the framework flow of the modeling process.



A validated physical model and a controlled process with known capability and repeatability

Figure 1.2 Schematic of the modeling process framework

The data analysis for this dissertation is driven by a null hypothesis based on current publications literature review. The review is related to the CVD grown VA-SWNTs synthesis process and growth mechanism. For that purpose, the CVD is presumed to be controllable by researchers to improve the yield. The expectation is that an understanding of the process controllable variables will be developed with performing the examination and analyzing the data. That will result in better designs to control the whole growth process. This dissertation research was created based upon certain assumptions. Input

variables are independent and will yield statistical significant results. Without such assumption the experimental design results will be hindered and obsolete. All the efforts are forced to obtain the best quantitative and qualitative data for the analytical model. Similar assumptions will be applied to the data analysis.

This dissertation will add to the understanding of the VA-SWNTs fabrication Process, however, certain limitations to the study exist. The data were collected using traditional sampling methods, which only assess data perceptions of the independent and dependent variables at one point in time.

The analysis of the CVD grown CNTs process was reported in the literature before but not for the current process under study. Hence, all variables have to be considered without the benefit of previous recommendations from old experiments. The dissertation will examine a metamodel of the CVD VA-SWNTs synthesis process. The Purpose of the Study is to improve the current understanding of the VA-SWNTs yield controllability and length. The study significance lies in the results of such purposes achieved in using such VA-SWNTs in nanomanufacturing.

The dissertation content is organized as follows. Chapter 2 will go over the properties and growth mechanism of VA-SWNTs. In addition, it will also

describe their importance toward the advancement of nanotechnology.

Moreover, a brief introduction to experimental designs is described including design of experiment for (Full/Fractional Factorial Designs, Taguchi), Artificial Neural Networks, and some instances where CNT growth was enhanced by an experimental design. The method for VA-SWNTS growth and catalyst preparation with small illustration of the characterization method are discussed in Chapter 3. Chapter 4 discusses the VA-SWNTs controllability by a metamodel of an ANN phase and an Experimental Design phase. Chapter 5 will start by an analysis of the VA-SWNTs length assurance experiments results followed by a general analysis using a similar to chapter 4 metamodel. CVD gas flow rate relation with the growth time will be analyzed in chapter 6. In chapter 7, we will detail some scientific formulation of the previous metamodels. Finally, Chapter 8 will present the conclusion and touch on the future research directions.

2. Literature Review

This chapter will give a background on VA-SWNTs and Computational methods related to this dissertation. The VA-SWNTs section is related to their remarkable properties and how they were discovered. Then, an illustration of how they are grown with CVD, growth mechanism and possible future applications. Here, Computational methods are discussed and related to the research proposed metamodel. Specifically Artificial neural networks and design of experiments will be introduced.

2.1 Vertically Aligned Single Walled Carbon Nanotubes

Iijima et al. used arc discharge method to discover CNTs in 1991 (see Figure 2.1) and it fueled the research about those tubes [5]. Superior morphology and fascinating physical features of vertically aligned single walled carbon nanotubes (VA-SWNTs) can result in interesting applications. Therefore, we need to address the control of their structural growth and organization. Growing VA-SWNTs on a substrate surface is an important step toward manufacturing nanoscale devices like field emission displays [4].

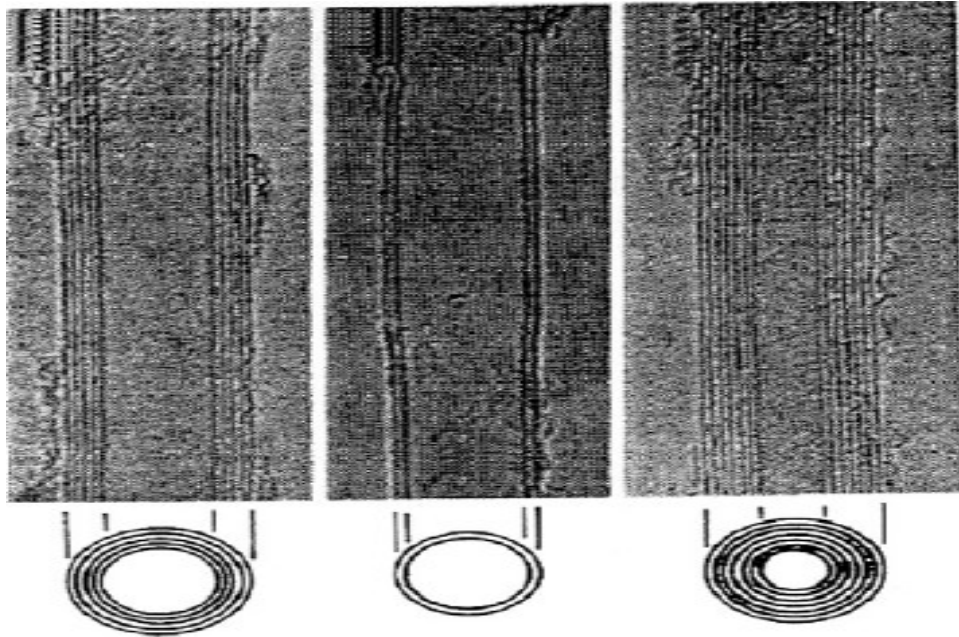


**Figure 2.1 Homogenous MWNT samples in a network characterized by TEM
done by Iijima in 1991 [6]**

In general, they bears higher physical quality than other nanoscale carbon materials [4]. Furthermore, their astonishing purity of 99.98% in a sample present them as being the purest and highest quality of carbon nanotubes [6]. Their ratio of SWNT to catalyst weight exceeds 50,000% to the other processes [6]. We can define Multi Walled Carbon Nanotubes (MWNTs) as multiple rolled concentric tubes of graphite while Single Walled Carbon Nanotubes (SWNTs) has only one tube [1]. Carbon comes in different molecular structure like diamond and graphite (Figure 2.2).

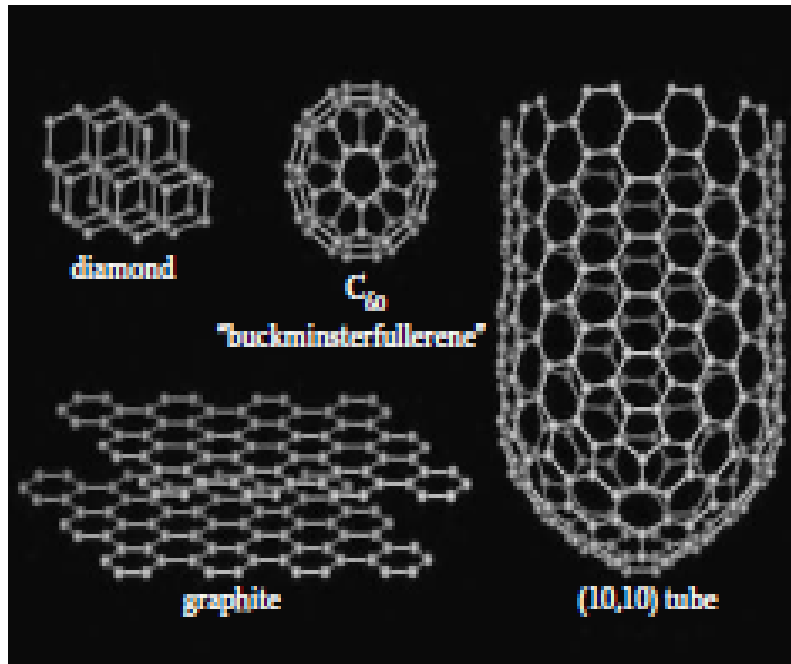


Figure 2.2 Schematic of the types of pure Carbon forms like Carbon Nanotubes, Graphite and Diamond [7]

CNT science is a well-researched topic in literature especially for Multi Walled Carbon Nanotubes (MWNTs)[7]. However, manufacturing those tubes at a large scale is still an emerging research area [8]. Hence, several researchers are investigating the large-scale production of CNTs [9]. Our research considers the nanomanufacturing of VA-SWNTs at a mass production scale. Current methods for producing VA-SWNTs by CVD have high quality and yield in comparison to other methods like arc discharge and laser ablation.

The task to review VA-SWNTs in literature is made challenging by several issues. Mainly, there is huge variability of carbon nanotubes. In addition, there is large amount of published literature researching their physical properties as pure or compound materials. That literature is produced over a long period and is generated under very different environments. Therefore, most probably it discusses very different experimental conditions. Those reasons have driven us to focus our analysis on more recent work, assuming that older studies are made obsolete by the new ones.

2.1.1 Experimental Methods

There are three major ways to grow CNTs (SWNT, MWNTs, VA-SWNTs): electric arc discharge, laser ablation, and chemical vapor deposition (CVD). Arc discharge was the method used to discover CNT in 1991 by Iijima [5]. Here is a brief discussion about those main techniques and their characteristics.

Electric Arc Discharge

In 1991 Iijima discovered MWNT by the Electric Arc Discharge process [10]. Figure 2.3 shows a drawing of the arc discharge machine [11]. The anode and cathode are made of graphite. It works by flowing electricity between the anode

and cathode where a plasma will occur resulting in a CNTs accumulated on the cathode. Other variables in the process include high temperatures (3000-4000 K) and the presence of inert gas in the chamber [11].

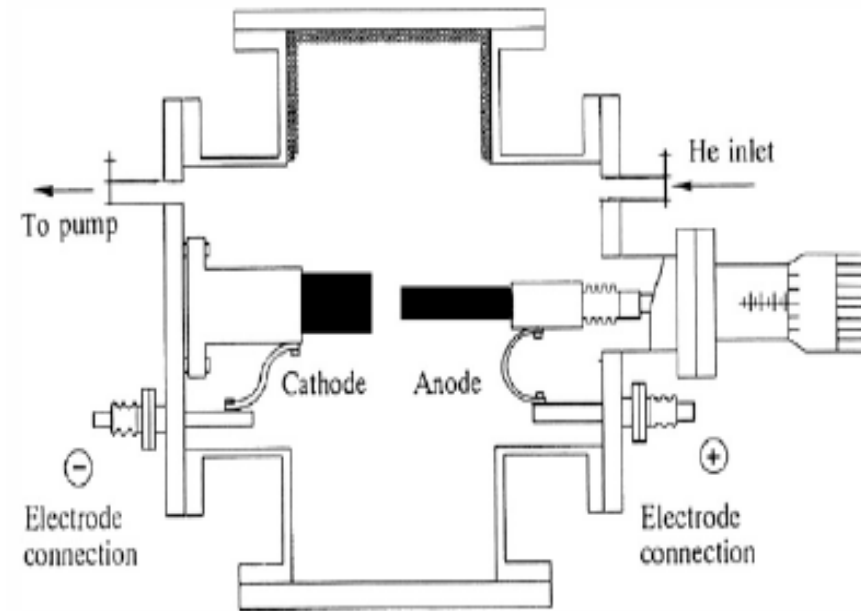


Figure 2.3 Schematic of the arc-discharge apparatus employed for CNT production [12]

The structure and yield of CNTs synthesized by this reactor are comparable to the CVD processes. Therefore, current researchers resolve to the CVD especially that it is less expensive and can be operated at lower temperatures.

Laser Ablation Method

An alternative to using electric arc discharge is laser ablation. As shown in Figure 2.4 it utilizes high-energy lasers in high temperature furnaces [11]. The laser will be used to vaporize metallicity catalyzed graphite in the presence of high temperatures. Similar to the previous process this process is less usable than the CVD especially that lasers are very costly.

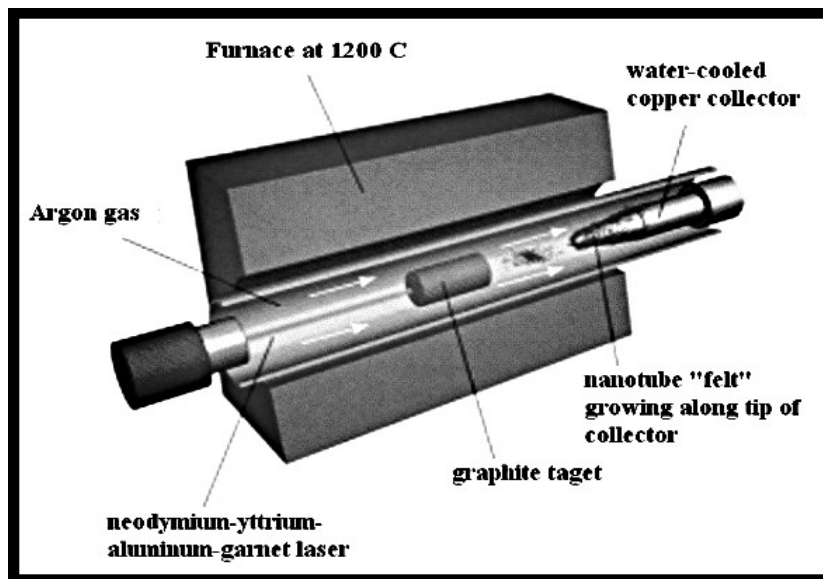


Figure 2.4 Laser ablation schematic for growing CNTs [12]

Chemical Vapor Deposition

In the CVD furnace, a carbonaceous gas is flown over a metallic catalyst. The carbon under pressure will react with the catalyst and start growing to form the

CNT (Figure 2.5) [7]. In contrast, to the previous methods the CVD factors involved are of moderate ranges. Consequently, the viability of the process for high yield is promising especially if more research is done in the area. Current methods for producing CNT by CVD have high quality and yield in comparison to other methods.

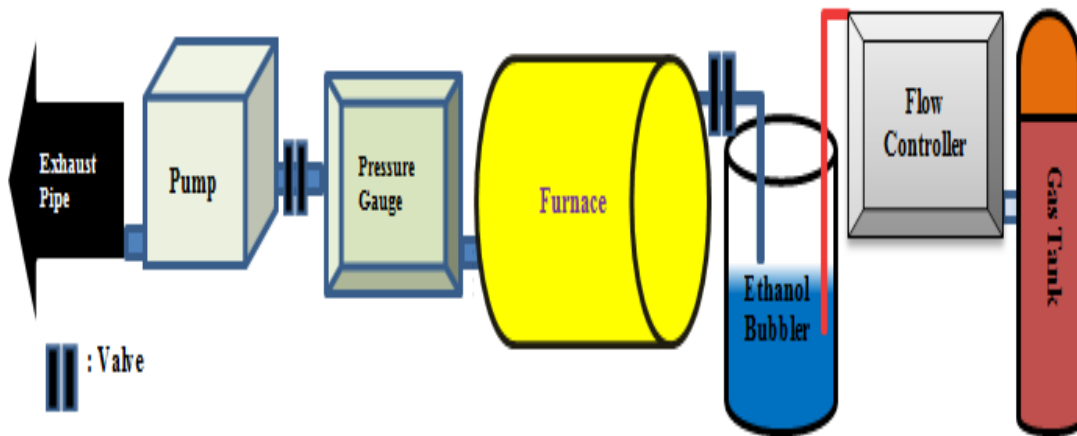


Figure 2.5 Schematics of ethanol CVD systems and experimental procedures for the growth of VA-SWNTs

Historically, the research and discoveries in CNTs were happening in rapid pace (Table 2.1) [12]. CNTs researchers come from different fields with different scientific background [5]. Such criteria enabled the development of different techniques and different materials to be utilized.

Table 2.1 Historical timeline of CNT growth methods [19]

Discovery	Year	Method	Carbon Nanotubes
1	1991	Arc discharge	Multi walled
2	1993	Pre-deposited CVD	Multi walled
3	1993	Arc discharge	Single walled
4	1995	Laser ablation	Multi walled
5	1995	Laser ablation	single walled
6	1996	Pre-deposited CVD	Single walled
7	2000	Flame	Multi walled
8	2002	Flame	Single walled

The current VA-SWNTs fabrication methods like electric arc discharge and laser ablation are not suitable for high-quality, high-purity and inexpensive VA-SWNTs mass production [4]. Therefore, mass production issues such as continuous CVD production and increasing the substrate region while decreasing it is cost need to be studied [4]. Moreover, the overall cost must be cut down to the level of common industrial materials like activated carbon [4].

In contrast to other methods, CVD based growth processes produce higher quality VA-SWNTs with higher process yield [5]. In addition, CVD processes

require process variables such as temperature and pressure in moderate ranges, reflecting its potential as cost effective manufacturing technique[13].

In 1996, multi-walled Carbon nanotubes were first aligned utilizing a CVD process [14]. However, researchers could not grow VA-SWNTs until Murakami et al. demonstrated their growth in 2004 [15] which were short $\sim 1.5 \mu\text{m}$ and not suitable for manufacturing devices. Later, Hata et al. used the assistance of water to grow VA-SWNTs to $2500 \mu\text{m}$ [6]. The addition of water prolonged the catalyst lifetime resulting in taller tubes [6].

The majority of SWNTs grown by CVD use a flow of a gaseous carbon feedstock over catalyst nanoparticles at medium to high temperature, which reacts with the catalyst nanoparticles [7]. During CVD growth, VA-SWNTs self-assemble into vertical structures on the patterned substrate at the catalyst locations [4,16]. They self-orient and grow perpendicular to the substrate because of the of van der Waals forces rigidity [7].

Researchers have already mastered the alignment of multiwall carbon nanotubes while VA-SWNTs alignment understanding is still a challenging task [17]. Multiple researchers have studied their growth conditions and found that uncontaminated CVD chamber, gas flow rate and water addition are important

control factors and that the vertical or parallel alignment of SWNTs depends largely on the density of catalyst particles and their distribution in the substrate [17].

2.1.2 Growth Mechanism

Forming CNT on a substrate surface is an important step toward manufacturing nanoscale devices. For instance, the vertical forming of CNTs is particularly essential for field emission displays. The rigidity of MWNT made them easier for alignment than the flexible SWNT. That VA-SWNTS has higher quality than other materials.

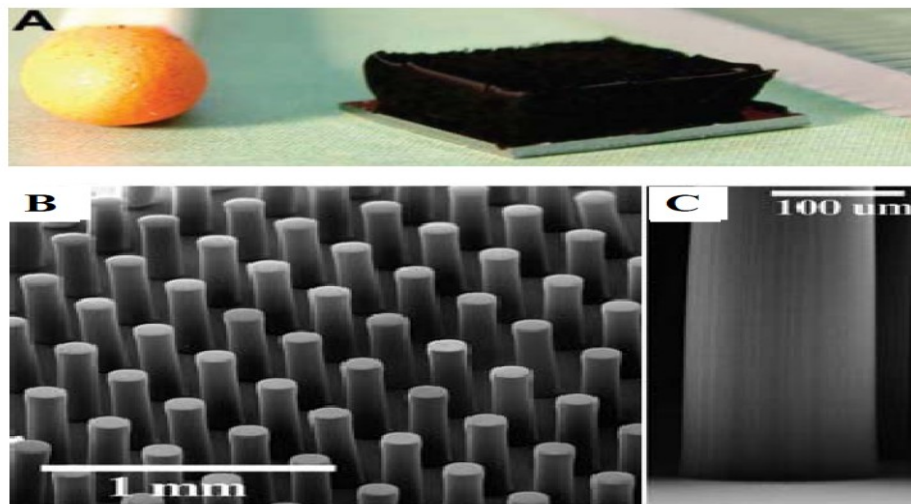


Figure 2.6 (a) An image of the 2.5-mm-height VA-SWNTS (b) & (c) SEM images of VA-SWNTs [6]

Another method of achieving VA-SWNTs is with metallic templates. As shown on Table 2.2 researchers used a lot of different substrate materials to produce the tubes [12]. Recently, more focus is been on Silicon material substrates. By using Silicon, templates with a lot of different nanoscale carbon are produced. For example, hierarchically branched nanoscale porous can be produced with a patterned catalyst.

Table 2.2 Researchers used many substrate materials to produce the tubes [19]

Year	Substrate	Catalyst	Source	CVD	CNTs
1996	Silica	Fe	Acetylene	Pre-deposited metal catalyst	MWNTs
1997	Silica	Co	Triazine	Pre-deposited metal catalyst	MWNTs, Pattern
1998	Quartz	Quartz	Quartz	Plasma-enhanced	MWNTs
1999	Porous Si	Fe	Ethylene	Pre-deposited metal catalyst	MWNTs, Pattern
1999	Si	Pd	Methane	Plasma-enhanced	MWNTs
2000	Si	Co	Acetylene	Pre-deposited metal catalyst	MWNTs
2004	Quartz	Co/Mo	Ethanol	Pre-deposited metal catalyst	SWNTs
2004	Si, Quartz,	Fe, Al/Fe,	Ethylene	Pre-deposited metal	SWNT,

	Metal Foil	Al ₂ O ₃ /Fe Al ₂ O ₃ /Co		catalyst	Pattern
2005	Si	Al ₂ O ₃ /Fe/ Al ₂ O ₃	Methane	Plasma-enhanced	SWNTs

There are four main assumptions about SWNTs growth mechanism [7]. First, a carbon feedstock and active transition metal nanoparticles are necessary for their growth unless high temperature is used to heat graphitic carbon nanoparticles. Second, their diameter is set from the onset of the nanotubes growth and only a small change will happen if there is a defect. Third, both the catalyst nanoparticle and the SWNT have the same size (diameter). Fourth, one catalyst nanoparticle will result in only one nanotube unless the diameters are different.

There are two types of CNTs diffusion on the substrate, surface or bulk carbon diffusion [7]. Surface diffusion is related to substrate growth where catalyst nanoparticles are deposited on a substrate such as SiO₂ [7]. The carbon cracks and nucleates around the solid catalyst and start growing SWNT [7]. Bulk diffusion can be called a gas phase growth because the formation of catalyst and nanotube occur in the air [7]. Here the metal nanoparticle dissolve the cracked carbon until saturation and the growth starts [7]. The growth continues

on both types until the carbon source is stopped or the particle is fully coated with amorphous or graphitic carbon [7].

VA-SWNTs grows either from the catalyst base or from tip and its growth type depends on the position and size of the catalyst particles (See Figure 2.7) [7].

Thus, the particles detach from the surface of the support material and move at the tip of growing CNTs for tip-growth. The base growth happens when nanoscale particles remain attached to the supporting material and CNTs grow upwards from those metal particles. Figure 2.7 shows both CNTs growth mechanism.

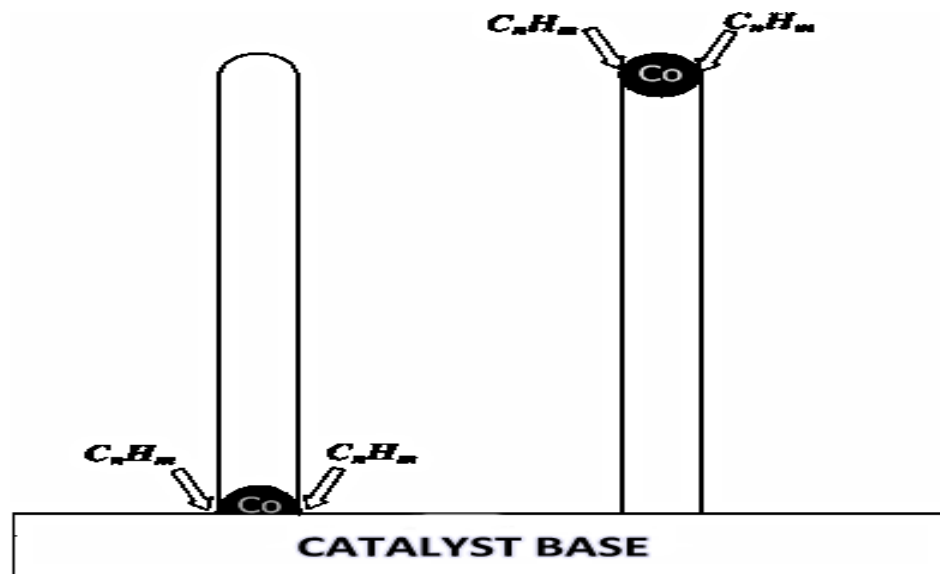
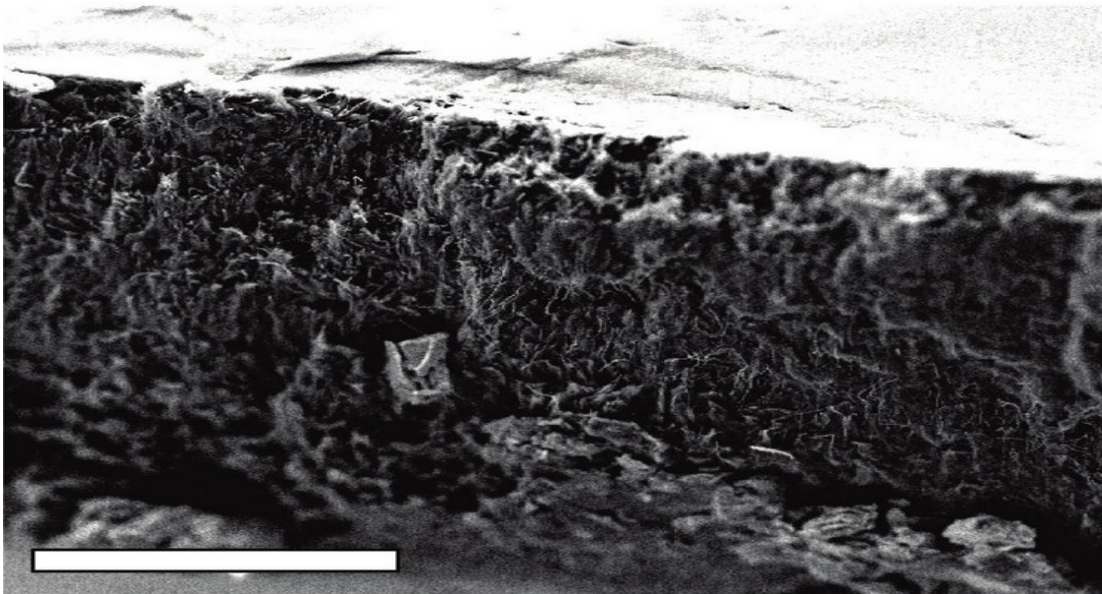


Figure 2.7 CVD grown VA-SWNTS base or tip growth mechanism schematic with catalyst as Cobalt

2.1.3 Applications

Remarkable applications may result from VA-SWNTs superior morphology and fascinating physical features. Transport processes for gas and liquid through CNTs are subjects of deep theoretical and experimental research. One study uses VACNTs to make gas and liquid membranes [18]. Figure 2.8 shows a Scanning electron microscope image of that membrane.



**Figure 2.8 Scanning electron microscope image of a VA-CNTs membrane
(scale bar = 10 μm) [18]**

The VA-CNTs hydrophobic graphitic walls, and nanoscale internal diameters give rise to an exceptional physical process of ultra-efficient water and gas

transport [19]. Water and gas molecules move through nanotube pores 20 or 30 times faster than through other pores of comparable size (see Figure 2.9). Hence, they will aspire future applications for water desalination, water purification, nanofiltration, and gas separation.

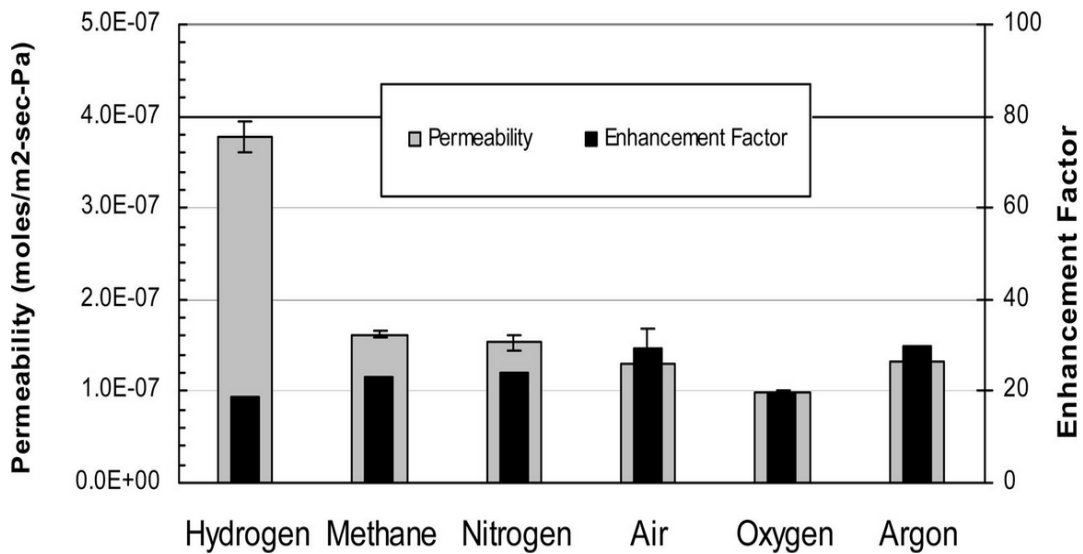


Figure 2.9 Histogram of observed permeability in VA-CNTs [18]

Another application is made from an array of 5 mm aligned titanium oxide/vertically aligned carbon nanotube (TiO₂/CNT) [20]. It was prepared by electrochemically coating the CNTs with a uniform layer of TiO₂ nanoparticles [20]. The resultant arrays exhibit minimized recombination of photo induced electron-hole pairs and fast electron transfer from the aligned TiO₂/CNT arrays to external circuits [20]. This enables the assembly of TiO₂/CNT arrays for

various device applications, like photovoltaic cells for harvesting solar energy.

Figure 2.10 shows image of 5 mm long CNT arrays with electrodeposition of TiO_2 .

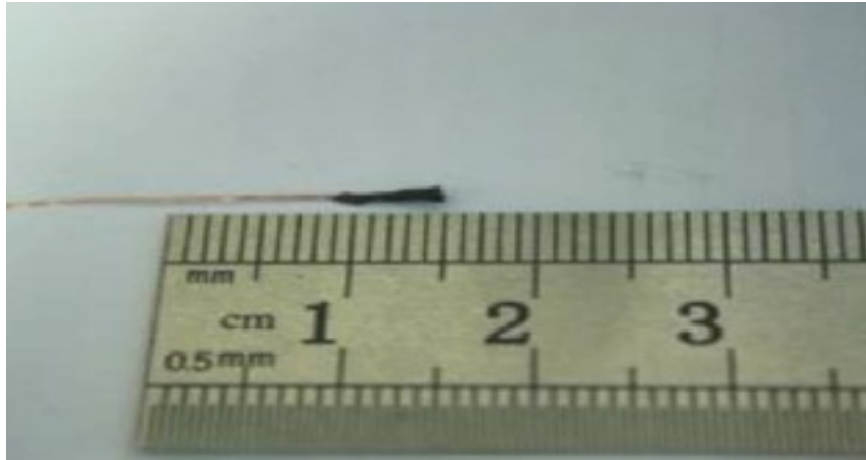


Figure 2.10 5 mm long TiO_2/CNT arrays [20]

2.2 Computational Methods

Our proposed analysis approach uses Artificial Neural Network (ANN) and Design of Experiment (DOE). The network we will use in our work is A Multilayer Perceptron (MLP). Statistical experimental design can be defined as the science of obtaining the largest possible amount of information about a system with the smallest number of experiments [21]. Contrary to ANN, there is a lot of research utilizing DOE in nanotechnology [8]. For example,

researchers used full and fractional factorial designs to optimize SWNTs [22-25].

2.2.1 Multi-Layer Perceptron

MLPs are an important class of highly connected feed-forward neural networks (Figure 2.10). Typically, an MLP consists of a layer of input nodes, one or more layers of hidden neurons, and a layer of output nodes. The input signal propagates forward layer by layer with every neuron in the layers representing a smooth and differentiable nonlinear activation function. The hidden neurons help the network learn complex features of the relation between input patterns and outputs. MLPs use a popular supervised learning algorithm named back propagation, which works in two phases [26].

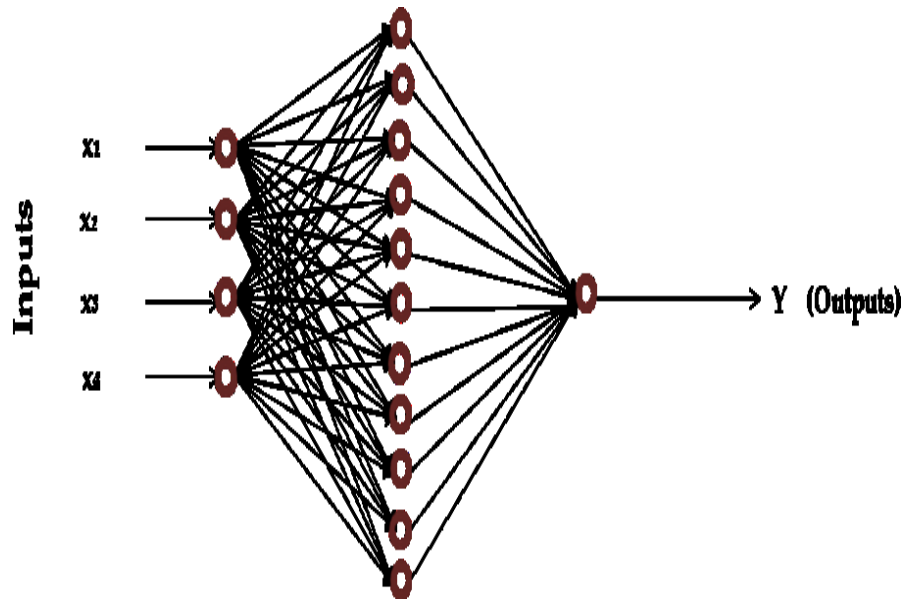


Figure 2.11 Architecture of a Multilayer Perceptron

2.2.2 Design of Experiments

DOE was first used first used in agriculture and has been for over 70 years.

Before information technology DOE was a hard job which requires a skilled statistician with a wholesome physical knowledge of the process under study to make an inference about the process [8].

In DOE, factors are the controllable parameters of the process, which have different levels usually determined by scientific method or experience. Barker et al. illustrated all of the possible factorial designs in Table 2.3 where the columns

are number of factors , rows are number of runs, and III, IV etc. is the fractional factorial designs [27].

Table 2.3 The feasible factorial design either for full or fractional factorial designs, which can be utilized to optimize processes

		Number Of Factors										
		2	3	4	5	6	7	8	9	10	11	12
Number of Runs	4	FULL	III									
	8		FULL	IV	III	III	III					
	16			FULL	V	IV	IV	IV	III	III	III	III
	32				FULL	VI	IV	IV	IV	IV	IV	IV
	64					FULL	VII	V	IV	IV	IV	IV
	128						FULL	VIII	VI	V	V	IV

Now we can design the experiment in less time and even analyze the output with vast speed. Toward this end, choosing a design is the first step, which requires an understanding of the process input and output. The most used designs are full and fractional factorial design with high and low levels (two levels). Other designs like Box–Behnken Design (BBD) are more geared toward studying the curvature of the design after optimality to deeper understanding

of the variables interaction. Another technique is the Taguchi methodology where the researcher chooses an array and optimizes the process based on it, as mentioned on Bourgeois et al. which is also illustrated on Table 2.4 [28].

Table 2.4 Taguchi Designs orthogonal arrays

		Number Of Parameters (P)										
		2	3	4	5	6	7	8	9	10	11	12
Number of Levels	2	L4	L4	L8	L8	L8	L8	L12	L12	L12	L12	L16
	3	L9	L9	L9	L18	L18	L18	L18	L27	L27	L27	L27
	4	L16	L16	L16	L16	L32	L32	L32	L32	L32		
	5	L25	L25	L25	L25	L25	L50	L50	L50	L50		

2.3 Design of Experiments for CVD Grown Carbon

Nanotubes

This sections will present instances of using experimental designs in nanotechnology. Currently, the research on using ANN to study nanotechnology is very limited. The number of journals, which include CNTs

DOE works, is also very limited. Moreover, most of those journals are related to the nanoscience. Hence, DOE utilization for producing CNTs is still limited and there is a lot of work to move it to mass production scale. Table 2.5 shows number of publications available where they used DOE with nanoscale carbon materials [13,22-25,29-43].

Table 2.5 Journals including nanotechnology papers utilizing DOE

Item	Year	Papers	Journal
1	2007	1	AIP Conference Proceedings
2	2004	1	Carbon nanotubes. MRS BULLETIN
3	2007	1	Nanotechnology
4	2007	1	Analytica chimica acta
5	2010	1	Analytical and bioanalytical chemistry
6	2008	1	Biotechnology Letters
7	2005,2005, 2008	3	Carbon
8	2007	1	IEEE Transactions on Reliability
9	2007	1	Industrial & Engineering Chemistry Research
10	2008	1	International Journal of Nanomanufacturing
11	2007	1	Journal of Materials Science: Materials in Electronics
12	2005	1	Journal of Nanoscience and Nanotechnology
13	2009	1	Journal of Quality Technology
14	2006	1	Journal of Vacuum Science & Technology B: Microelectronics and Nanometer Structures,
15	2004,2005	2	Microporous and Mesoporous Materials

16	2009	1	Polymer Letters
17	2007	1	Powder Technology
18	2007	1	Quality Progress
19	2006	1	Thin Solid Films

Most of the papers use full factorial design because of its understanding ease and depth of information. Such technique is very useful for a technology in its start like CNTs. Those designs are useful in most nanotechnology experiments especially for the physical characteristics enhancements of innovative nanostructures.

Table 2.6 illustrates instances of research using DOE and CNT. Table also 2.6 shows how most researchers often use the full factorial than other techniques. Using fractional factorial design is used if the number of runs is high like for two level seven factors experiment ($2^7=128$). However, this technique will help when the full design with high number of runs is not feasible and the goal is to get the main effects and low order factors interactions. Table 2.7 explains in more details why some researchers use full or the other techniques.

Table 2.6 Publications using variable conventional processes and designs for the optimization of carbon nanotubes characteristic [23-26,31,32,34,38,45-49]

Authors	Year	Design	Runs	TYPE	Title
Cotasanchez, et	2005	FFD	16	BUCKY	Induction plasma

al.					synthesis of fullerenes and nanotubes using carbon black–nickel particles
Desai, et al.	2008	FFD	16	SWNT	Understanding conductivity in a composite resin with Single Wall Carbon Nanotubes (SWCNTs) using design of experiments
Kukovecz, et al.	2005	Fractional	22	SWNT	Optimization of CCVD synthesis conditions for single-wall carbon nanotubes by statistical design of experiments (DoE)
Liu, et al.	2007	FFD	8	CNT	Electrocatalytic detection of estradiol at a carbon nanotube Ni (Cyclam) composite electrode fabricated based on a two-factorial design.
Ford, N.	2007	FFD	8	CNT	Plasma enhanced growth of carbon nanotubes
Nourbakhsh, et al.	2007	Fractional	25	MWNT	Morphology optimization of CCVD-synthesized multiwall carbon nanotubes, using statistical design of experiments
Yang, et al.	2005	FFD	27	SWNT	Statistical design of C10-Co-MCM-41 catalytic template for synthesizing smaller-diameter single-

					wall carbon nanotubes
Darsono, et al.	2007	FFD	8	CNT	Field emission properties of carbon nanotube pastes examined using design of experiments,
Gou, et al.	2004	FFD	8	BUCKY	Experimental design and optimization of dispersion process for single-walled carbon nanotube bucky dissertation
Cota-Sanchez, G	2003	FFD	16	MWNT	Synthesis of carbon nanostructures using a high frequency induction plasma reactor
Doddasanagouda, S.	2006	FFD	8	SSNT	Growth and Deterministic Assembly of Single Stranded Carbon Nanotube
Kuo, et al	2005	Fractional	16	MWNT	Diameter control of multiwalled carbon nanotubes using experimental Design
Yang, et al.	2004	Fractional	28	SWNT	Statistical analysis of synthesis of Co-MCM-41 catalysts for production of aligned single walled carbon nanotubes (SWNT)
Yeh, C.	2004	Fractional	30	Buckypaper	CHARACTERIZATION OF NANOTUBE BUCKYDISSERTATION MANUFACTURING PROCESS

Table 2.7 Nano-manufacturing improvements techniques

Technique	Nano-manufacturing Fabrication method	Examples
Full Factorial Designs	Those designs are useful in most nanotechnology experiments especially for the physical characteristics enhancements of innovative nanostructures	Induction Plasma (new method but currently with low yield)
Fractional Factorial Designs	This technique will help when the full design high number of runs is not feasible and the goal is to get the main effects and low order factors interactions	Catalyst Chemical vapor deposition (big number of variables)
Non-Conventional Designs	Such designs are used when techniques efficiency is not essential for the model	Injection Molding (old techniques)

An example of the use of full factorial can be seen in the dissertation about Induction Plasma [33]. This process is new and currently has low yield in comparison to other CNT synthesis methods. So, the author resolved to full design to get the complete statistical analysis for factors interactions. In contrast, other publications used fractional factorial for CVD. CVD is an old technique with most variables is known and only small fraction of their interactions is important [44].

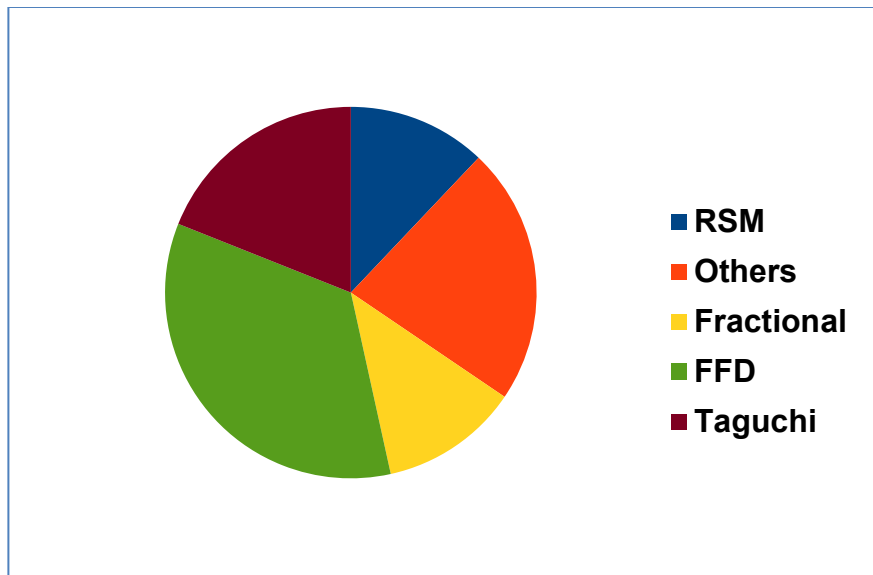


Figure 2.12 Most researchers utilize Full Factorial designs for their publications instead of other techniques like Fractional Factorial and Taguchi

In addition, there are some instances where some investigators used orthogonal array to study CNT (See figure 2.11). Such designs are used when technique's efficiency is not essential for the model. For example, the Injection Molding paper used an old technique's where there is no need for a full statistical analysis. Here the author can just study the new factors affecting the process rather than studying all the factors. In addition, only suspected interactions are examined since others might already have been proven insignificant. Figure 2.12 show an overview of the number of papers over the years who used orthogonal arrays and Table 2.8 details their titles and other information.

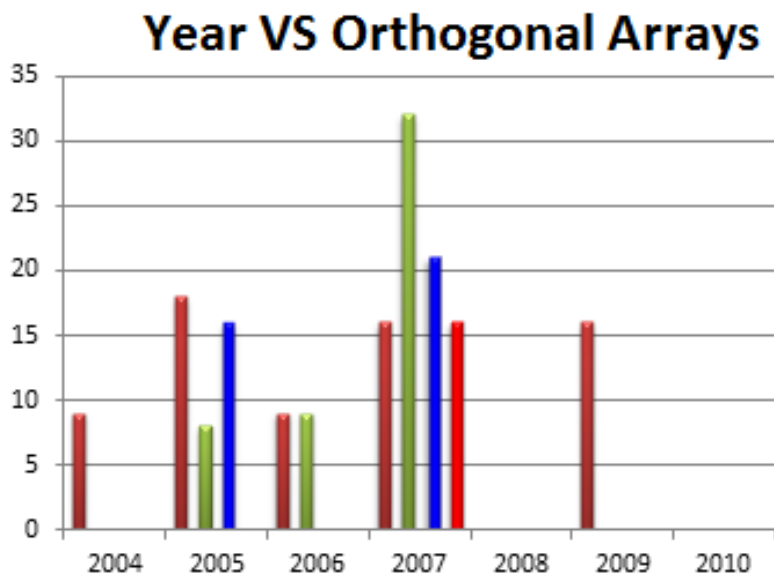


Figure 2.13 Histogram of years 2004-2009 of papers related to Orthogonal Arrays

Table 2.8 Summary of articles in the use of Orthogonal Arrays to optimize the processes and designs related to carbon nanotubes [30,39,41,44,51]

Authors	Year	Array	TYPE	Title
Ting, et al.	2006	9	CNT	Optimization of field emission properties of carbon nanotubes by Taguchi method
Maheshwar, et al.	2005	18	CNT	Application of the Taguchi Analytical Method for Optimization of Effective Parameters of the Chemical Vapor Deposition Process Controlling the Production

				of Nanotubes/Nanobeads
Lin, et al.	2006	9	Nano fibers	Improvement on superhydrophobic behavior of carbon nanofibers via the design of experiment and analysis of variance
Jahanshahi, M	2007	16	CNT	Application of Taguchi Method in the Optimization of ARC-Carbon Nanotube Fabrication
Prashantha, K.	2009	16	MW NT	Taguchi analysis of shrinkage and warpage of injection-moulded polypropylene/multiwall carbon nanotubes nanocomposites

2.3.1 Experiments and Discussion

Three papers used DOE to optimize CNTs fabrication will be discussed here [34, 36, 40]. The papers used two types of CVD to grow the CNTs, namely, catalyst chemical vapor deposition (CCVD) and vertical chemical vapor deposition (VCVD). Two papers research the use of CCVD to optimize the diameter and synthesis condition of CNTs. Those papers have similar input and

output variables but one of them synthesized SWNT and the other MWNT.

Figure 2.13 shows a schematic of their CVD system.

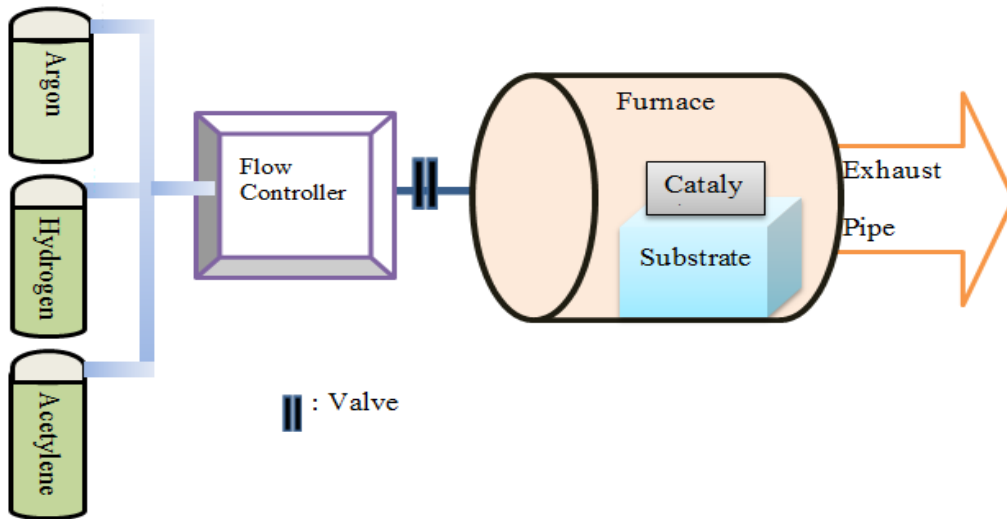


Figure 2.14 Schematic diagram of the CCVD setup for carbon nanotube synthesis

The third paper used VCVD, which has great promise for producing large quantities of CNT. Its vertical setup allow for the constant feeding of the catalyst material and carbon source to the furnace. However, it needs high temperature to operate and its initial capital investment is high. Figure 2.14 shows how the vertical alignment is structured.

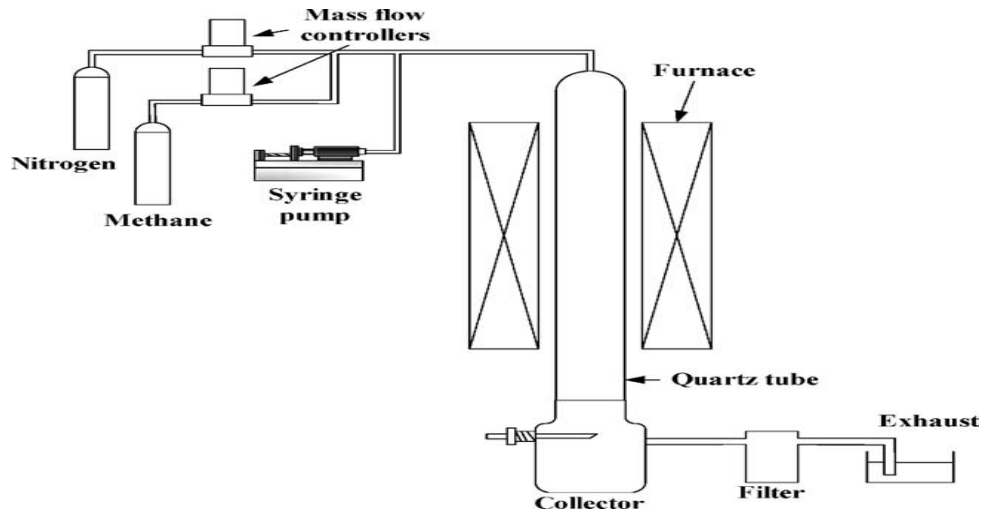


Figure 2.15 Schematic diagram of VCVD [50]

Both methods focused on the furnace temperature as an important factor to study initially. Then, all of the research regardless of the analytical method used concluded that it is a statistical significant factor. After that, the gas flow rate was considered significant. For the CCVD a C_2H_2 source was utilized while the VCVD used a methane source. Both the temperature and carbon source flow rate ranges were moderately similar for the two processes. The third common factor between the processes was carrier gas flow rate. Three gases were considered. H_2 , N_2 and Argon were varied dramatically between (50-2000Scm) to study their effect on CNTs. Table 2.9 summarizing the techniques used and the results.

Table 2.9 CCVD and VCVD process for growing CNTs synthesis conditions,

MRL: mean rectilinear length, C%: Carbon Deposit, QDN: quality descriptor number

	Nourbakhsh et al.	Kukovecz et al.	Kuo et al.
Year	2007	2005	2005
Process	CCVD	CCVD	VCVD
CNTs	MWNT	SWNT	MWNT
Temperature C°	700,800	850,900,950	1050,1150
Carbon Source Flow Rate	(3,12) C ₂ H ₂	(5,10,15) C ₂ H ₂	(125,250) CH ₄
Carrier Gas Flow Rate	(50,110) C ₂ H ₂	(100,300,500) Ar	(1000,2000) N ₂
Runs	64 = 2 ⁶⁻³ +BBD	128 = 2 ⁷⁻⁴ +BBD	32 = 2 ⁵⁻¹ +CCD
Goal	Diameter, MRL	C%, QDN	Diameter

(Kukovecz et al., 2005) used two level design with fractional factorial design [23]. They optimize the main seven factors influencing the carbon percentage and the ratio of radial breathing mode to the Raman spectrum d-band. The seven factors are reaction temperature, reaction time, preheating time, catalyst mass, C₂H₂ volumetric flow rate, Ar volumetric flow rate, and Fe: MgO molar ratio. The design confounds three factors using BBD and so reduces the run to 22 instead of 128. Which is an example of DOE saving time and cost.

BBD used for two factorial fractional designs is illustrated in (Nourbakhsh et al., 2007) [31]. Six parameters (synthesis time, synthesis temperature, catalyst mass, reduction time, acetylene flow rate and hydrogen flow rate) were optimized by only 25 runs, less than 39 runs of the FFD. MWCNT morphological responses like the average diameter and mean rectilinear length (MRL). A final run was performed to check the optimality. The main factors which were significant are H₂ flow rate, synthesis temperature and reduction time. In addition, it might have been useful if the paper used response surface methodology to find the global optimum combination for all responses.

Fractional factorial design was used in (Kuo, et al., 2005) to optimize MWNT Diameter by a CVD reaction. Equally important they utilized different tools like response surface methodology steepest ascent path to calibrate their findings. Thereupon, the diameter was controlled and precisely from 15 – 240 nm with a contentious CVD. 16 runs optimized the system while for full factorial it would need to be 32.

From previous discussion, it is clear that DOE is practical for optimizing CNTs fabrication. However, it needs be done with new experiments after the preliminary experiments were done. The preliminary experiments will be a

used to setup the input and output factors of the DOE and their levels. With ANN, we can utilize the preliminary results to build a process metamodel. Then, we utilize metamodel to setup the DOE method and analysis. That analysis will give us a better understanding of the CNTs fabrication without having to do additional experiments. So, in the following chapters will be more discussion on that metamodel and analysis.

3. Experimental Setup

This chapter will discuss growing VA-SWNTs experimental Setup and CVD setup. First, we describe the details of the growth system variables. Then, we discuss the catalyst preparation and generalization of the CVD setup especially the growth processes. The length controlled VA-SWNTs were synthesized by using an ethanol CVD technique.

Most of the experiment setup here is similar to work published before utilizing ethanol based CVD to grow VA-SWNTs [23, 46]. Figure 3.1 is a schematic showing the ethanol CVD system and experimental procedure for the growth of the highly aligned CNTs.

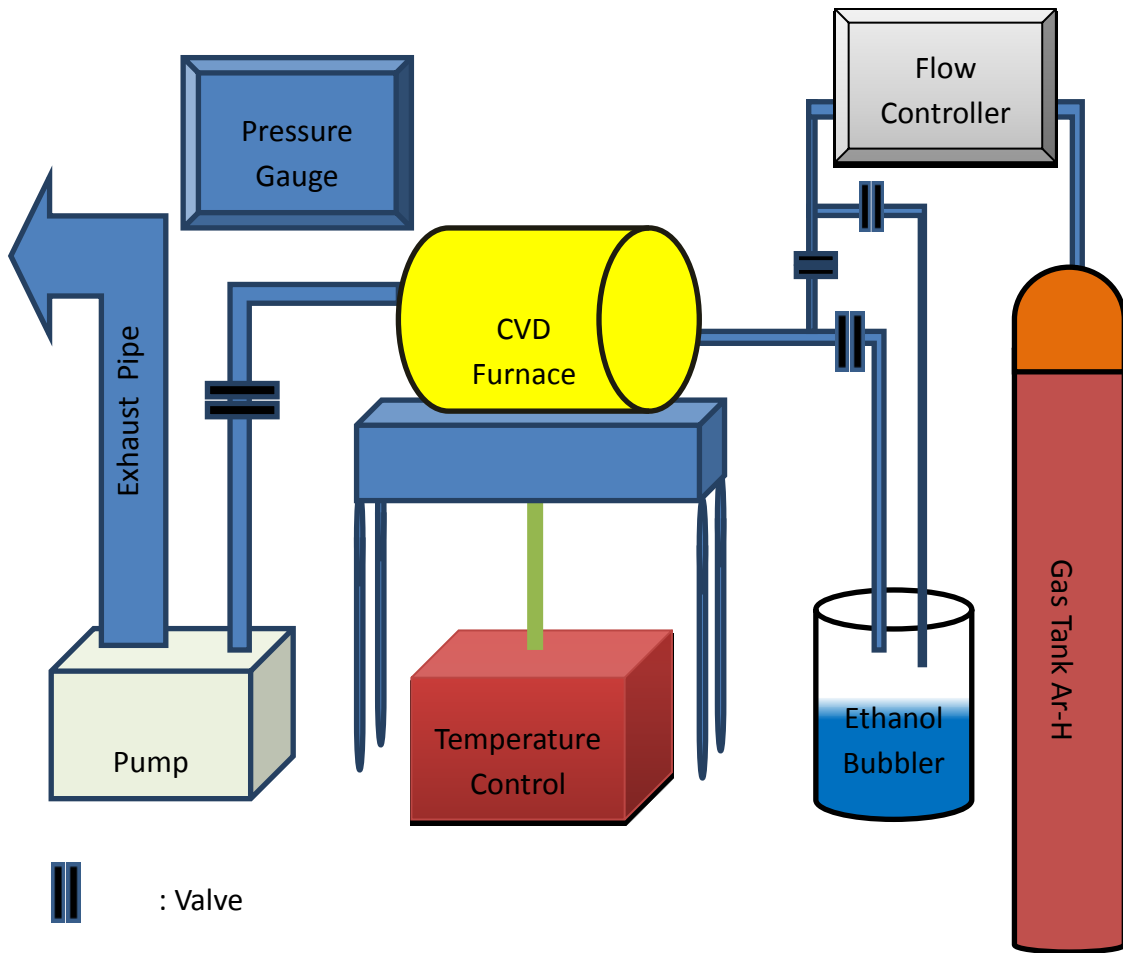


Figure 3.1 Schematics of ethanol CVD systems and experimental procedures for the growth of VASWMTs

The flow of the carbon source will react with the substrate in the furnace to form a nucleation region. The diameter of the VA-SWNTs is said to be determined by how fast the gas flow [44]. High or low flow means no growth of the CNTs.

3.1 System Variables

Figure 1.1 shows the input-output diagram of the CVD process to grow VA-SWNTs. As shown in the figure, temperature, gas flow rate and pressure are considered the important process inputs. VA-SWNTs length is considered the key performance indicator, i.e. process output.

Input Variables

1. *CVD temperature*: It is the temperature of the gas flowing through the furnace; it is measured by a thermocouple installed inside the furnace; the resolution of this measurement is 1°C.
2. *Gas flow rate*: it is the volumetric flow rate of the gas flowing through the furnace; it is measured by flow gauge; the unit of this measurement is Standard Cubic Centimeters per Minute (SCCM).
3. *CVD pressure*: it is the furnace pressure at the time of CNT growth; it is measured by a pressure gauge attached to the furnace; the control resolution of this apparatus is 1 Torr.
4. *Growth time*: It is the duration from the time the substrate is inserted in to the furnace until the process is terminated; it is measured in minutes.

Noise Factors

Noise factors are known or unknown variables affecting the VA-SWNTs growth and they have one thing in common; they are uncontrollable. Lot of variables affect the sample before, during, and after growth. Some are inside the furnace like the ambient temperature and rate of cooling. Others are from the environment like the gravity field. A Cause and Effect Diagram (Fishbone) Analysis is done to map each input variable to the output. The major inputs are classified to Measurement, Method, Machine, Manpower, Materials, and Environment. As shown in Figure 3.2 an analysis investigation is done on each of those inputs to study and classify the most important of them. More emphasis is aimed to classify them to either controllable or non-controllable (noise) factors.

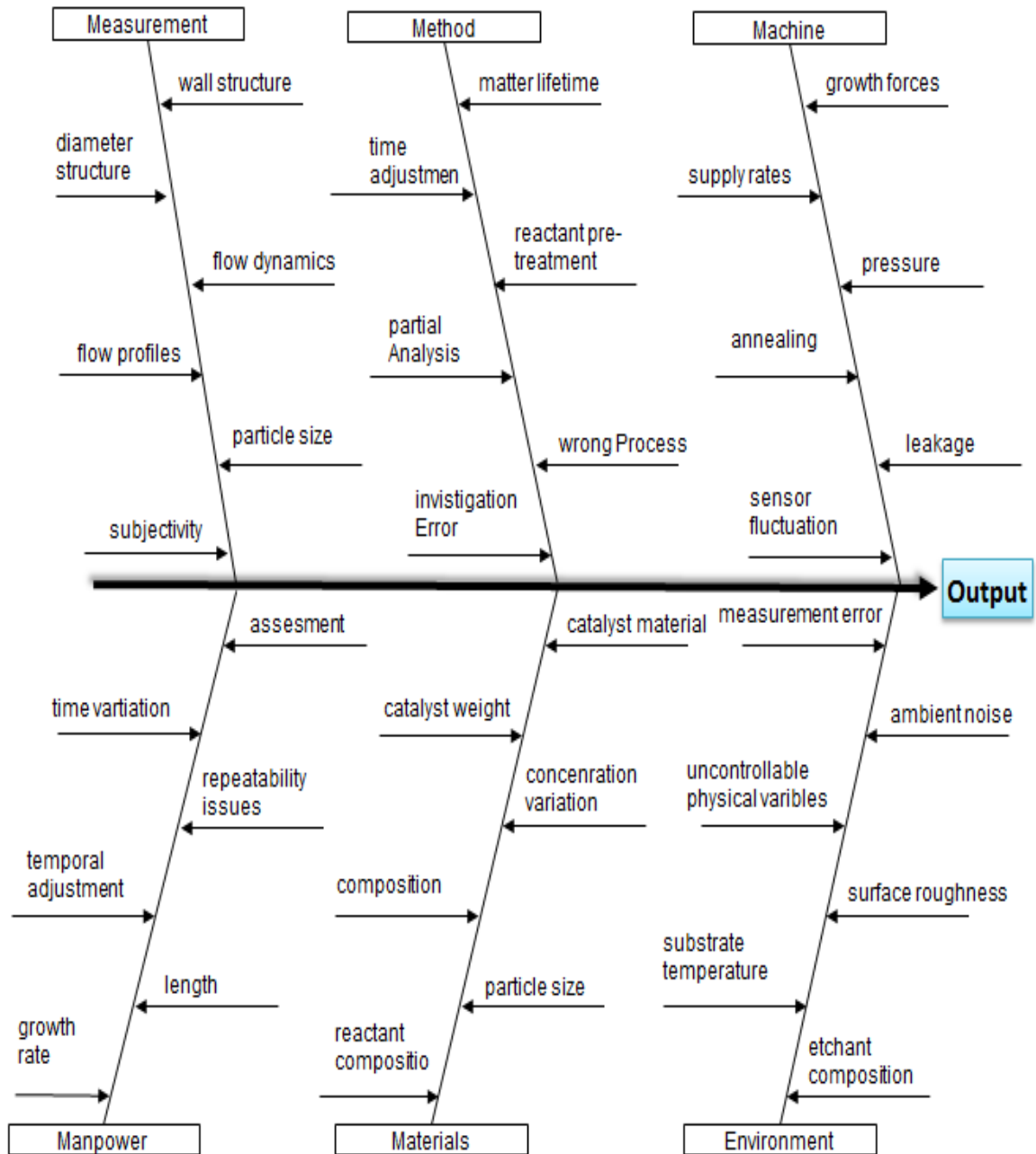


Figure 3.2 Cause and effect matrix of input variables

3.2 Catalyst Preparation

Catalyst system is prepared by sputter coating a 20 nm thick Aluminum layer onto a SiO₂ wafer as a buffer to grow VA-SWNTs. Then, the layer is exposed to the air for the formation of aluminum oxide. Using a sputter coater a 0.5-1 nm thick Cobalt (Co) catalyst film was deposited on top of the Al/SiO₂ layer with wide dispersion. Figure 3.3 shows a schematic of the preparation process.

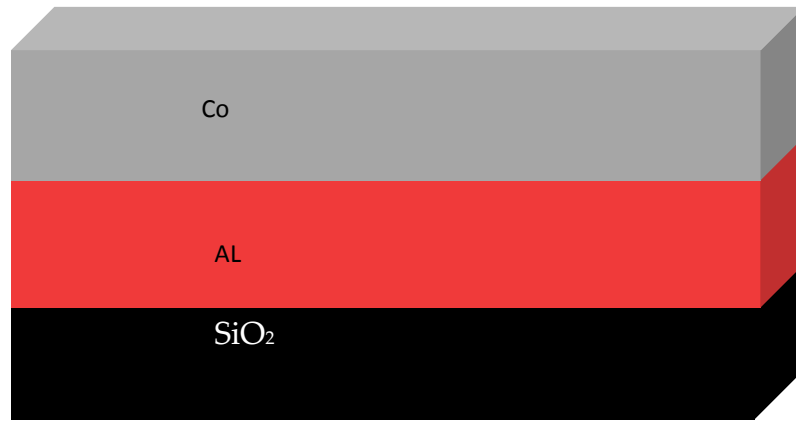


Figure 3.3 Schematic of the cross section of the substrate

3.3 CVD Process Setup

CVD setup is done through the following steps. First, put the substrate inside the furnace. Then, pressurize the furnace to prepare for the growth process. Meanwhile, a mixture of an argon-hydrogen (5% hydrogen) is supplied as the carrier gas to maintain the pressure at 700 Torr. Consequently, the temperature

inside the quartz tube furnace reaches 850°C. After that, a controlled high-purity anhydrous ethanol (99.95%) vapor is supplied from the bubbler as a carbon source for the growth of VA-SWNTs. Using different ethanol/argon/hydrogen mixture gas flow rates, different VA-SWNTs are synthesized. Resulting VA-SWNTs shown in two views and set of samples is shown in Appendix A. Also, Appendix A shows a set of pictures showing the whole CVD system, heat source and temperature sensor, pressure machine, gases locker, the ethanol bubbler, the gold plated furnace, the catalyst sputter.

4. Process Design for Controllability

In this dissertation, we study the controllability of VA-SWNTs growth via a hybrid process model of an experimental design and an artificial neural network (ANN). Controllability here means to selectively fabricate only VA-SWNTs. Our process analysis shows that CVD pressure and temperature are the most significant input factors [47]. In addition, interactions and response surface plots confirm these results and show that higher temperature and pressure will yield VA-SWNTs with high probability.

Our proposed approach aims to analyze experimental data from a CVD process, build neural network models, and perform statistical analysis with the goal of relating the CVD input parameters to the characteristics of the CNTs to gain better understanding of CNT properties. Our objective is to evaluate all input variables theoretically and experimentally to find the statistically significant ones.

The proposed methodology has two distinct stages. Stage 1 focuses on building a metamodel of the process using the experimental data and an ANN technique such as an MLP. A metamodel in this context captures the overarching behavior of the process by broadly encompassing the data available at hand. Using the

metamodel, Stage 2 generates multiple runs for a full-factorial experimental design.

4.1 Metamodel and Design of Experiments

Artificial Neural Network Design Stage

The following are the steps that make up the stage 1 of the research methodology.

- Delete records with missing data.
- Using the records retained in the previous step, train a set of MLPs for predicting the process outputs; given that input vectors are positioned densely in the input space, the neural networks is likely to learn the mapping between process inputs and outputs accurately.
- Compute the prediction accuracy of each MLP and retain the network that gives the highest prediction accuracy.

- The neural network selected in the previous step serves as a meta-model of the process. Compute the paired difference between the actual process outputs and the neural-network estimated process responses.
- Conduct the t-test on paired differences with level of significance $\alpha = 0.05$.
 $H_0: \mu_d = 0$ and $H_1: \mu_d > 0$, where μ_d is the mean of the paired differences.
 Compute t_0 , the t-statistic for the paired difference. If $|t_0| > t_{\alpha/2}$ then reject H_0 ; otherwise we fail to reject H_0 , and conclude that our metamodel is a viable statistical representation of the experiment.

Design of Experiment Stage

After building the MLP-based process metamodel, a DOE study is performed.

Following are the steps required for their implementation.

- Find the min-, mid- and max-points of each input variable for the records used for training the selected neural networks in stage 1.
- Create the level settings for the DOE using the min-, mid-, and max-points of the input variables.
- Conduct DOE analysis using the DOE runs.

System Variables

The process input variables are growth time; furnace temperature, gas flow rate, and chamber pressure (see Figure 1.1). The process output is one of three possible types of CNTs : VA-SWNTs, MWNTs or MWNTs-SWNTs mixture.

Seven hundred and fifty samples of VA-SWNTs were used in our study (see Appendix B). First, we eliminated the records that lack measurement quality or completeness of data. This brought down the number of available records to 702. We ignored the growth time since it has no effect on the type of CNTs that come out of the process. Using these records, we trained an MLP neural network with three input nodes, four output nodes, and a different number of hidden neurons. We found that an MLP with three inputs, seven hidden nodes, and four outputs (3-7-4) gives the best prediction (83%) for the training data as shown in Figure 4.1.

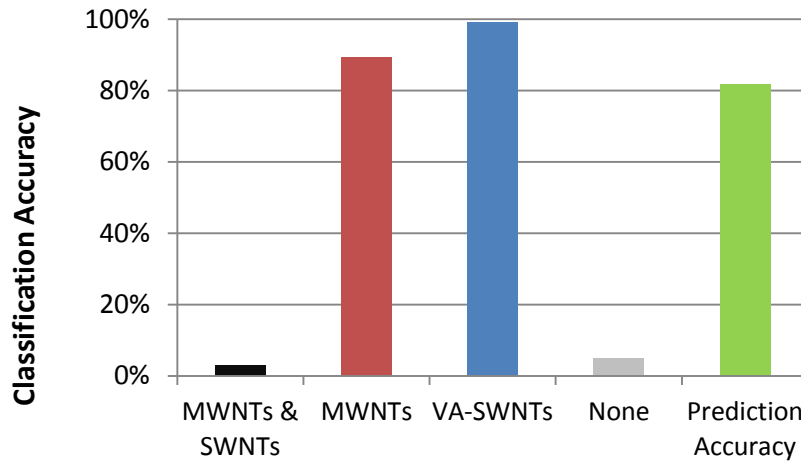


Figure 4.1 Classifications accuracy of process outcome

The ANN response is obtained from the trained MLP. Then, we computed the response estimation error (the absolute difference between the predicted and actual values) for the prediction. Subsequently, the paired t-test was conducted on the actual process output and the neural-network estimated process responses. We computed t_0 for the VA-SWNTs and found it to be $t_0 = 0.76$. So, the value of $|t_0| < t_{0.025} = 1.98$, and hence we concluded that there is no statistical evidence to say that the behavior of the metamodel is different from that of the actual process. This has given us the confidence that the DOE analysis conducted using metamodel will be statistically valid.

Design of Experiments

Using the boundaries of the final input space, we determined minimum, medium, and maximum values for each of the three variables. Using these settings, we created a full factorial experimental design (Table 4.1). The regression fit to the analysis show that the model is significant for prediction based on the Sig F value for output.

Table 4.1 CVD three level-three variables full factorial design of experiment

Independent Variable	Range and Level			
	Factor	-1	0	1
Temperature (°C)	X1	700	800	900
Pressure (torr)	X2	500	632	764
Gas Flow Rate (sccm)	X3	50	225	400

4.2 Comparison of Main Effects Plots

Figure 4.2 illustrates interactions plots for both key performance indicators with respect to the process variables. Response of those plots to the key performance indicators largely conforms to our general understanding of the process. Trends of interaction and main-effects plots for output ratios, as shown in Figure 4.1, are mostly converse of each other as expected. Effect of high reaction temperature on the controlled pressure is visible on the plot trends.

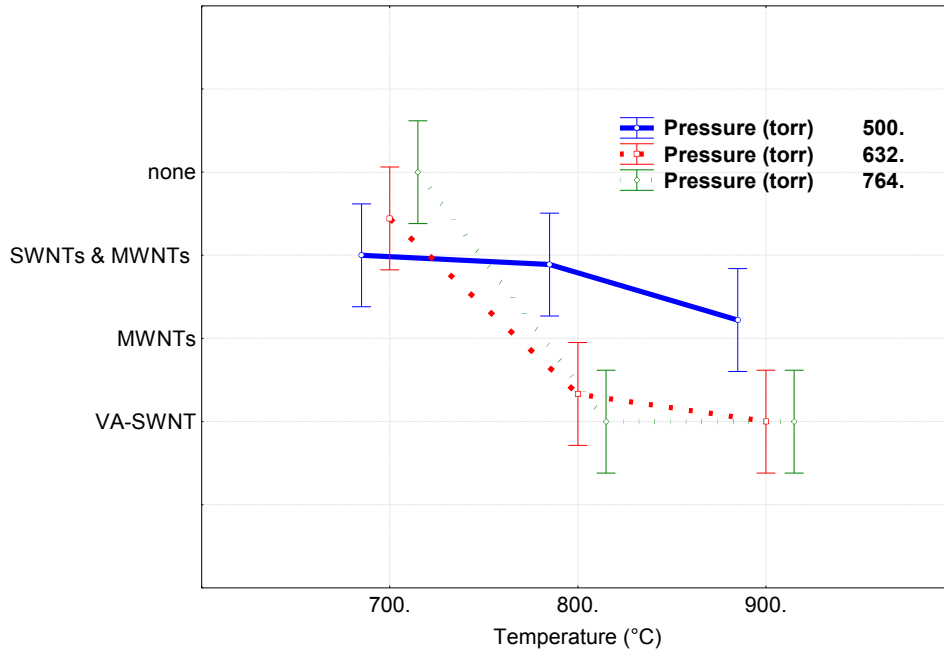


Figure 4.2 Interaction Plots between Temperature and Pressure for VA-SWNTS

Interaction plot serves as a secondary means to gauge the efficacy with which our metamodel simulate the actual process behavior in response to the changes in the input settings. Once we have the interaction plots for the generally anticipated behavior of the process, we go into variable specific analysis within the input variables space defined by the minimum and maximum values available in the experimental data.

4.3 Pareto and General Response Surface Plots

The R-squared value for the process is 0.89 and the standard error is 0.15. The Pareto chart of the analysis is presented in Figure 4.3. The Figure shows that CVD temperature and pressure are the most statistically significant factors ($\alpha = 0.05$). Therefore, any alteration of their values will affect the desired output (VA-SWNTs). Response surface plots in Figure 4.4 help illustrate the details of the growth changing aspects of VA-SWNTs with respect to individual behavior of the control variables. The figure shows that there is a more rapidly increasing ascent of the VA-SWNTs response surface along increasing temperature and pressure. This provides insight into the role of high temperature and pressure and its positive impact on VA-SWNTs growth.

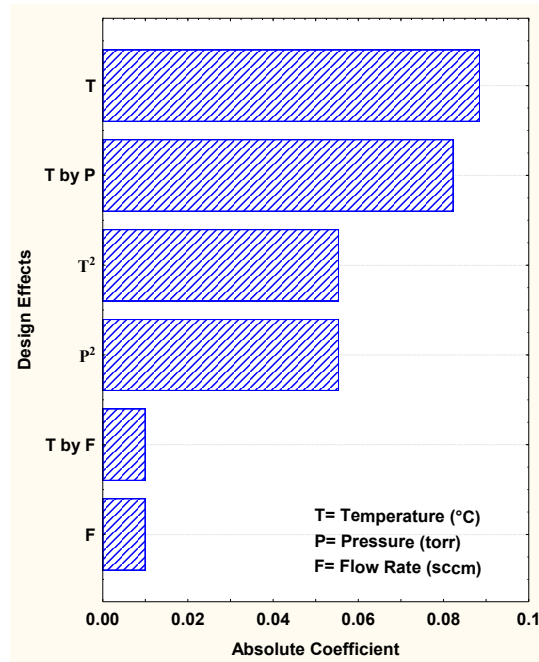


Figure 4.3 Process Analysis Pareto Plot

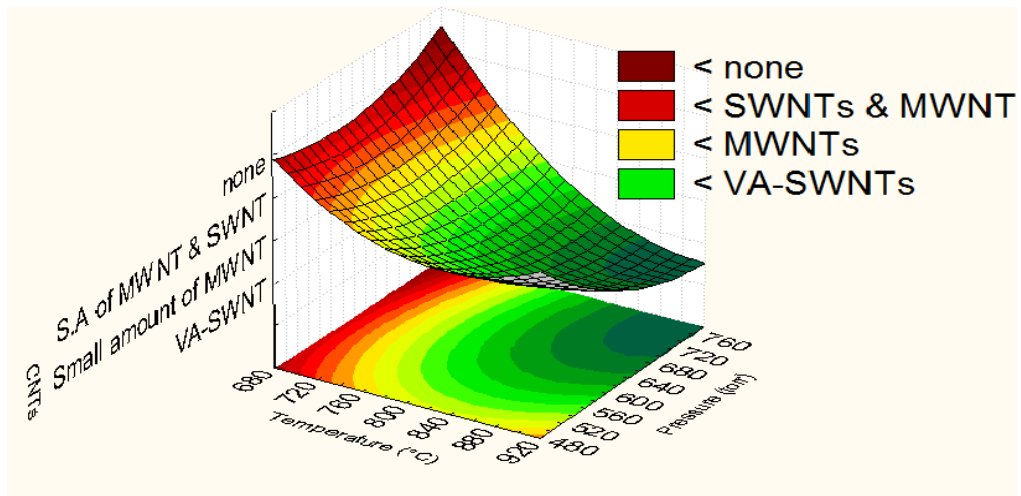


Figure 4.4 Response Surface Plots of VA-SWNTs Length (Temperature VS Pressure)

5. Process Design for Length Assurance

Chapter 4 researched the VA-SWNTs controllability while this chapter will research their length assurance. Chemical vapor deposition (CVD) is one of the several viable methods for growing VA-SWNTs. Utilizing Co supported on multilayer Al/SiO₂ as the catalyst and a hydrocarbon feedstock, VA-SWNTs are grown in excess of a millimeter high. To control VA-SWNTs length, one has to use the right combination of process inputs such as hydrocarbon flow, growth time, temperature, and pressure.

This dissertation presents a process metamodel-based full factorial experimental design and analysis to study the yield of tall VA-SWNTs. All of the process variables under the study play a role in influencing VA-SWNTs length; the current study which under review in the “International Journal of Advanced Manufacturing Technology” investigates their main effects and interactions [48]. The neural network metamodel-based analysis demonstrates that the hydrocarbon flow rate and the pressure are the most statistically significant factors that influence the length of VA-SWNTs. In addition, the response surface graph confirms the factors of significance and adds that higher flow with lower pressure will consistently yield tall VA-SWNTs.

We found that gas flow rate is the most significant of the control variables and only the optimum value of the gas flow can ensure the growth of tall VA-SWNTs. We also found that the interaction of flow rate with temperature of the gases in the chamber is extremely significant to the quality of output indicating towards velocity related dynamic pressure of the fluid to be a way to simplify the understanding of the process. Outcomes of this investigation are beneficial for moving closer to producing VA-SWNTs on production scale.

5.1 Metamodel and Design of Experiments

The methodology employed [26] has two phases. Phase 1 focuses on building the process metamodel using the experimental data. The metamodel in this context captures the overarching behavior of the process by broadly encompassing the data available at hand. Using the metamodel, in Phase 2 we generate multiple runs for a full-factorial experimental design to study the influence of the process input variables (Figure 5) on the length of the VA-SWNTs.

We explored different data modeling techniques keeping in view that the anticipated behavior of the control variables is highly nonlinear. First technique we considered is non-parametric regression, which is one of the most

established modeling techniques in statistical theory as presented by *Dasguta et al.* [27]. However, its dependence on the valid statistical design of training data is the major challenge to its applicability to the problem at hand. The basic fitting parameter, i.e. R^2 for the response surface regression with linear, paired interaction and nonlinear coefficients was 0.32, a low number of valid results. Thus, we use neural networks as an alternative modeling technique.

There are different types of neural networks like self-organizing maps and radial basis functions that can be used for modeling process input-output relationship [28]. Most MLPs contain highly connected feed-forward connections with a layer of input nodes, one or more layers of hidden nodes, and a layer of output nodes [29]. The input signal propagates forward layer-by-layer with every node in the hidden and output layers representing a smooth and differentiable nonlinear activation function.

Therefore, we used multi-layer perceptron based on back propagation algorithm, which is well known as a universal approximate of the non-linearities in the training data. Using these experimental data records, we trained multi-layer perceptions with three input nodes, one output node. The architecture of the MLP used in the current dissertation is shown in Figure 5.1.

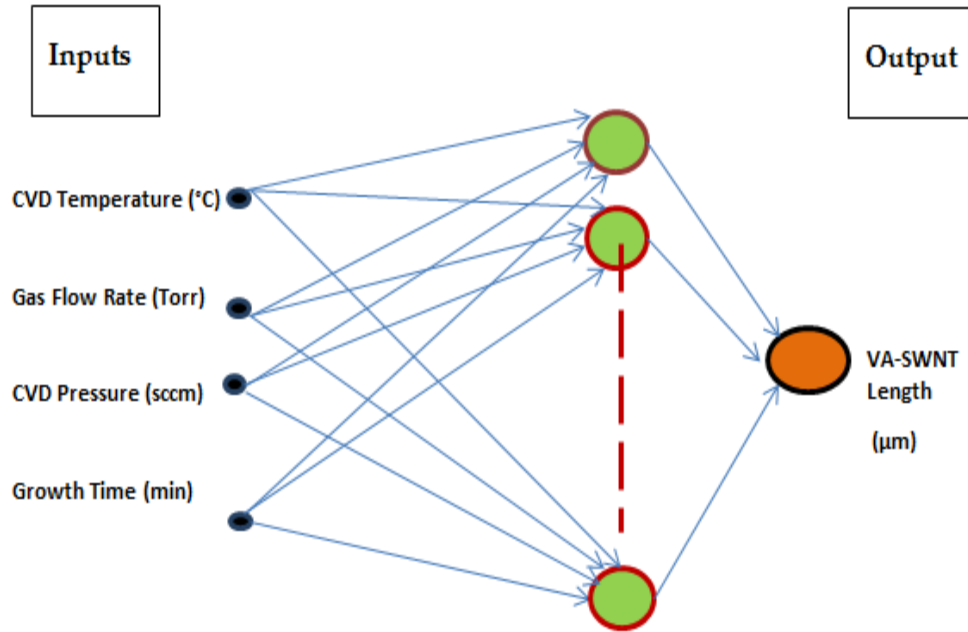


Figure 5.1 Architecture of a multi-layer perceptron network

As shown in Figure 5.2 R^2 value of 0.5 for the network architecture with three input nodes, 21 hidden nodes and one output node renders it as a better meta-model for the process with the available data at hand. Once the best available process meta-model is selected, we used a full factorial design of experiments to design a set of computer experiments with 30 replication for each record for studying the details of process behavior. We compute t_0 for the VA-SWNTs length and find it to be $t_0 = 0.9188$. So, the value of $|t_0| < t_{0.025} = 1.98$. On this basis, we decide that there is no statistical evidence to say that the behavior of the metamodel is different from that of the actual process with 97.25% confidence level.

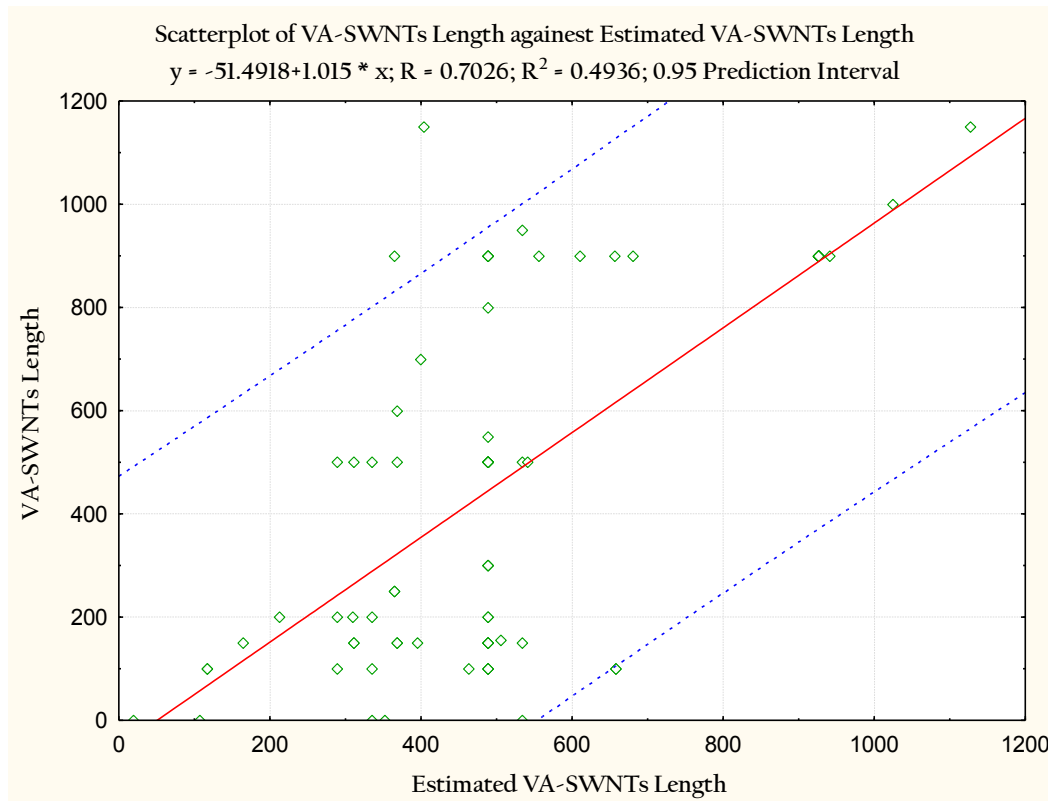


Figure 5.2 VA-SWNTs length (target) versus estimated VA-SWNTs length (output) regressions graph for the MLP 4-21-1 network

Metamodel

The following are the steps to construct the computer model:

- Eliminate experimental data records with missing data.
- Normalize the values of each process control variable in [0, 1] range. This transformation brings all control variables into the same numerical range to give equal weight to each variable in clustering process described below.

- Using the records retained in the previous step, train the neural networks for estimating the performance variables, given that control variable vectors are most likely positioned densely in the input space, the neural networks are likely to learn the mapping between process inputs and outputs accurately.
- Compute the estimation errors, i.e., the paired differences between the actual process outputs and neural-network-estimated process responses.
- By examining the distribution of the estimation errors, retain the training records whose estimation error is smaller than $\mu+2\sigma$, and ignore the remaining training records; here μ and σ are the mean and standard deviation of the estimation errors respectively; this process eliminates 2.28% of the training records that are considered outliers. Here most of the records eliminated would be the ones with erroneous experimental measurements.
- Using the records retained in the previous step, retrain the neural networks for estimating the process outputs; these trained neural networks serves as computer models of the CVD process.
- Compute the paired difference between the actual process outputs and the neural-network estimated process responses.

- Conduct the t -test on paired differences with a level of significance, say $\alpha = 0.05$ (this can be tightened or relaxed if necessary). $H_0: \mu_d = 0$ and $H_1: \mu_d > 0$, where μ_d is the mean of the paired differences. Compute t_0 , the t -statistic for the paired difference. If $|t_0| > t_{\alpha/2}$ then reject H_0 ; otherwise we fail to reject H_0 , which would mean that statistically we do not have evidence to the effect that the behavior of the metamodel is different from that of the actual process.

Design of Experiment Phase

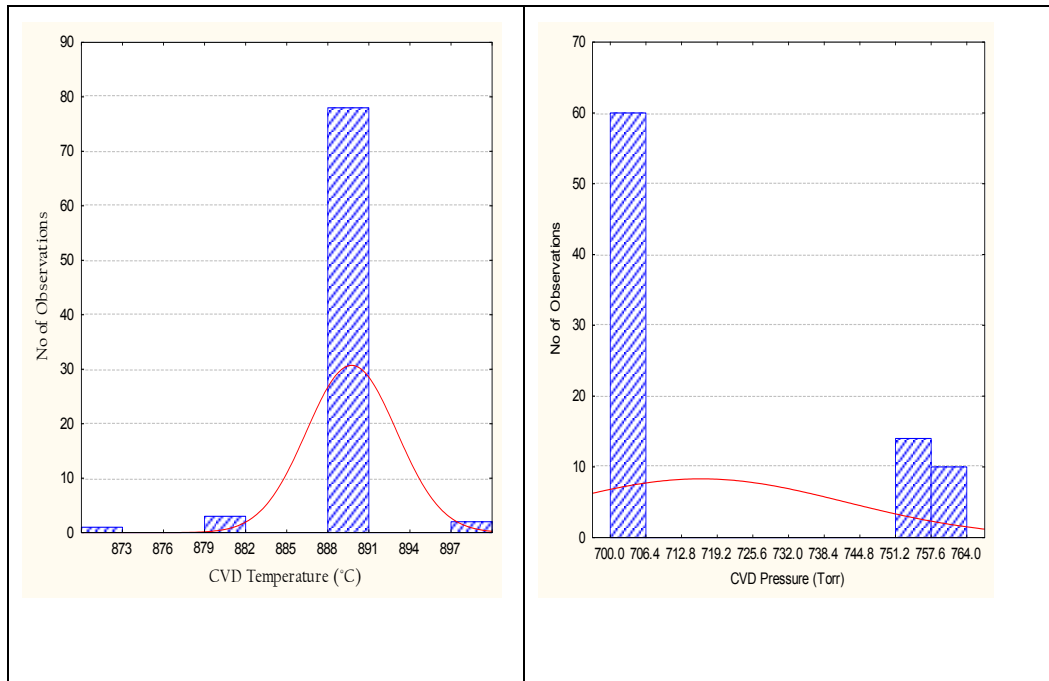
After building the multi-layer perceptron based process metamodel, we perform a design of experiment study. The following steps are used to conduct the study.

- Find the min-, mid- and max-points of each input variable for the records used in training the neural networks in phase 1.
- Create the three level settings for the DOE using the min-, med-, and max-points of the input variables.
- Create 30 replications of each pattern by adding a Gaussian noise to each variable. The Gaussian noise was added with mean equal to zero and

standard deviation equal to 1% of the minimum value of each variable in the training data.

- Conduct DOE analysis using the DOE runs.

We started with 100 records of VA-SWNTs growth using the same experimental setup for chapter 3 (See Appendix C). First, we eliminated records with errors in measurements and missing data. This brought down the number of available records to 84 samples. The distribution of the control variables in these 84 records is shown in Figure 5.3.



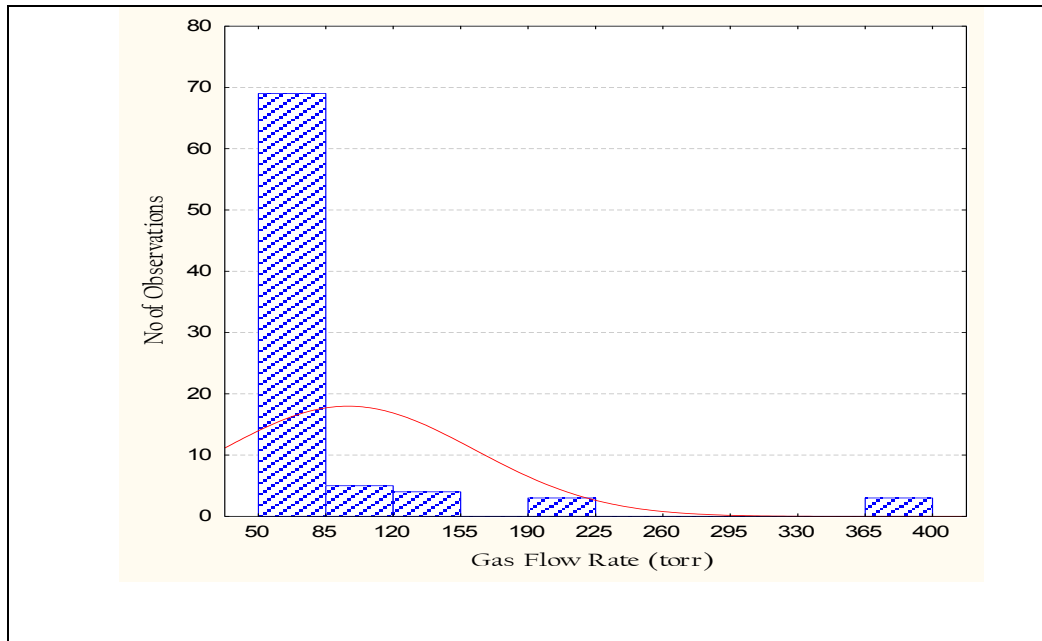


Figure 5.3 Histograms showing the distribution of control variables in the training data for neural networks

Using the boundaries of the final input space, we determine minimum, medium, and maximum values for each of the four input variables. Table 5.1 shows the min, mid, and max values of the records used for the analysis.

Table 5.1 Experimental records of the CVD process input and output variables

Variable	Min	Mid	Max
CVD Temperature (°C)	870	889	900
CVD Pressure (sccm)	700	717	764

Gas Flow Rate (Torr)	50	97	400
----------------------	----	----	-----

5.2 Pareto Chart Analysis

The comparison of significance of control variables, their quadratic effects, and or their paired interactions is presented in Pareto and the coefficients of regression Figure 5.4. The most significant of the variables is the quadratic effect of the gas flow in the chamber during growth. After that linear effect of chamber pressure, interaction of pressure and flow and linear effect of chamber pressure bear almost the same significance of effect on the length of VA-SWNTs grown.

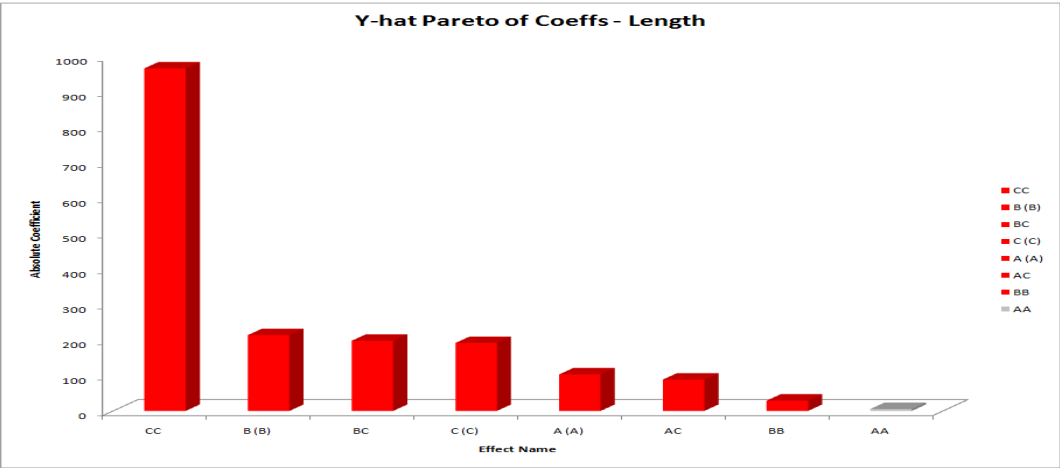


Figure 5.4 Process Pareto Analysis, (A) CVD Temperature (°C), (B) CVD Pressure (scm), (C) Gas Flow Rate (Torr)

5.3 Marginal Mean Plots

Marginal mean plots are the generalized three level process behaviors with trend of each variable plotted at the mid value of its peers. Figure 5.5 presents the marginal mean plots of the responses of neural network meta-model to the full factorial design of computer experiments where A = CVD Temperature (°C), B= CVD Pressure (sccm), C= Gas Flow Rate (Torr). Assessing from the marginal means we can see that pressure and flow are the two most significant control variables and flow has a two level effect on the length of VA-SWNTs.

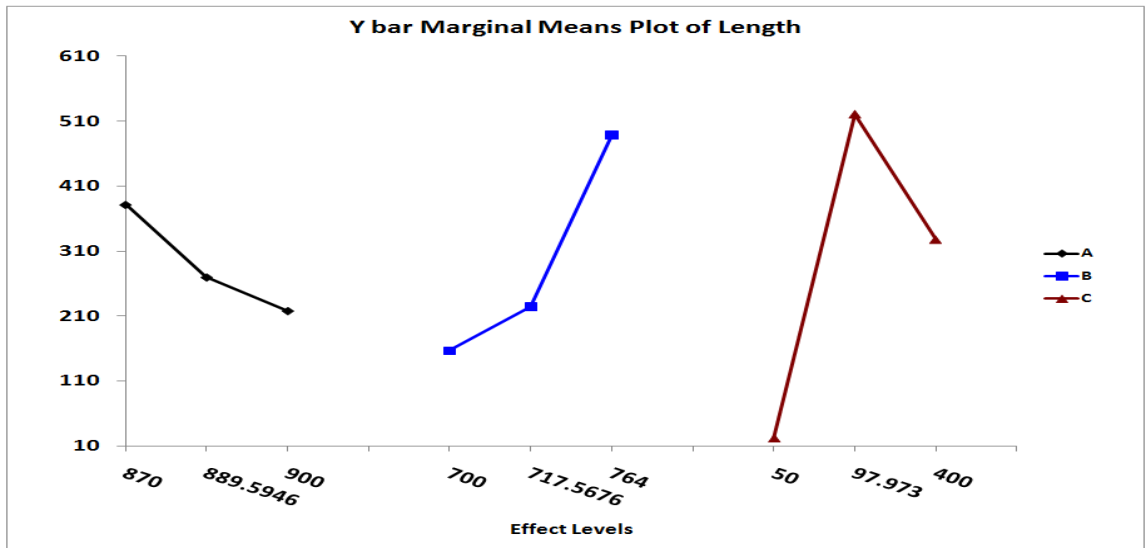


Figure 5.5 Marginal mean plots, (A) CVD Temperature (°C), (B) CVD Pressure (sccm), (C) Gas Flow Rate (Torr)

5.4 Comparison of Main Effects Plots

In order to investigate the details of interaction between chamber pressure and flow of the constituent gases (Ethanol, Hydrogen, and Argon), we performed the main effects analysis on this interaction. Figure 5.6 shows the interaction plots for the key performance indicator (length of VA-SWNTs) with respect to the significance process variables, namely, pressure and flow rate. The interaction plots largely confirm our belief that the process pressure and flow rate are the most influential process input parameters. The sensitivity trends of chamber pressure, which directly relates to the availability of gases for growth reaction at min, mid, and max values of net flow rate of the gases, indicate towards the details of nature of two level effect of the flow rate on the length of the VA-SWNTs. The minimum extreme of flow rate, which in a way indicates towards the sustained supply of fresh mix of gases, shows almost no growth. However, the extreme high-end values of the flow, i.e., 400 sccm refer to a saturation effect that can be forced to yield taller SWNTs if coupled with higher pressure. Pressure here seems to ensure sustained concentration of reactant at catalyst locations to maintain the growth mechanism. The fundamental conclusion which we can draw from this is that the velocity of arriving

constituent atoms at the cobalt catalyst locations needs to be maintained high but the momentum must not exceed the strength of the van der Waals forces that initiate and maintain the growth reaction. However, this growth phenomenon appears to optimize the length of VA-SWNTs grown at the optimum range of flow rate (225 sccm) revealing that pressure may only ensure the supply of right amount of constituent atoms to some extent. The main influences that flow rate has on the growth phenomenon are ensuring the optimum compensation of reaction constituents to the depleted stoichiometry in the vicinity of the catalyst location and guaranteeing the right amount of momentum these atoms have.

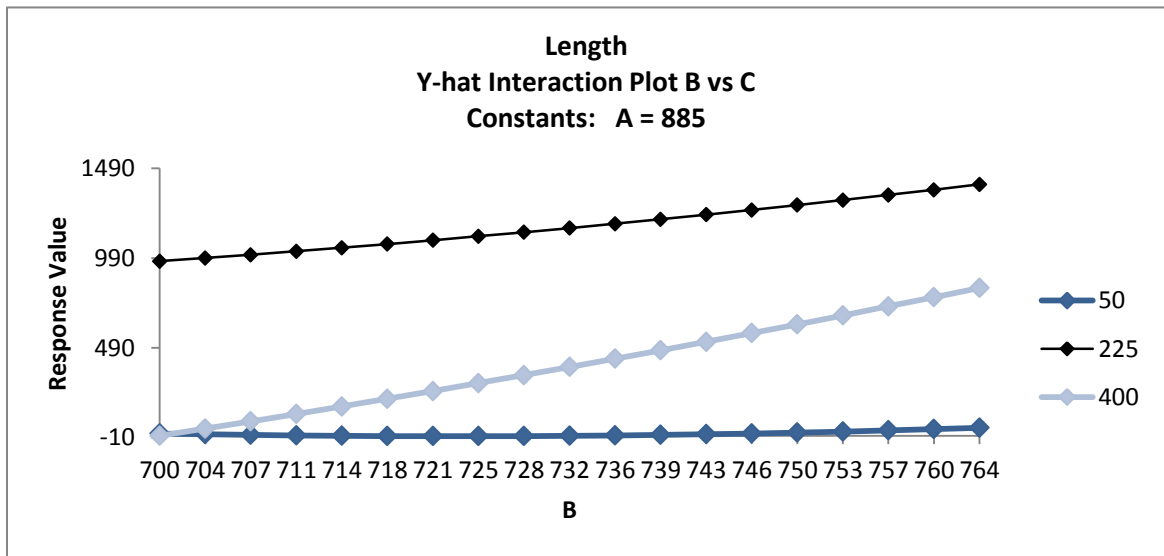


Figure 5.6 Main effect plots for VA-SWNTs length of pressure and flow

5.5 General Response Surface Plot

A. Response Surface (Length versus Flow and Pressure)

A further deeper and concise insight in the growth mechanism can be attained by analyzing the response surface between chamber pressure and flow rate and the length of the VA-SWNTs as shown in the Figure 5.7. The minimum and maximum values of the chamber pressure are not significant in terms of the concentrating effect they may have on the flowing mixture of gases with very small flow rate, i.e., 50 sccm. Similarly, at the highest flow rate values in the training data, i.e., 400 sccm stepping the chamber pressure up to 764 Torr can support the growth reaction to the extent that the resultant VA-SWNTs length of 900 μm can be achieved as explained in Figure 10. However, the two level effect of the flow rate can optimize the length to 990 μm and $\approx 1390 \mu\text{m}$ at 700 Torr and 764 Torr respectively.

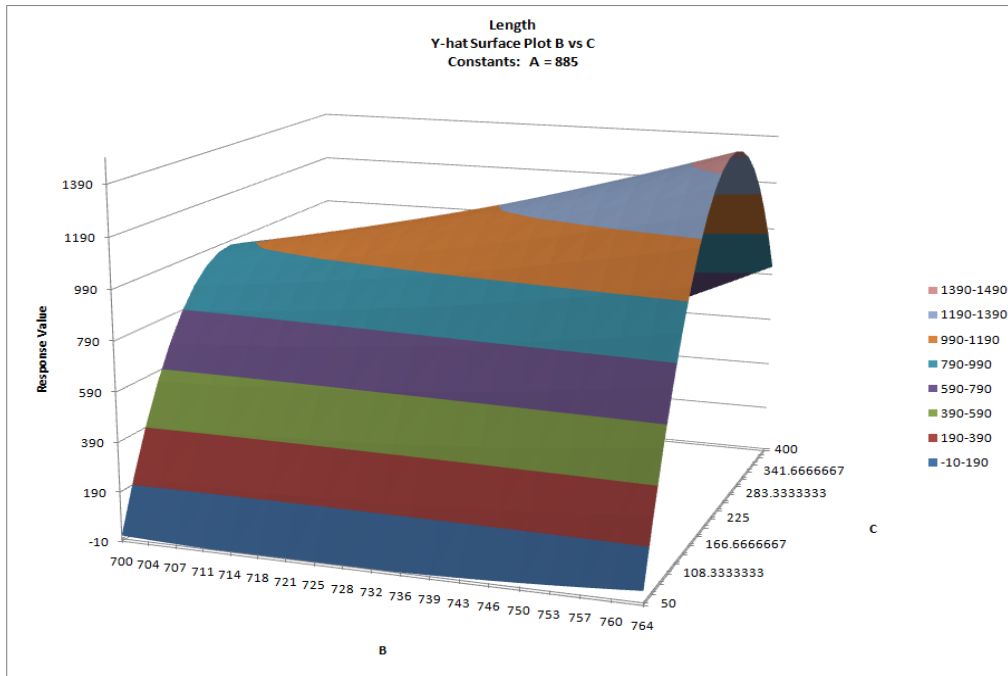


Figure 5.7 Response surface plot of VA-SWNTs length VS flow rate VS pressure

B. Response Surface (Length w.r.t Flow and Temperature)

In order to further test the theory of effect of momentum on the van der Waals forces that ensure the stiction of incoming constituent atoms at the cobalt location, we investigated the impact of temperature on the flow of the gases in the chamber even though the temperature turned out to be the relatively insignificant variable in the Pareto of coefficients (Figure 5.4). Figure 5.7 is the response surface of the length w.r.t flow and temperature at the mid setting of the pressure of constituent gases in the chamber, i.e., 732 Torr. Figure 5.8 is the

main effect plot of the two control variables in order to elaborate the significance of impact of temperature on flow of constituents along the hidden edge of the response surface in Figure 5.9. As anticipated, the impact of temperature on the dominant nonlinear flow rate is minimum at the optimum flow rate, i.e., 225 sccm. However, its impact is magnified where the a large amount of constituents is arriving at the cobalt locations with already too high momentum and the temperature only adds to the volatility of the saturation condition of the supply of constituents.

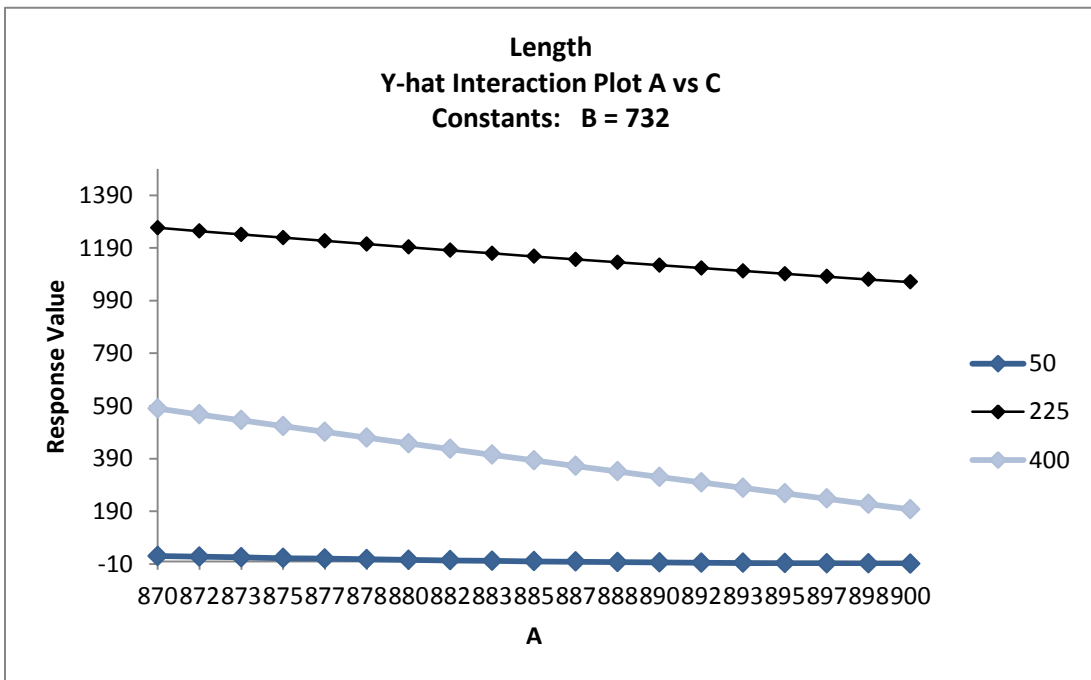
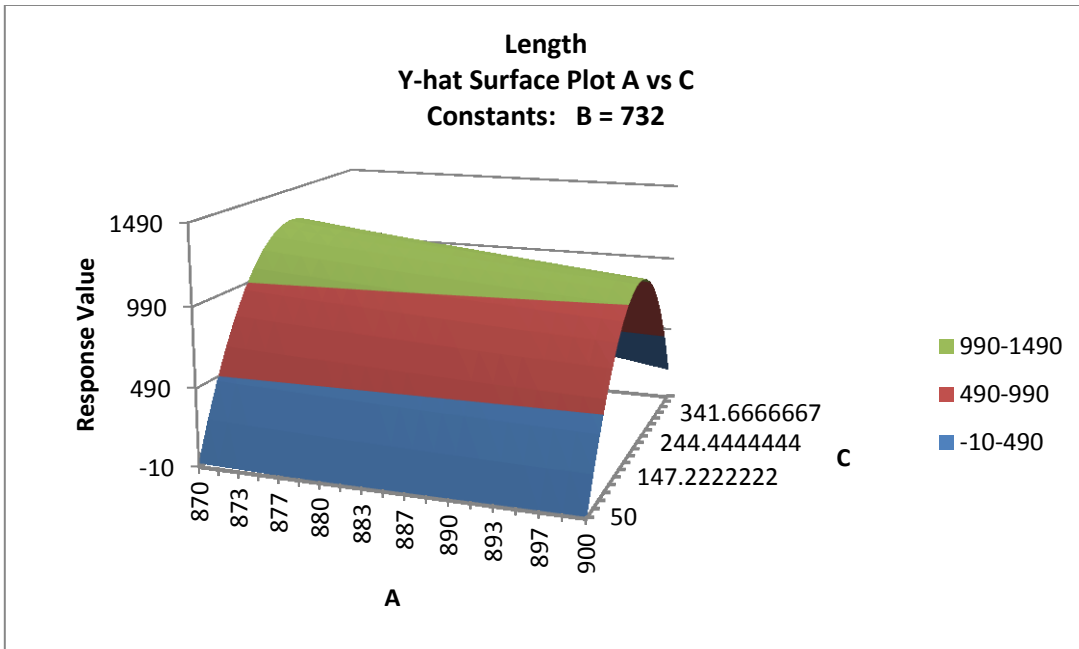


Figure 5.8 Main effect plots for VA-SWNTs length of temperature and flow



**Figure 5.9 Response surface plot of VA-SWNTs length VS flow rate VS
temperature**

6. Process Design for CVD Flow

This chapter discusses in depth the relation between the gas flow and time. The methodology employed [26] has two phases and somewhat similar to the one employed in the previous chapter.

As shown in Figure 6.1 R^2 value of 0.8 for the network architecture with two input nodes, 12 hidden nodes and one output node renders it as a better meta-model for the process with the available data on hand (See Appendix D). Once the best available process meta-model is selected, we used a full factorial design of experiments to design a set of computer experiments for each record for studying the details of process behavior. We compute t_0 for the VA-SWNTs length and find it to be $t_0 = 0.17$. So, the value of $|t_0| < t_{0.025} = 1.98$. On this basis, we decide that there is no statistical evidence to say that the behavior of the metamodel is different from that of the actual process with 97.25% confidence level.

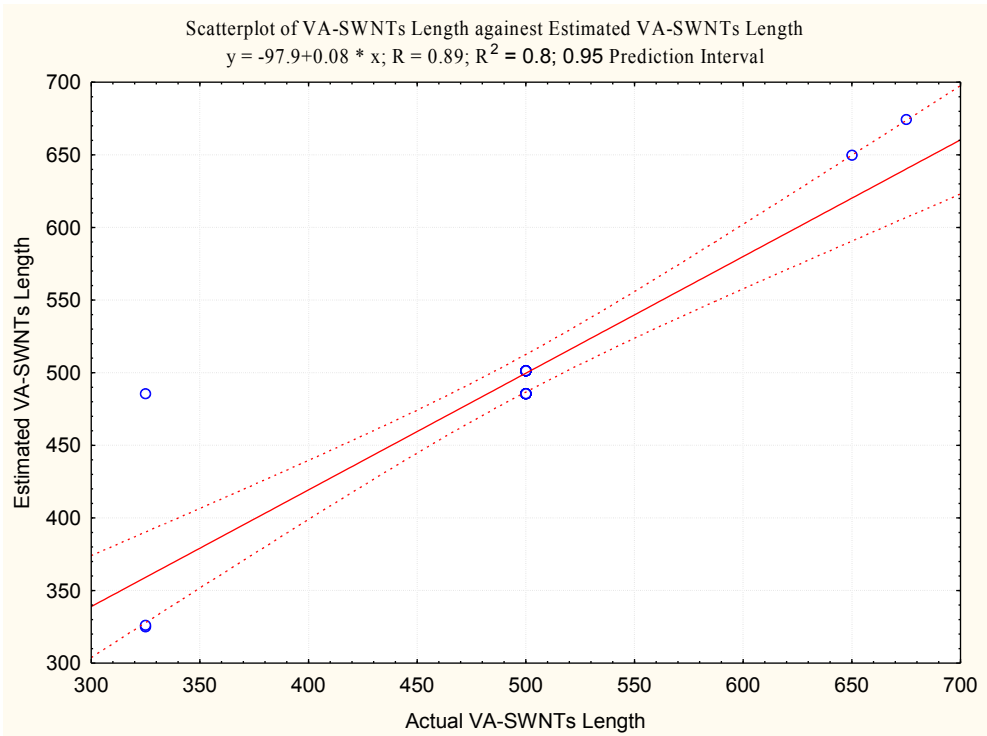


Figure 6.1 VA-SWNTs length (target) versus estimated VA-SWNTs length (output) regressions graph for the MLP 2-12-1 network

The following are the steps to construct the computer model:

- Eliminate experimental data records with missing data.
- Normalize the values of each process control variable in $[0, 1]$ range. This transformation brings all control variables into the same numerical range to give equal weight to each variable in clustering process described below.
- Using the records retained in the previous step, train the neural networks for estimating the performance variables; given that control variable vectors

are most likely positioned densely in the input space, the neural networks are likely to learn the mapping between process inputs and outputs accurately.

- Compute the estimation errors, i.e., the paired differences between the actual process outputs and neural-network-estimated process responses.
- Using the records retained in the previous step, retrain the neural networks for estimating the process outputs; these trained neural networks serves as computer models of the MBE process.
- Compute the paired difference between the actual process outputs and the neural-network estimated process responses.
- Conduct the t -test on paired differences with a level of significance, say $\alpha = 0.05$ (this can be tightened or relaxed if necessary). $H_0: \mu_d = 0$ and $H_1: \mu_d > 0$, where μ_d is the mean of the paired differences. Compute t_0 , the t -statistic for the paired difference. If $|t_0| > t_{\alpha/2}$ then reject H_0 ; otherwise we fail to reject H_0 , which would mean that statistically we do not have evidence to the effect that the behavior of the meta model is different from that of the actual process.

Design of Experiment Phase

After building the multi-layer perceptron based process metamodel, we perform a design of experiment study. The following steps are used to conduct the study.

- Find the min-, mid- and max-points of each input variable for the records used in training the neural networks in phase 1.
- Create the three level settings for the DOE using the min-, med-, and max-points of the input variables.
- Conduct DOE analysis using the DOE runs.
- We started with 42 records of VA-SWNTs growth using the experimental setup described in chapter 3. First, we eliminated records with errors in measurements and missing data. This brought down the number of available records to 25 samples.

Using the boundaries of the final input space, we determine minimum, medium, and maximum values for each of the four input variables. Table 1 shows the min, mid, and max values of the records used for the analysis.

Table 6.1 Experimental records of the CVD process input and output variables

Variable	Min	Mid	Max
Growth Time (min)	5	32	60
Gas Flow Rate (Torr)	20	85	150

6.1 Pareto Chart Analysis

The comparison of significance of control variables, their quadratic effects, and or their paired interactions is presented in Pareto and the coefficients of regression Figure 6.2. The most significant of the variables is the quadratic effect of the time and gas flow in the chamber during growth.

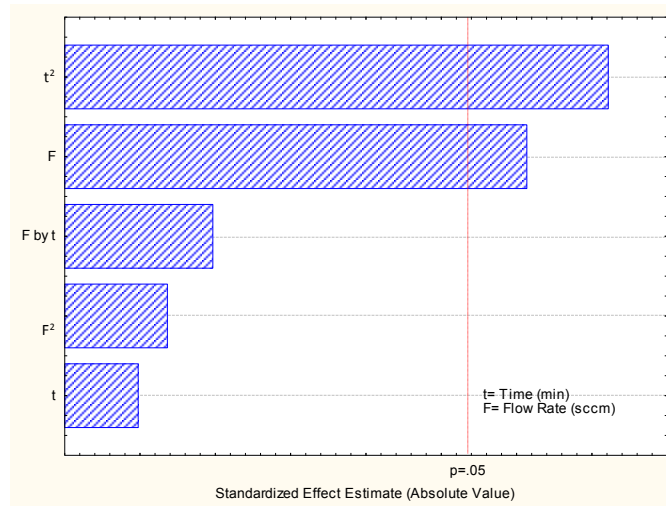


Figure 6.2 Process Pareto analysis

6.2 Comparison of Main Effects Plots

In order to investigate the details of interaction between growth time and gas flow we performed the main effects analysis on this interaction. Figure 6.3 shows the interaction plots for the length of VA-SWNTs with respect to the process input variables, namely, time and flow rate. The sensitivity trends of growth time, which directly relates to the availability of gases for growth reaction at min, mid, and max values of net flow rate of the gases, indicate towards the details of nature of time low level effect of the flow rate on the length of the VA-SWNTs.

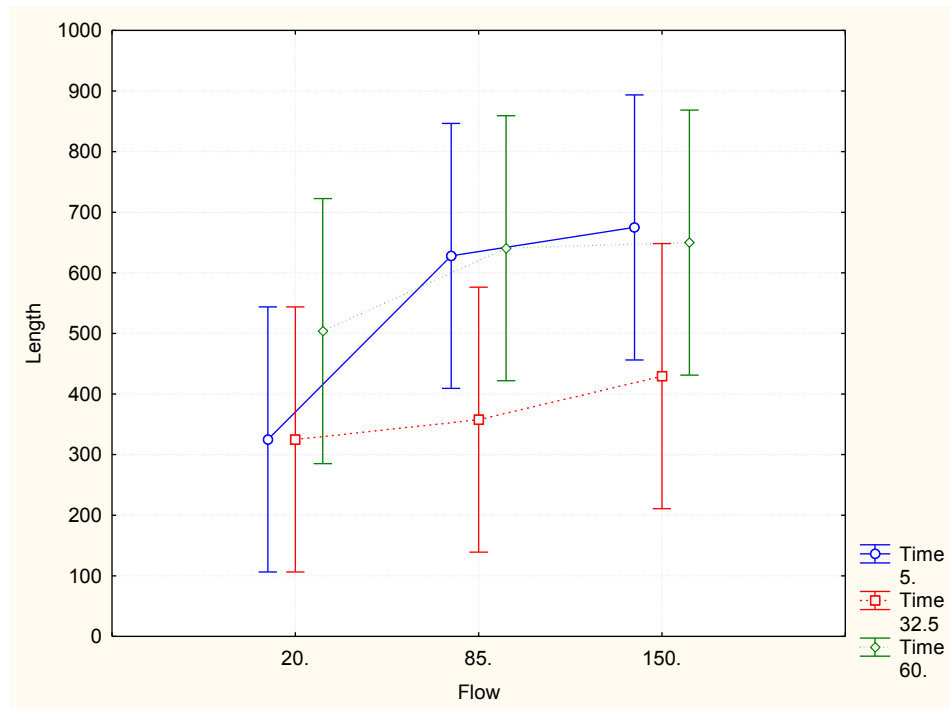


Figure 6.3 Main effect plots for VA-SWNTs length of time and flow

6.3 General Response Surface Plot

A further deeper and concise insight in the growth mechanism can be attained by analyzing the response surface between growth time and flow rate and the length of the VA-SWNTs as shown in the Figure 6.4. The minimum and maximum values of the growth time are not significant in terms of the concentrating effect they may have on the flowing mixture of gases with flow rate. Higher VA-SWNTs length will be achieved at less than 20 minute and flow rate fewer than 150 sccm. This would be suitable for repeatedly producing medium length VA-SWNTs.

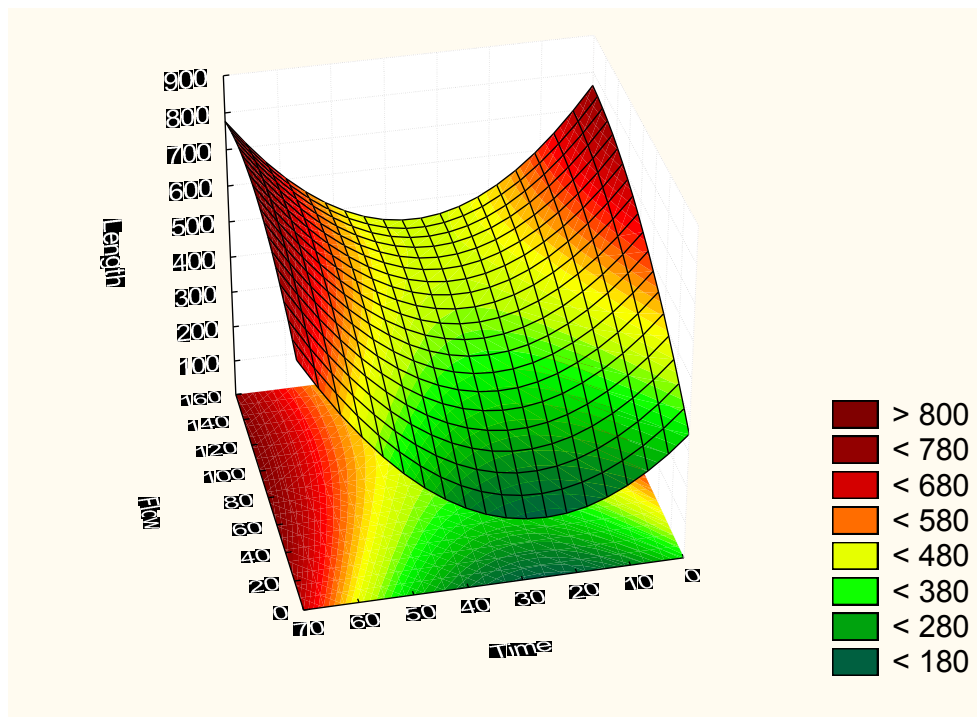


Figure 6.4 Response surface plot of VA-SWNTs length VS flow rate VS time

7. Scientific Formulation of the Process Input

Variables

Previous chapters discuss the CVD grown VA-SWNTs input and output variables. In addition, they discuss which of them are most significant for the controllability or the length assurance. We used the pressure gauge to check the reliability of the pressure sensor during the growth time. We found that the pressure sensor is slightly fluctuating. Therefore, an investigation of the fluctuating was performed to Figure out if the setup value is a good representative of the CVD pressure. The following Figure 7.1 shows that the pressure average of two 30 minutes runs. From figure it is clear that the fluctuation is between 680 torr and 730 torr for a setup value of 700 torr. This mean that we can approximate the pressure by its setup value. Therefore, we used the setup value as a measure of the CVD pressure. The exact values observed for the two runs are shown in appendix E.

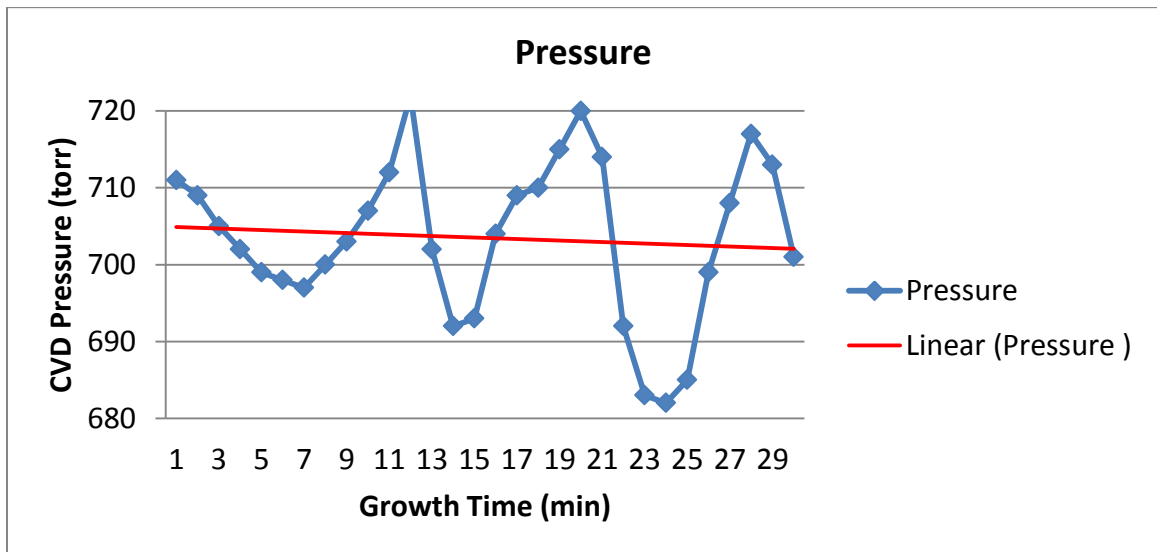
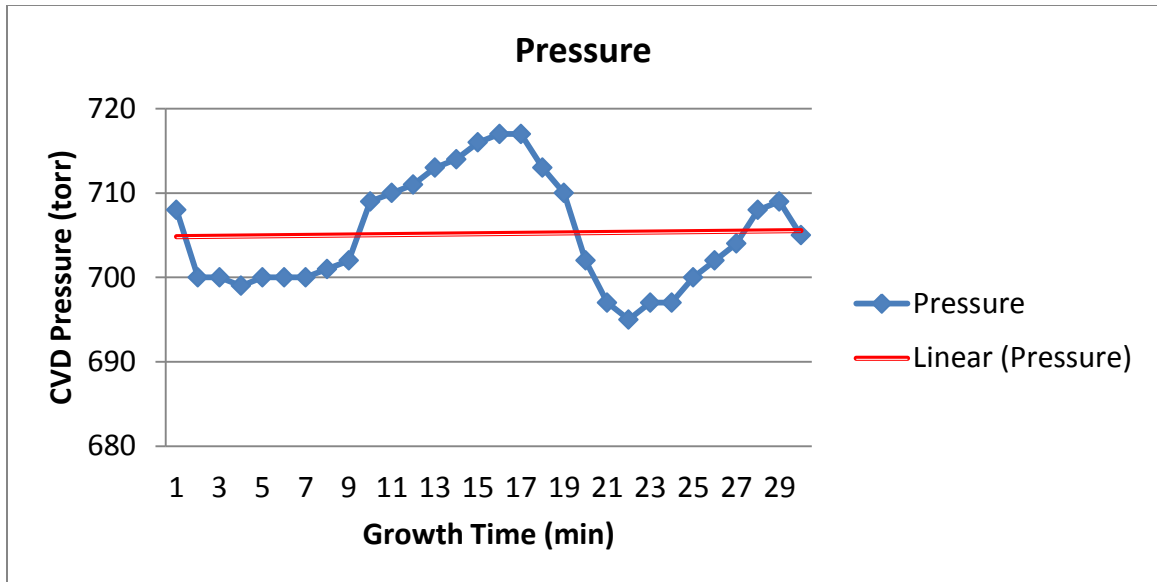


Figure 7.1 First and second runs graphs to measure the stability of pressure sensor during VA-SWNTs growth time (average = 705.2 torr, 703.5 torr)

Based on the plots of marginal means, interactions, and response surfaces the overall relationship between the VA-SWNTs controllability and length with the four controlled inputs can be iterated as follows:

For Controllability

$$\text{VA-SWNTs} \propto F \quad (7.1)$$

$$\text{VA-SWNTs} \propto P \quad (7.2)$$

$$\text{VA-SWNTs} \propto 1 / T \quad (7.3)$$

$$\text{VA-SWNTs} \propto t \quad (7.4)$$

For Length Assurance

$$\text{VA-SWNTs } L \propto F^2 \quad (7.5)$$

$$\text{VA-SWNTs } L \propto P \quad (7.6)$$

$$\text{VA-SWNTs } L \propto 1/ T \quad (7.7)$$

$$\text{VA-SWNTs } L \propto t \quad (7.8)$$

Where F = flow rate, P = pressure, T= temperature and L= length and t= time.

They can be combined to represent an aggregated relationship as:

For Controllability

$$\text{VA-SWNTs} \propto F * P / T \quad (7.9)$$

For Length Assurance

$$L \propto F^2 * P / T \quad (7.10)$$

7.1 Ideal Gas Law

We can derive an approximate equation from the Ideal Gas Law formula [52].

That law is part of the thermodynamics theory relating pressure, temperature, and volume.

$$P * Vol = n * R_u * T \quad (7.11)$$

Where R_u = specific gas constant , Vol = volume of gases, and n = chemical amount of gases. Since volume is the multiplication between flow and cross sectional area of the system (A).

$$Vol = F * A \quad (7.12)$$

Substituting all the values, we get the following formula:

$$P * F * A = n * R_u * T \quad (7.13)$$

Assuming that n and R_u divided by A is proportional to the desired output, we rewrite it as:

$$P * F / T = n * R_u / A \quad (7.14)$$

Figure 7.1 shows the slight correlation between controllability of VA-SWNTs and the above formulation extracted from the ideal gas law.

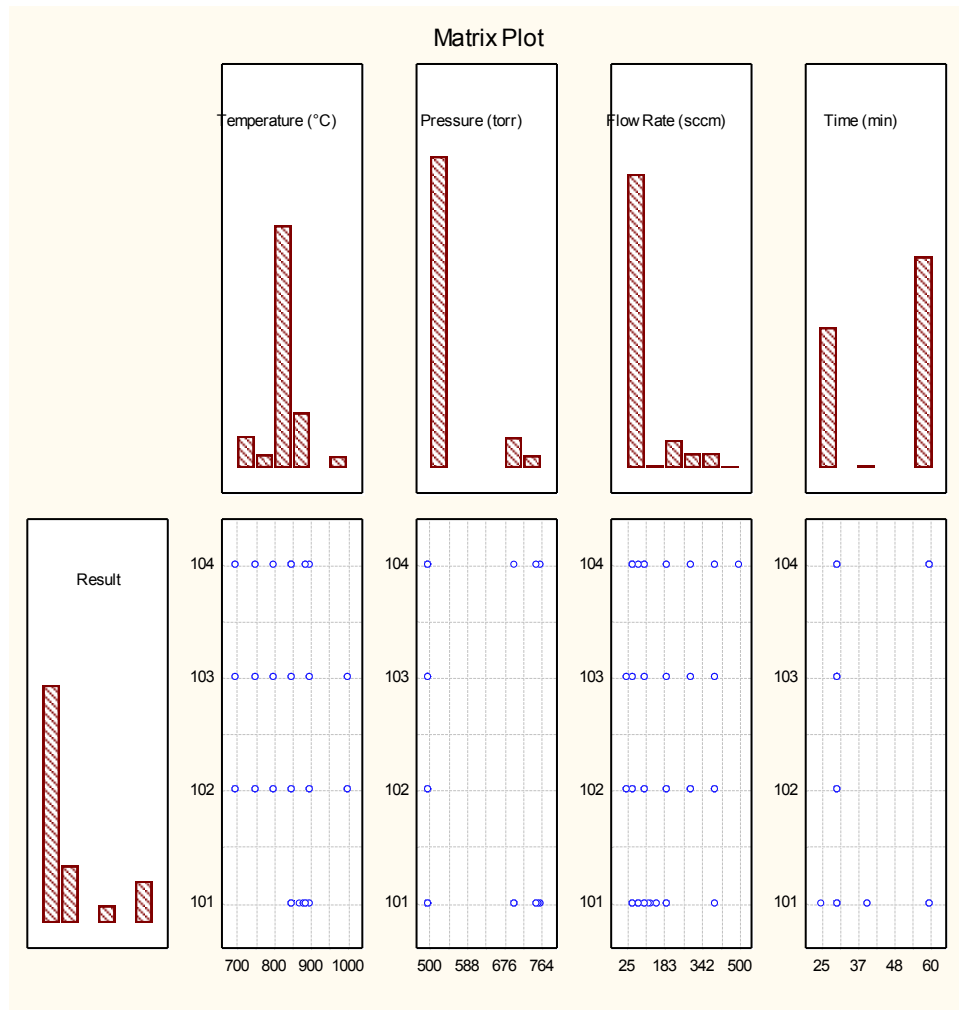


Figure 7.2 Matrix plots between flow, temperature and pressure for VA-SWNTS (101 = VA-SWNTs, 102 = MWNTs, 103 = MWNTs & SWNTs, 104 = None)

This refers to a possibility of relationship between the macro scale physical quantity of the gases in the CVD chamber and quantum level phenomenon. Our detailed designed experimental studies corroborated this hypothesis,

which explains the physics of the growth process for customization chamber designs for high rate manufacturing.

7.2 Dynamic Pressure

An approximate equation from the formula of Bernoulli dynamic (P_d) pressure can be derived for the VA-SWNTs length assurance [52]. Since, dynamic pressure is part of the Bernoulli theory relating pressure and velocity.

$$P_d = \frac{1}{2} * \gamma * \rho * V^2 \quad (7.15)$$

Where γ = heat capacity ratio, and M is the Mach number ($M = v/a$), a = speed of sound.

$$M = V / a, \quad a = (R * T * \gamma)^{1/2} \quad (7.16)$$

Since velocity is the ratio between flow and cross sectional area of the system.

$$V = F / A \quad (7.17)$$

Substituting all the values, we get the following formula.

$$P_d = (1 / 2 * A^2 * R) F^2 * \rho / T \quad (7.18)$$

Assuming that half of squared area multiplied by the specific gas constant to be a constant term (K) for the process, we rewrite it as

$$P_d = K * F^2 * \rho / T \quad (7.19)$$

Figure 7.3 shows an approximate linear relationship between length of VA-SWNTs and the dynamic pressure with an offsetting constant K.

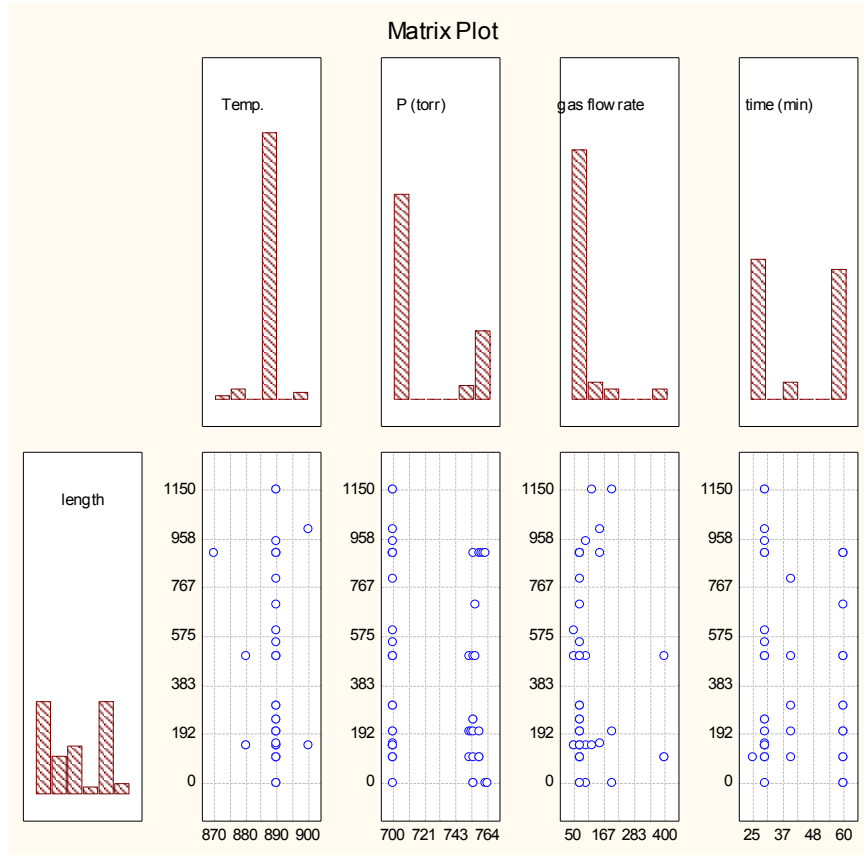


Figure 7.3 Interaction plots between temperature and pressure for VA-SWNTs

This relation refers to a possibility of relationship between the macro scale physical quantity, i.e., dynamic pressure of the gases in the CVD chamber and quantum level phenomenon of CVD growth reaction at selected catalyst sites on the substrate. Detailed and carefully designed experimental studies are

required to validate this hypothesis, which if validated, can simplify the physics of the growth process for customizing chamber designs for high rate manufacturing. Table 7.1 summaries this chapter recommended input ranges with the main two goals (controllability and length assurance) and the four inputs.

Table 7.1 Process inputs combinations based on the desired output

Inputs ranges	Gas flow rate (sccm)	CVD pressure (torr)	CVD temperature (°c)	Growth time (min)
VA-SWNTs controllability	25-500	500-764	700-1000	25-60
Recommended VA-SWNTs controllability	50-400	632-764	800-920	40-60
VA-SWNTs length	50-400	700-764	870-900	25-60
Recommended VA-SWNTs length	150	700	880	60

8. Conclusion and Future Work

In summary, this dissertation shows that VA-SWNTs mass production is a multidisciplinary research area requiring collaboration between nanoscience and nanomanufacturing. Generally, there are many variables influencing the CVD process. In the preceding chapters, several questions were raised on the VA-SWNTs growth input factors role. We found that, carbon flow rate, furnace temperature, CVD pressure, and growth time are the most influential factors. In addition, the study discusses some exercises of applying models of ANN and DOE to help understand the nanotubes growth mechanism.

The start of VA-SWNTs growth mechanism is an area that requires further investigation. We found that CVD pressure and its interaction with the CVD temperature have the most significant influence on the controllability of VA-SWNTs. In addition, higher temperature with elevated pressure will produce higher yield of VA-SWNTs.

In addition, we found that CVD pressure and its interaction with the CVD flow have the most significant influence on the VA-SWNTs length. Higher flow with depressed pressure will produce taller VA-SWNTs. Dynamic pressure equation drawn from Bernoulli equation showed that dynamic pressure at

macro level might be, directly, related to molecular level growth reaction of VA-SWNT and helps simplify the understanding of control parameters of the process.

In addition to the previous discussion, future research related challenges are briefly outlined below.

1. Control the catalyst particle diameter to control the VA-SWNTs diameter.
2. Determine the VA-SWNTs physical, chemical, electronic, and optical properties of each catalyst used in growing the nanotubes and research the visibility of building devices like nanomembrane for water desalination and photovoltaic cells for solar energy.
3. Figure out the nucleation crucial steps to help decide what is significant for mass production.
4. Investigate the growth mechanism at room temperature to lower the cost of CVD process.
5. Eliminate or mitigate the impurities from the catalyst or support materials.
6. Employ the recent technologies in Quality Engineering to and standardized them among nanotechnology fields.

References

- [1] Tanaka K., Yamabe T., and Fukui K., 1999, The science and technology of carbon nanotubes, Elsevier.
- [2] Hosokawa M., 2007, Nanoparticle technology handbook, Elsevier Science Ltd.
- [3] Board E., 2006, Understanding Carbon Nanotubes, Springer Berlin Heidelberg.
- [4] Jorio A., Dresselhaus G., and Dresselhaus M. S., 2008, Carbon nanotubes: Advanced topics in the synthesis, structure, properties and applications, Springer.
- [5] Dresselhaus M., 2001, “Carbon nanotubes: Synthesis, structure, properties, and applications.”
- [6] Hata K., Futaba D., and Mizuno K., 2004, “Water-assisted highly efficient synthesis of impurity-free single-walled carbon nanotubes,” Science.
- [7] Oconnell M. J., 2006, Carbon nanotubes: properties and applications, CRC press.

- [8] Yuangyai C., and Nembhard H. B., 2009, "Design of Experiments: A Key to Innovation in Nanotechnology," *Emerging Nanotechnologies for Manufacturing*, Elsevier Inc., pp. 207-234.
- [9] Busnaina A. A., 2007, *Nanomanufacturing handbook*, CRC Press/Taylor & Francis.
- [10] Iijima S., 1991, "Helical microtubules of graphitic carbon," *Nature*.
- [11] Harris P., 2007, "Solid state growth mechanisms for carbon nanotubes," *Carbon*.
- [12] Li X., 2008, "Tailoring vertically aligned carbon nanotube growth and fabrication of carbon nanotube membrane filters," RPI.
- [13] Dresselhaus, M.S. , Dresselhaus, G. and Avouris P., 2004, "Carbon nanotubes," *MRS Bulletin*, 33(7), p. 237.
- [14] Li W., Xie S., Qian L., and Chang B., 1996, "Large-scale synthesis of aligned carbon nanotubes," *Science*.
- [15] Murakami Y., 2004, "Growth of vertically aligned single-walled carbon nanotube films on quartz substrates and their optical anisotropy," *Chemical Physics Letters*, 385(3-4), pp. 298-303.

- [16] Miller G. P., 2007, Carbon Nanotubes, Properties and Applications. CRC Press and Taylor & Francis Group: Boca Raton, FL. 2006.
- [17] Klabunde K. J., Richards R., 2009, Nanoscale materials in chemistry, Wiley Online Library.
- [18] Majumder M., Chopra N., and Hinds B. J., 2011, “Mass transport through carbon nanotube membranes in three different regimes: Ionic diffusion and gas and liquid flow.,” ACS nano, 5(5), pp. 3867-77.
- [19] Majumder M., Stinchcomb A., and Hinds B. J., 2010, “Towards mimicking natural protein channels with aligned carbon nanotube membranes for active drug delivery.,” Life Sciences, 86(15-16), pp. 563-8.
- [20] Zhao Y., Hu Y., Li Y., Zhang H., Zhang S., Qu L., Shi G., and Dai L., 2010, “Super-long aligned TiO₂/carbon nanotube arrays.,” Nanotechnology, 21(50), p. 505702.
- [21] Kohonen T., 2001, Self-organizing maps, Springer.
- [22] Desai S., Mohan R., Sankar J., and Tiano T., 2008, “Understanding conductivity in a composite resin with Single Wall Carbon Nanotubes (SWCNTs) using design of experiments,” International Journal of Nanomanufacturing, 2(4), pp. 292–304.

- [23] Kukovecz a, Mehn D., Nemesnagy E., Szabo R., and Kiricsi I., 2005, "Optimization of CCVD synthesis conditions for single-wall carbon nanotubes by statistical design of experiments (DoE)," *Carbon*, 43(14), pp. 2842-2849.
- [24] Yang Y., York J. D., Xu J., Lim S., Chen Y., and Haller G. L., 2005, "Statistical design of C10-Co-MCM-41 catalytic template for synthesizing smaller-diameter single-wall carbon nanotubes," *Microporous and Mesoporous Materials*, 86(1-3), pp. 303-313.
- [25] Yang Y., Lim S., Wang C., Du G., and Haller G. L., 2004, "Statistical analysis of synthesis of Co-MCM-41 catalysts for production of aligned single walled carbon nanotubes (SWNT)," *Microporous and Mesoporous Materials*, 74(1-3), pp. 133-141.
- [26] Haykin S., 2009, *Neural networks and learning machines*, Pearson.
- [27] Barker T., 1994, "Quality by experimental design". CRC
- [28] Bourgeois, J., Kravchenko, M., Parsons N., 2010, "Design of experiments via factorial designs - ControlsWiki." https://controls.engin.umich.edu/wiki/index.php/Design_of_experiments_via_factorial_designs

- [29] Jahanshahi M., Jahan-Bakhsh R., Solmaz H., and Razieh J., 2007, "Application of Taguchi Method in the Optimization of ARC-Carbon Nanotube Fabrication," AIP Conference Proceedings, p. 77.
- [30] Liu X., and Wong D. K. Y., 2007, "Electrocatalytic detection of estradiol at a carbon nanotube|Ni(Cyclam) composite electrode fabricated based on a two-factorial design.," *Analytica chimica acta*, 594(2), pp. 184-91.
- [31] Nourbakhsh A., Ganjipour B., Zahedifar M., and Arzi E., 2007, "Morphology optimization of CCVD-synthesized multiwall carbon nanotubes, using statistical design of experiments," *Nanotechnology*, 18(11), p. 115715.
- [32] Luo F., 2008, "Application of Tagushi Method in the Optimization of ARC Carbon Nanotube Fabrication," *Biotechnology Letters*, 31(4), pp. 221-649.
- [33] Cotasanchez G., Soucy G., Huczko A., and Lange H., 2005, "Induction plasma synthesis of fullerenes and nanotubes using carbon black–nickel particles," *Carbon*, 43(15), pp. 3153-3166.
- [34] Maultzsch J., and Thomsen C., 2008, "Characterization of Carbon Nanotubes by Optical Spectroscopy," *Carbon*, 8.

- [35] Jeng S. L., Lu J. C., and Wang K., 2007, "A review of reliability research on nanotechnology," *IEEE Transactions on Reliability*, 56(3), pp. 401–410.
- [36] See C. H., and Harris A. T., 2007, "A Review of Carbon Nanotube Synthesis via Fluidized-Bed Chemical Vapor Deposition," *Industrial & Engineering Chemistry Research*, 46(4), pp. 997-1012.
- [37] Darsono N., Kwon S.-W., Yoon D.-H., Kim J., Moon H., and Park S.-U., 2007, "Field emission properties of carbon nanotube pastes examined using design of experiments," *Journal of Materials Science: Materials in Electronics*, 19(1), pp. 17-23.
- [38] Maheshwar S., Apte P., Purandare S., and Renju Z., 2005, "Application of the Taguchi Analytical Method for Optimization of Effective Parameters of the Chemical Vapor Deposition Process Controlling the Production of Nanotubes/Nanobeads," *Journal of Nanoscience and Nanotechnology*, 5(2), pp. 288–295.
- [39] Lu J.-C., Jeng, Shuen-Lin J., Kaibo W., And Jye-Chyi L. U. S. L. I. N. J., 2009, "A Review of Statistical Methods for Quality Improvement and Control in Nanotechnology," *Journal of Quality Technology*, 41(2).
- [40] Lin T.-S., Wu C.-F., and Hsieh C.-T., 2006, "Improvement on superhydrophobic behavior of carbon nanofibers via the design of experiment and analysis of variance,"

Journal of Vacuum Science & Technology B: Microelectronics and Nanometer Structures, 24(2), p. 855.

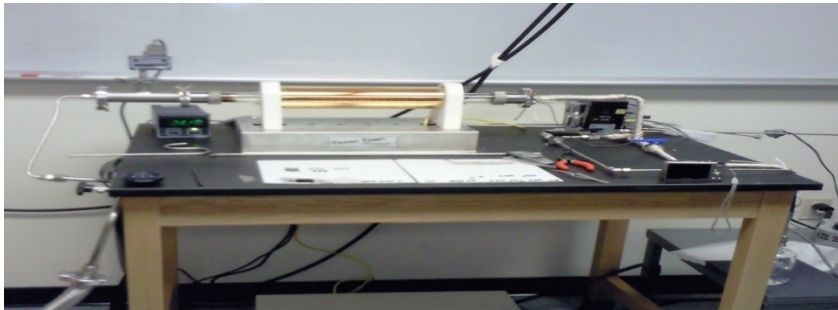
- [41] Hou T.-H., Su C.-H., and Liu W.-L., 2007, "Parameters optimization of a nano-particle wet milling process using the Taguchi method, response surface method and genetic algorithm," Powder Technology, 173(3), pp. 153-162.
- [42] Nembhard H. B., 2007, "Nanotechnology : A Big Little Frontier For Quality," Quality Progress, (July), pp. 23-29.
- [43] Ting J., Chang C., Chen S., Lu D., Kung C., and Huang F., 2006, "Optimization of field emission properties of carbon nanotubes by Taguchi method," Thin Solid Films, 496(2), pp. 299-305.
- [44] Kuo C. C. S., Bai A., Huang C. C. M., Li Y. Y. Y., Hu C. C., and Chen C. C., 2005, "Diameter control of multiwalled carbon nanotubes using experimental strategies," Carbon, 43(13), pp. 2760–2768.
- [45] Hahm M., Kwon Y., and Busnaina A., 2011, "Structure Controlled Synthesis of Vertically Aligned Carbon Nanotubes Using Thermal Chemical Vapor Deposition Process," Journal of Heat Transfer, 133(3), p. 31001-31004.

- [46] Hahm M. G., Kwon Y.-K., Lee E., Ahn C. W., and Jung Y. J., 2008, "Diameter Selective Growth of Vertically Aligned Single Walled Carbon Nanotubes and Study on Their Growth Mechanism," *Journal of Physical Chemistry C*, 112(44), pp. 17143-17147.
- [47] Abuhimd H., Zeid A., Jung Y.G., Kamarthi S. K., 2011, "Process design for the controllability of chemical vapor deposition grown Vertically Aligned Single Walled Carbon Nanotubes," *IMECE* 2011.
- [48] Abuhimd H., Zeid A., Jung Y.G., Kamarthi S. K., Uddin G. M., 2011, "Chemical Vapor Deposition grown Vertically Aligned Single Walled Carbon Nanotubes Length Assurance," *The International Journal of Advanced Manufacturing Technology*, (Special Issue).
- [49] Uddin G. M., Cai Z., Ziemer K. S., Zeid A., and Kamarthi S., 2010, "Analysis of Molecular Beam Epitaxy Process for Growing Nanoscale Magnesium Oxide Films," *Journal of Manufacturing Science and Engineering*, 132(3), p. 030913.
- [50] Dasgupta T., Weintraub B., and Joseph V. R., 2011, "A physical–statistical model for density control of nanowires," *IIE Transactions*, 43(4), pp. 233-241.
- [51] Haykin S., 2009, *Neural networks and learning machines*, Prentice Hall.

[52] Liepmann H. W., and Roshko A., 1957, Elements of gasdynamics, Courier Dover Publications.

Appendix A

Set of pictures showing CVD experimental setup (courtesy Prof. Jung's Research Group)



whole CVD system



heat source and temperature



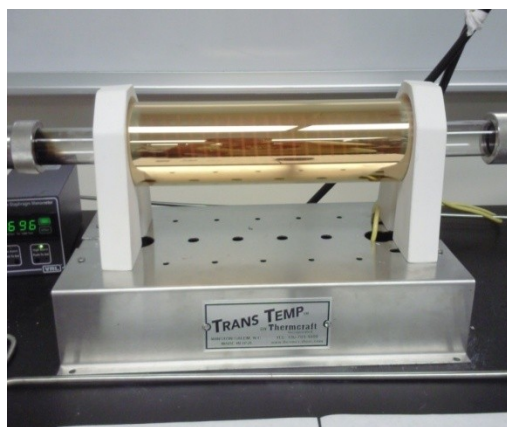
pressure machine



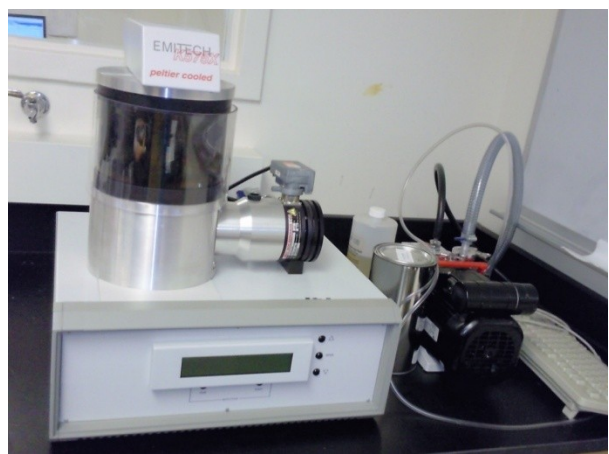
gases locker



ethanol bubbler

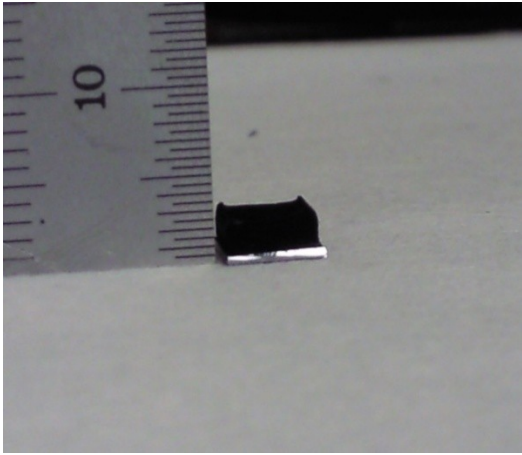
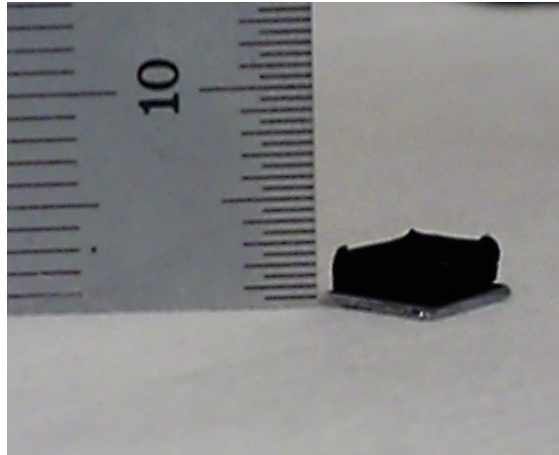
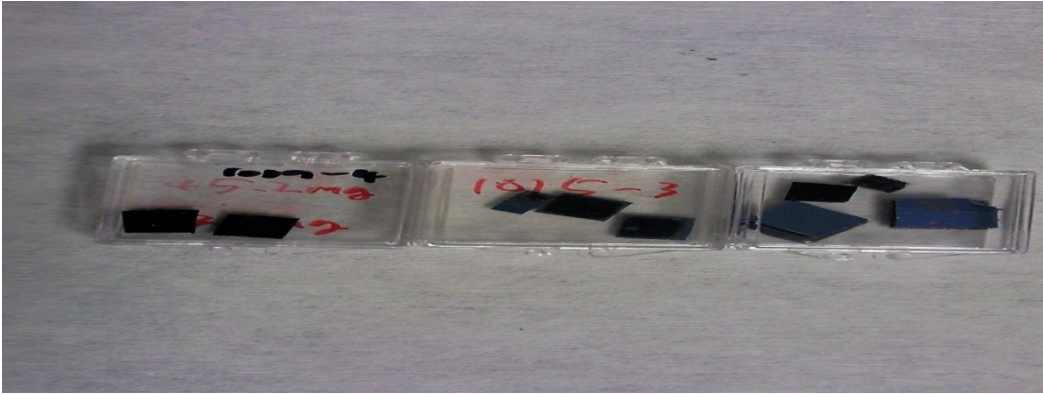


gold plated furnace(inner diameter
1.26 inch and length 24 inches)



catalyst sputter

Samples of VA-SWNTs pictures (courtesy Prof. Jung's Research Group)

	
<p>Picture of VA-SWNTs shown from side</p>	<p>Picture of VA-SWNTs shown from oblique view</p>
	
<p>Set of samples view from top</p>	

850	500	50	30	VA-SWNT
850	500	50	30	VA-SWNT
850	500	50	30	VA-SWNT
850	500	50	30	VA-SWNT
850	500	50	30	VA-SWNT
850	500	50	30	VA-SWNT
850	500	50	30	VA-SWNT
850	500	50	30	VA-SWNT
850	500	50	30	VA-SWNT
850	500	50	30	VA-SWNT
850	500	50	30	VA-SWNT
850	500	50	30	VA-SWNT
850	500	50	30	VA-SWNT
850	500	50	30	VA-SWNT
850	500	50	30	VA-SWNT
850	500	50	30	VA-SWNT
850	500	50	30	VA-SWNT
890	754	75	25	VA-SWNT
1000	500	400	30	Small amount of MWNT
1000	500	400	30	Small amount of MWNT
900	500	400	30	Small amount of MWNT
900	500	400	30	Small amount of MWNT
850	500	400	30	Small amount of MWNT
850	500	400	30	Small amount of MWNT
850	500	400	30	Small amount of MWNT
800	500	400	30	Small amount of MWNT
800	500	400	30	Small amount of MWNT
800	500	400	30	Small amount of MWNT
750	500	400	30	Small amount of MWNT
750	500	400	30	Small amount of MWNT
750	500	400	30	Small amount of MWNT
700	500	400	30	Small amount of MWNT
700	500	400	30	Small amount of MWNT
700	500	400	30	Small amount of MWNT

700	500	400	30	Small amount of MWNT
1000	500	300	30	Small amount of MWNT
1000	500	300	30	Small amount of MWNT
1000	500	300	30	Small amount of MWNT
900	500	300	30	Small amount of MWNT
900	500	300	30	Small amount of MWNT
900	500	300	30	Small amount of MWNT
850	500	300	30	Small amount of MWNT
850	500	300	30	Small amount of MWNT
850	500	300	30	Small amount of MWNT
800	500	300	30	Small amount of MWNT
800	500	300	30	Small amount of MWNT
800	500	300	30	Small amount of MWNT
750	500	300	30	Small amount of MWNT
750	500	300	30	Small amount of MWNT
750	500	300	30	Small amount of MWNT
700	500	300	30	Small amount of MWNT
700	500	300	30	Small amount of MWNT
700	500	300	30	Small amount of MWNT
700	500	300	30	Small amount of MWNT
700	500	300	30	Small amount of MWNT
1000	500	200	30	Small amount of MWNT
1000	500	200	30	Small amount of MWNT
1000	500	200	30	Small amount of MWNT
900	500	200	30	Small amount of MWNT
900	500	200	30	Small amount of MWNT
900	500	200	30	Small amount of MWNT
850	500	200	30	Small amount of MWNT
850	500	200	30	Small amount of MWNT
850	500	200	30	Small amount of MWNT
800	500	200	30	Small amount of MWNT
800	500	200	30	Small amount of MWNT
800	500	200	30	Small amount of MWNT

750	500	200	30	Small amount of MWNT
750	500	200	30	Small amount of MWNT
750	500	200	30	Small amount of MWNT
700	500	200	30	Small amount of MWNT
700	500	200	30	Small amount of MWNT
700	500	200	30	Small amount of MWNT
700	500	200	30	Small amount of MWNT
700	500	200	30	Small amount of MWNT
700	500	200	30	Small amount of MWNT
1000	500	100	30	Small amount of MWNT
1000	500	100	30	Small amount of MWNT
1000	500	100	30	Small amount of MWNT
900	500	100	30	Small amount of MWNT
900	500	100	30	Small amount of MWNT
900	500	100	30	Small amount of MWNT
850	500	100	30	Small amount of MWNT
850	500	100	30	Small amount of MWNT
850	500	100	30	Small amount of MWNT
800	500	100	30	Small amount of MWNT
800	500	100	30	Small amount of MWNT
800	500	100	30	Small amount of MWNT
750	500	100	30	Small amount of MWNT
750	500	100	30	Small amount of MWNT
750	500	100	30	Small amount of MWNT
700	500	100	30	Small amount of MWNT
700	500	100	30	Small amount of MWNT
700	500	100	30	Small amount of MWNT
700	500	100	30	Small amount of MWNT
1000	500	50	30	Small amount of MWNT
1000	500	50	30	Small amount of MWNT
1000	500	50	30	Small amount of MWNT
900	500	50	30	Small amount of MWNT
900	500	50	30	Small amount of MWNT

900	500	50	30	Small amount of MWNT
850	500	50	30	Small amount of MWNT
850	500	50	30	Small amount of MWNT
850	500	50	30	Small amount of MWNT
800	500	50	30	Small amount of MWNT
800	500	50	30	Small amount of MWNT
800	500	50	30	Small amount of MWNT
750	500	50	30	Small amount of MWNT
750	500	50	30	Small amount of MWNT
750	500	50	30	Small amount of MWNT
700	500	50	30	Small amount of MWNT
700	500	50	30	Small amount of MWNT
700	500	50	30	Small amount of MWNT
1000	500	25	30	Small amount of MWNT
1000	500	25	30	Small amount of MWNT
1000	500	25	30	Small amount of MWNT
900	500	25	30	Small amount of MWNT
900	500	25	30	Small amount of MWNT
900	500	25	30	Small amount of MWNT
850	500	25	30	Small amount of MWNT
850	500	25	30	Small amount of MWNT
850	500	25	30	Small amount of MWNT
800	500	25	30	Small amount of MWNT
800	500	25	30	Small amount of MWNT
800	500	25	30	Small amount of MWNT
750	500	25	30	Small amount of MWNT
750	500	25	30	Small amount of MWNT
750	500	25	30	Small amount of MWNT
700	500	25	30	Small amount of MWNT
700	500	25	30	Small amount of MWNT
700	500	25	30	Small amount of MWNT
1000	500	400	30	S.A of MWNT & SWNT
900	500	400	30	S.A of MWNT & SWNT

850	500	400	30	S.A of MWNT & SWNT
800	500	400	30	S.A of MWNT & SWNT
750	500	400	30	S.A of MWNT & SWNT
1000	500	300	30	S.A of MWNT & SWNT
900	500	300	30	S.A of MWNT & SWNT
850	500	300	30	S.A of MWNT & SWNT
800	500	300	30	S.A of MWNT & SWNT
750	500	300	30	S.A of MWNT & SWNT
1000	500	200	30	S.A of MWNT & SWNT
900	500	200	30	S.A of MWNT & SWNT
850	500	200	30	S.A of MWNT & SWNT
800	500	200	30	S.A of MWNT & SWNT
750	500	200	30	S.A of MWNT & SWNT
700	500	200	30	S.A of MWNT & SWNT
1000	500	100	30	S.A of MWNT & SWNT
900	500	100	30	S.A of MWNT & SWNT
850	500	100	30	S.A of MWNT & SWNT
800	500	100	30	S.A of MWNT & SWNT
750	500	100	30	S.A of MWNT & SWNT
700	500	100	30	S.A of MWNT & SWNT
1000	500	50	30	S.A of MWNT & SWNT
900	500	50	30	S.A of MWNT & SWNT
850	500	50	30	S.A of MWNT & SWNT
800	500	50	30	S.A of MWNT & SWNT
750	500	50	30	S.A of MWNT & SWNT
700	500	50	30	S.A of MWNT & SWNT
1000	500	25	30	S.A of MWNT & SWNT
900	500	25	30	S.A of MWNT & SWNT
850	500	25	30	S.A of MWNT & SWNT
800	500	25	30	S.A of MWNT & SWNT
750	500	25	30	S.A of MWNT & SWNT
700	500	25	30	S.A of MWNT & SWNT
890	755	200	60	none

850	500	50	60	none
850	500	50	60	none
850	500	50	60	none
850	500	50	60	none
850	500	500	30	none
850	500	500	30	none
850	500	400	30	none
850	500	400	30	none
750	500	400	30	none
700	500	400	30	none
850	500	300	30	none
850	500	300	30	none
700	500	300	30	none
850	500	200	30	none
850	500	200	30	none
900	500	100	30	none
900	500	100	30	none
850	500	100	30	none
850	500	100	30	none
850	500	100	30	none
850	500	100	30	none
800	500	100	30	none
800	500	100	30	none
750	500	100	30	none
750	500	100	30	none
750	500	100	30	none
750	500	100	30	none
700	500	100	30	none
700	500	100	30	none
700	500	100	30	none
890	754	75	30	none
850	500	50	30	none
850	500	50	30	none

850	500	50	30	none
850	500	50	30	none
850	500	50	30	none
850	500	50	30	none
850	500	50	30	none
850	500	50	30	none
850	500	50	30	none
850	500	50	30	none
850	500	50	30	none
850	500	50	30	none
850	500	50	30	none
850	500	50	30	none
850	500	50	30	none
850	500	50	30	none
850	500	50	30	none
850	500	50	30	none

DOE Data

Temperature	Pressure	Flow	Time	Result
700	500	50	250	none
700	500	50	420	S.A of MWNT & SWNT
700	500	50	600	none
700	500	225	250	Small amount of MWNT

700	500	225	420	S.A of MWNT & SWNT
700	500	225	600	none
700	500	400	250	Small amount of MWNT
700	500	400	420	S.A of MWNT & SWNT
700	500	400	600	Small amount of MWNT
700	632	50	250	S.A of MWNT & SWNT
700	632	50	420	none
700	632	50	600	none
700	632	225	250	S.A of MWNT & SWNT
700	632	225	420	none
700	632	225	600	none
700	632	400	250	S.A of MWNT & SWNT
700	632	400	420	Small amount of MWNT
700	632	400	600	none
700	764	50	250	none
700	764	50	420	none

700	764	50	600	none
700	764	225	250	none
700	764	225	420	none
700	764	225	600	none
700	764	400	250	none
700	764	400	420	none
700	764	400	600	none
800	500	50	250	Small amount of MWNT
800	500	50	420	S.A of MWNT & SWNT
800	500	50	600	none
800	500	225	250	Small amount of MWNT
800	500	225	420	S.A of MWNT & SWNT
800	500	225	600	none
800	500	400	250	Small amount of MWNT
800	500	400	420	S.A of MWNT & SWNT
800	500	400	600	S.A of MWNT & SWNT

800	632	50	250	VA-SWNT
800	632	50	420	VA-SWNT
800	632	50	600	VA-SWNT
800	632	225	250	VA-SWNT
800	632	225	420	VA-SWNT
800	632	225	600	VA-SWNT
800	632	400	250	VA-SWNT
800	632	400	420	VA-SWNT
800	632	400	600	none
800	764	50	250	VA-SWNT
800	764	50	420	VA-SWNT
800	764	50	600	VA-SWNT
800	764	225	250	VA-SWNT
800	764	225	420	VA-SWNT
800	764	225	600	VA-SWNT
800	764	400	250	VA-SWNT

800	764	400	420	VA-SWNT
800	764	400	600	VA-SWNT
900	500	50	250	none
900	500	50	420	VA-SWNT
900	500	50	600	VA-SWNT
900	500	225	250	Small amount of MWNT
900	500	225	420	S.A of MWNT & SWNT
900	500	225	600	VA-SWNT
900	500	400	250	none
900	500	400	420	S.A of MWNT & SWNT
900	500	400	600	VA-SWNT
900	632	50	250	VA-SWNT
900	632	50	420	VA-SWNT
900	632	50	600	VA-SWNT
900	632	225	250	VA-SWNT
900	632	225	420	VA-SWNT

900	632	225	600	VA-SWNT
900	632	400	250	VA-SWNT
900	632	400	420	VA-SWNT
900	632	400	600	VA-SWNT
900	764	50	250	VA-SWNT
900	764	50	420	VA-SWNT
900	764	50	600	VA-SWNT
900	764	225	250	VA-SWNT
900	764	225	420	VA-SWNT
900	764	225	600	VA-SWNT
900	764	400	250	VA-SWNT
900	764	400	420	VA-SWNT
900	764	400	600	VA-SWNT

C Source File

//Analysis Type - Classification


```

#include <stdio.h>
#include <conio.h>
#include <math.h>
#include <stdlib.h>
double input_hidden_weights[12][4]=
{
    {-1.10626389895333e+000, -3.73643496006291e-003, 5.96566965299829e+000,
    2.12499984937343e+000 },
    {6.57731612579698e-001, -2.92481134061285e+000, -7.85101897381701e-001,
    1.64231401512658e+000 },
    {-1.16058873730090e+001, -8.92886691018749e+000, 5.43316705908870e+000, -
    4.83392243846306e+000 },
    {-5.21276960171781e+000, -6.62498586125943e-001, -2.53690312098249e+000,
    5.80096137446396e-001 },
    {1.95455434574576e-001, 2.27916688256394e+000, 1.95448650355832e+000,
    1.07630239317822e+000 },
    {3.16576736733244e+000, -4.14960880259401e+000, -4.92500806780292e+000, -
    3.48665624799860e+000 },
    {8.74702498089894e+000, -4.58648936262645e+000, -2.26116853452984e+000, -
    1.11784635782786e+000 },
    {1.04861692985922e+000, -4.30718908920277e+000, -1.45599407693833e+000, -
    3.83921115266548e+000 },
    {1.20344648378913e+000, 4.91528926944447e+000, -1.35668049826802e+000, -
    1.45964626930918e+000 },
    {-1.40925587887915e+000, -3.73382786683886e+000, -2.07472417539196e+001, -
    3.05847487083543e+000 },

```

```

{2.89719585458340e-001, -2.86859795404039e+000, -7.99821806345248e-001,
3.14126157045974e-001 },

{2.57779598097478e+000, -3.70422470781917e+000, -4.13173188587870e+000, -
7.20501918350059e-001 }

};

double hidden_bias[12]={ -3.98566483194604e+000, -9.43831760189939e-001,
5.17789669494765e+000, 9.65571074908640e-001, -5.69755420045899e-001, -
3.74927386846146e-001, -3.41779205020830e+000, -7.12520353454542e-001, -
1.07829605709090e+000, 2.65972689551957e+000, 1.71014648061759e-001, -
9.25008699698261e-002 };

double hidden_output_wts[4][12]=
{
{3.79361473524166e-001, -4.42293097221627e+000, -6.95536471294875e-004, -
6.26475374686074e-001, -1.12462198943676e+000, 3.09203595031522e-001,
3.77856184512851e-002, 1.27552964135618e+000, -1.75567973130942e+000,
1.73495548739488e-001, -1.99319110089557e+000, -6.59944854194473e-001 },
{-4.94462713236383e-001, -4.10065790869239e+000, 1.18290472182240e-004, -
1.47770701847982e-001, 2.89119115325853e-001, -2.02500595416126e-001,
2.22915702640809e-002, 3.85382053492280e+000, -4.13326836232414e+000,
1.14046369358423e-001, 3.73791241241672e-001, 4.94510325402918e-002 },
{1.62526284591701e-001, 4.69852312118827e-002, -5.33852531663558e+000, -
6.68527743098429e-002, -9.28439519529504e-003, 3.37202788325939e+000, -
2.29854749015291e+000, 2.73951374354158e+000, -2.90720424550613e-003, -
1.76806579230098e+000, 1.54873415426241e-001, 8.31978976118578e-001 },
{5.00692372344648e-002, 6.92434479070777e-001, -2.31526502993601e-002,
4.16740293309858e+000, 7.02582997480717e-001, 2.03961158903557e+000, -
9.80452572039321e-001, -1.43400429584647e-001, -2.10235980310695e+000, -
2.17975138935412e+000, -6.14022135063163e+000, 2.80423145063388e+000 }
};

```

```

double output_bias[4]={ 4.80480210266358e+000, 6.83717178164568e-001,
9.78925664392187e-002, 1.50652260101541e+000 };

double max_input[4]={ 10000000000e+003, 7.64000000000000e+002,
50000000000e+002, 60000000000e+001 };

double min_input[4]={ 70000000000e+002, 50000000000e+002,
2.50000000000000e+001, 2.50000000000000e+001 };

double input[4];
double hidden[12];
double output[4];
void ScaleInputs(double* input, double minimum, double maximum, int size)
{
    double delta;
    long i;
    for(i=0; i<size; i++)
    {
        delta = (maximum-minimum)/(max_input[i]-min_input[i]);
        input[i] = minimum - delta*min_input[i]+ delta*input[i];
    }
}

void ComputeFeedForwardSignals(double* MAT_INOUT,double*
V_IN,double* V_OUT, double* V_BIAS,int size1,int size2,int layer)
{
    int row,col;

```

```

for(row=0;row < size2; row++)
{
    V_OUT[row]=0.0;
for(col=0;col<size1;col++)V_OUT[row]+=(*(MAT_INOUT+(row*size1)+col)*V_I
N[col]);
    V_OUT[row]+=V_BIAS[row];
    if(layer==0) V_OUT[row] = exp(V_OUT[row]);
    if(layer==1) V_OUT[row] = exp(V_OUT[row]);
}
}
void RunNeuralNet_Classification ()
{
    ComputeFeedForwardSignals((double*)input_hidden_weights,input,hidden,hi
dden_bias,4, 12,0);
    ComputeFeedForwardSignals((double*)hidden_output_wts,hidden,output,out
put_bias,12, 4,1);
}
int main()
{
    int index;
    int i=0;
    int keyin=1;
    double max;
    while(1)
    {

```

```

max=3.e-300;
printf("\nEnter values for Continuous inputs\n");
printf("Cont. Input-0(Temperature (°C)): ");
scanf("%lg",&input[0]);
printf("Cont. Input-1(Pressure (torr)): ");
scanf("%lg",&input[1]);
printf("Cont. Input-2(Flow Rate (sccm)): ");
scanf("%lg",&input[2]);
printf("Cont. Input-3(Time (min)): ");
scanf("%lg",&input[3]);
ScaleInputs(input,0,1,4);
RunNeuralNet_Classification();
for(i=0;i<4;i++)
{
if(max<output[i])
{
max=output[i];
index=i+1;
}
}
printf("\nPredicted category = ");

switch(index)
{

```

```

    case 1: printf("S.A of MWNT & SWNT\n"); break;
    case 2: printf("Small amount of MWNT\n"); break;
    case 3: printf("VA-SWNT\n"); break;
    case 4: printf("none\n"); break;
    default: break;
}
printf("\nConfidence level = %.14f",max);
    printf("\n\nPress any key to make another prediction or enter 0 to quit
the program.\n");
    keyin=getch();
    if(keyin==48)break;
}
    return 0;
}

```

XML Document

```

<?xml version="1.0" encoding="UTF-8"?>
<PMML version="3.0"><Header copyright="Copyright (c) StatSoft, Inc. All
Rights Reserved."><Application name="STATISTICA Automated Neural
Networks (SANN)" version="2.0"/></Header><DataDictionary
numberOfFields="5"><DataField name="Result" optype="categorical"><Value
value="S.A of MWNT & SWNT"/><Value value="Small amount of
MWNT"/><Value value="VA-SWNT"/><Value
value="none"/></DataField><DataField name="Temperature (°C)"
optype="continuous"/><DataField name="Pressure (torr)"
optype="continuous"/><DataField name="Flow Rate (sccm)"
optype="continuous"/><DataField name="Time (min)"

```

```

optype="continuous"/></DataDictionary><NeuralNetwork modelName="Book1
c_MLP 4-12-4" functionName="classification"><MiningSchema><MiningField
name="Result" usageType="predicted"/><MiningField name="Temperature
(°C)" lowValue="70000" highValue="100000"/><MiningField name="Pressure
(torr)" lowValue="50000" highValue="76400"/><MiningField name="Flow Rate
(sccm)" lowValue="2500" highValue="50000"/><MiningField name="Time (min)"
lowValue="2500" highValue="6000"/></MiningSchema><NeuralInputs
numberOfInputs="4"><NeuralInput id="0"><DerivedField><NormContinuous
field="Temperature (°C)"><LinearNorm orig="700000000000e+002"
norm="000"/><LinearNorm orig="100000000000e+003"
norm="100"/></NormContinuous></DerivedField></NeuralInput><NeuralInput
id="1"><DerivedField><NormContinuous field="Pressure (torr)"><LinearNorm
orig="50000000000e+002" norm="000"/><LinearNorm
orig="7.640000000000000e+002"
norm="100"/></NormContinuous></DerivedField></NeuralInput><NeuralInput
id="2"><DerivedField><NormContinuous field="Flow Rate
(sccm)"><LinearNorm orig="2.500000000000000e+001"
norm="000"/><LinearNorm orig="50000000000e+002"
norm="100"/></NormContinuous></DerivedField></NeuralInput><NeuralInput
id="3"><DerivedField><NormContinuous field="Time (min)"><LinearNorm
orig="2.500000000000000e+001" norm="000"/><LinearNorm
orig="60000000000e+001"
norm="100"/></NormContinuous></DerivedField></NeuralInput></NeuralInput
ts><NeuralLayer numberOfNeurons="12"
activationFunction="exponential"><Neuron id="4" bias="-
3.98566483194604e+000"><Con from="0" weight="-
1.10626389895333e+000"/><Con from="1" weight="-3.73643496006291e-
003"/><Con from="2" weight="5.96566965299829e+000"/><Con from="3"
weight="2.12499984937343e+000"/></Neuron><Neuron id="5" bias="-
9.43831760189939e-001"><Con from="0" weight="6.57731612579698e-001"/><Con
from="1" weight="-2.92481134061285e+000"/><Con from="2" weight="-
7.85101897381701e-001"/><Con from="3"
weight="1.64231401512658e+000"/></Neuron><Neuron id="6"

```

bias="5.17789669494765e+000"><Con from="0" weight="-
 1.16058873730090e+001"/><Con from="1" weight="-
 8.92886691018749e+000"/><Con from="2"
 weight="5.43316705908870e+000"/><Con from="3" weight="-
 4.83392243846306e+000"/></Neuron><Neuron id="7" bias="9.65571074908640e-
 001"><Con from="0" weight="-5.21276960171781e+000"/><Con from="1"
 weight="-6.62498586125943e-001"/><Con from="2" weight="-
 2.53690312098249e+000"/><Con from="3" weight="5.80096137446396e-
 001"/></Neuron><Neuron id="8" bias="-5.69755420045899e-001"><Con from="0"
 weight="1.95455434574576e-001"/><Con from="1"
 weight="2.27916688256394e+000"/><Con from="2"
 weight="1.95448650355832e+000"/><Con from="3"
 weight="1.07630239317822e+000"/></Neuron><Neuron id="9" bias="-
 3.74927386846146e-001"><Con from="0" weight="3.16576736733244e+000"/><Con
 from="1" weight="-4.14960880259401e+000"/><Con from="2" weight="-
 4.92500806780292e+000"/><Con from="3" weight="-
 3.48665624799860e+000"/></Neuron><Neuron id="10" bias="-
 3.41779205020830e+000"><Con from="0"
 weight="8.74702498089894e+000"/><Con from="1" weight="-
 4.58648936262645e+000"/><Con from="2" weight="-
 2.26116853452984e+000"/><Con from="3" weight="-
 1.11784635782786e+000"/></Neuron><Neuron id="11" bias="-7.12520353454542e-
 001"><Con from="0" weight="1.04861692985922e+000"/><Con from="1"
 weight="-4.30718908920277e+000"/><Con from="2" weight="-
 1.45599407693833e+000"/><Con from="3" weight="-
 3.83921115266548e+000"/></Neuron><Neuron id="12" bias="-
 1.07829605709090e+000"><Con from="0"
 weight="1.20344648378913e+000"/><Con from="1"
 weight="4.91528926944447e+000"/><Con from="2" weight="-
 1.35668049826802e+000"/><Con from="3" weight="-
 1.45964626930918e+000"/></Neuron><Neuron id="13"
 bias="2.65972689551957e+000"><Con from="0" weight="-
 1.40925587887915e+000"/><Con from="1" weight="-

3.73382786683886e+000"/><Con from="2" weight="-
 2.07472417539196e+001"/><Con from="3" weight="-
 3.05847487083543e+000"/></Neuron><Neuron id="14" bias="1.71014648061759e-
 001"><Con from="0" weight="2.89719585458340e-001"/><Con from="1" weight="-
 2.86859795404039e+000"/><Con from="2" weight="-7.99821806345248e-
 001"/><Con from="3" weight="3.14126157045974e-001"/></Neuron><Neuron
 id="15" bias="-9.25008699698261e-002"><Con from="0"
 weight="2.57779598097478e+000"/><Con from="1" weight="-
 3.70422470781917e+000"/><Con from="2" weight="-
 4.13173188587870e+000"/><Con from="3" weight="-7.20501918350059e-
 001"/></Neuron></NeuralLayer><NeuralLayer numberOfNeurons="4"
 activationFunction="exponential"><Neuron id="16"
 bias="4.80480210266358e+000"><Con from="4" weight="3.79361473524166e-
 001"/><Con from="5" weight="-4.42293097221627e+000"/><Con from="6"
 weight="-6.95536471294875e-004"/><Con from="7" weight="-6.26475374686074e-
 001"/><Con from="8" weight="-1.12462198943676e+000"/><Con from="9"
 weight="3.09203595031522e-001"/><Con from="10" weight="3.77856184512851e-
 002"/><Con from="11" weight="1.27552964135618e+000"/><Con from="12"
 weight="-1.75567973130942e+000"/><Con from="13"
 weight="1.73495548739488e-001"/><Con from="14" weight="-
 1.99319110089557e+000"/><Con from="15" weight="-6.59944854194473e-
 001"/></Neuron><Neuron id="17" bias="6.83717178164568e-001"><Con from="4"
 weight="-4.94462713236383e-001"/><Con from="5" weight="-
 4.10065790869239e+000"/><Con from="6" weight="1.18290472182240e-
 004"/><Con from="7" weight="-1.47770701847982e-001"/><Con from="8"
 weight="2.89119115325853e-001"/><Con from="9" weight="-2.02500595416126e-
 001"/><Con from="10" weight="2.22915702640809e-002"/><Con from="11"
 weight="3.85382053492280e+000"/><Con from="12" weight="-
 4.13326836232414e+000"/><Con from="13" weight="1.14046369358423e-
 001"/><Con from="14" weight="3.73791241241672e-001"/><Con from="15"
 weight="4.94510325402918e-002"/></Neuron><Neuron id="18"
 bias="9.78925664392187e-002"><Con from="4" weight="1.62526284591701e-
 001"/><Con from="5" weight="4.69852312118827e-002"/><Con from="6"

```

weight="-5.33852531663558e+000"/><Con from="7" weight="-6.68527743098429e-
002"/><Con from="8" weight="-9.28439519529504e-003"/><Con from="9"
weight="3.37202788325939e+000"/><Con from="10" weight="-
2.29854749015291e+000"/><Con from="11"
weight="2.73951374354158e+000"/><Con from="12" weight="-
2.90720424550613e-003"/><Con from="13" weight="-
1.76806579230098e+000"/><Con from="14" weight="1.54873415426241e-
001"/><Con from="15" weight="8.31978976118578e-001"/></Neuron><Neuron
id="19" bias="1.50652260101541e+000"><Con from="4"
weight="5.00692372344648e-002"/><Con from="5" weight="6.92434479070777e-
001"/><Con from="6" weight="-2.31526502993601e-002"/><Con from="7"
weight="4.16740293309858e+000"/><Con from="8" weight="7.02582997480717e-
001"/><Con from="9" weight="2.03961158903557e+000"/><Con from="10"
weight="-9.80452572039321e-001"/><Con from="11" weight="-
1.43400429584647e-001"/><Con from="12" weight="-
2.10235980310695e+000"/><Con from="13" weight="-
2.17975138935412e+000"/><Con from="14" weight="-
6.14022135063163e+000"/><Con from="15"
weight="2.80423145063388e+000"/></Neuron></NeuralLayer><NeuralOutputs
numberOfOutputs="4"><NeuralOutput outputNeuron="16"><DerivedField
optype="categorical"><NormDiscrete field="Result" value="S.A of MWNT
& amp; SWNT"/></DerivedField></NeuralOutput><NeuralOutput
outputNeuron="17"><DerivedField optype="categorical"><NormDiscrete
field="Result" value="Small amount of
MWNT"/></DerivedField></NeuralOutput><NeuralOutput
outputNeuron="18"><DerivedField optype="categorical"><NormDiscrete
field="Result" value="VA-
SWNT"/></DerivedField></NeuralOutput><NeuralOutput
outputNeuron="19"><DerivedField optype="categorical"><NormDiscrete
field="Result"
value="none"/></DerivedField></NeuralOutput></NeuralOutputs></NeuralNet
work></PMML>

```

Appendix C

Experimental Data

Temp.	P (torr)	Flow (sccm)	time (min)	length
870	700	150	30	900
880	700	75	30	150
880	700	75	30	150
880	700	75	30	500
890	700	100	60	0
890	754	75	30	0
890	755	200	60	0
890	763	80	60	0
890	764	80	60	0
890	700	75	30	100
890	700	400	30	100
890	700	400	30	100
890	700	75	40	100
890	700	75	60	100
890	752	75	60	100
890	754	75	25	100
890	758	75	30	100
890	759	80	30	100
890	759	80	60	100
890	700	50	30	150
890	700	50	30	150
890	700	75	30	150

890	700	75	30	150
890	700	75	30	150
890	700	75	30	150
890	700	100	30	150
890	700	120	30	150
890	700	150	30	155
890	700	75	40	200
890	700	75	60	200
890	752	75	60	200
890	753	75	60	200
890	754	75	60	200
890	758	200	30	200
890	755	75	30	250
890	755	75	30	250
890	700	75	40	300
890	700	75	60	300
890	700	75	60	300
890	700	50	30	500
890	700	75	30	500
890	700	75	30	500
890	700	75	30	500
890	700	75	40	500
890	700	75	60	500
890	700	75	60	500
890	700	75	60	500
890	700	100	60	500
890	752	75	30	500
890	754	75	30	500
890	756	400	30	500
890	700	75	30	550
890	700	50	30	600

890	756	75	60	700
890	700	75	40	800
890	700	75	30	900
890	700	75	30	900
890	700	80	30	900
890	700	80	30	900
890	700	75	60	900
890	700	75	60	900
890	700	80	60	900
890	700	80	60	900
890	700	80	60	900
890	700	80	60	900
890	700	80	60	900
890	700	80	60	900
890	700	80	60	900
890	700	80	60	900
890	700	80	60	900
890	700	80	60	900
890	700	80	60	900
890	700	80	60	900
890	700	80	60	900
890	700	80	60	900
890	755	75	60	900
890	758	80	60	900
890	760	80	60	900
890	761	80	60	900
890	762	80	60	900
890	700	100	30	950
890	700	125	30	1150
890	700	200	30	1150
900	700	75	30	150
900	700	150	30	1000

DOE data

Temperature	Pressure	Flow	Time
870	700	50	250
870	700	50	42.50000
870	700	50	600
870	700	225	250
870	700	225	42.50000
870	700	225	600
870	700	400	250
870	700	400	42.50000
870	700	400	600
870	732	50	250
870	732	50	42.50000
870	732	50	600
870	732	225	250
870	732	225	42.50000
870	732	225	600
870	732	400	250
870	732	400	42.50000
870	732	400	600
870	764	50	250
870	764	50	42.50000
870	764	50	600
870	764	225	250
870	764	225	42.50000
870	764	225	600
870	764	400	250
870	764	400	42.50000

870	764	400	600
885	700	50	250
885	700	50	42.50000
885	700	50	600
885	700	225	250
885	700	225	42.50000
885	700	225	600
885	700	400	250
885	700	400	42.50000
885	700	400	600
885	732	50	250
885	732	50	42.50000
885	732	50	600
885	732	225	250
885	732	225	42.50000
885	732	225	600
885	732	400	250
885	732	400	42.50000
885	732	400	600
885	764	50	250
885	764	50	42.50000
885	764	50	600
885	764	225	250
885	764	225	42.50000
885	764	225	600
885	764	400	250
885	764	400	42.50000
885	764	400	600
900	700	50	250
900	700	50	42.50000
900	700	50	600

900	700	225	250
900	700	225	42.50000
900	700	225	600
900	700	400	250
900	700	400	42.50000
900	700	400	600
900	732	50	250
900	732	50	42.50000
900	732	50	600
900	732	225	250
900	732	225	42.50000
900	732	225	600
900	732	400	250
900	732	400	42.50000
900	732	400	600
900	764	50	250
900	764	50	42.50000
900	764	50	600
900	764	225	250
900	764	225	42.50000
900	764	225	600
900	764	400	250
900	764	400	42.50000
900	764	400	600

C Source File

```
//Analysis Type - Regression
#include <stdio.h>
```



```

#include <conio.h>
#include <math.h>
#include <stdlib.h>
double input_hidden_weights[16][4]=
{
    {6.88538167880656e+001, 5.19705031137239e+001, 1.96349725020864e-001, -
3.96837035101177e+001 },
    {-9.41151995629373e+001, -1.13003504340434e+002, 3.81656846849003e+001,
5.23240862449531e+001 },
    {4.01810908021807e+001, -9.18610797701283e+001, -1.04453192467511e+001,
5.36469081765266e+001 },
    {-1.56383045945218e+001, -9.06987638452360e+001, -1.01933995373302e+000,
8.40483484092657e+001 },
    {5.22265263772885e+001, 8.89616582166964e+001, -3.93660084263335e+001, -
4.43438171715207e+001 },
    {1.42040275574771e+001, 1.84972652282273e+001, 3.96386196954803e+000, -
7.87681671339185e+000 },
    {3.36355319990229e+001, -1.25864192194514e+002, -4.65829507148270e+001,
6.53305874680016e+001 },
    {-7.52932016934223e+001, 5.83281611885973e+001, 3.30854101777050e+000, -
1.31102191213292e+001 },
    {1.02433398178607e+001, 1.33528450578865e+002, 9.86575161041711e-001, -
1.26542861376054e+002 },
    {-5.45262588816080e+001, -8.60668501080394e+000, -3.21967335331254e+001,
5.00334975291107e+001 },
    {-3.36133417636788e+000, -1.27130873750613e+002, -2.28795241300012e+001, -
5.93673720091773e+000 },

```

```

{-4.94871677241414e+000, 1.75006370691987e+001, 4.70229690719144e+000,
1.61215658839238e+001 },

{-7.82230091690304e+001, -1.54029768119110e+001, -1.27426390300539e+002,
1.61760741125225e+000 },

{3.45486568045511e+001, 6.27126567698776e+001, -9.12086705919135e+001,
4.75735499149714e+000 },

{3.55321485300413e+001, -6.05696311234928e+000, -1.46376742164126e+001, -
3.04507464104846e+001 },

{-3.21699982266888e+001, 1.19627496082985e+002, -7.65554470841906e+001, -
1.42725907753947e+002 }

};

double hidden_bias[16]={ 1.35327813428559e+001, 1.41134751024459e+001,
1.76482123707594e+001, -2.41673416249054e+001, -1.59566330977438e+000, -
1.00669497804693e+001, 3.08661961534460e+001, 6.60304331325891e+001,
8.84922792181880e+000, 1.11914973077307e+001, 7.33639561516985e+000, -
3.20387893627937e+001, 7.09087687782888e+001, 1.49338018849561e+001,
1.45155945812972e+001, 6.17382693600943e+001 };

double hidden_output_wts[1][16]=
{
{-1.83866503181541e+002, -9.08345298647669e+001, 7.35533974495154e+001,
4.73836303200020e+001, 4.87935957704203e+001, -5.98846120080697e+001,
8.34668938379424e+001, -9.83377480284121e+001, 1.23223156059255e+002, -
8.15416774789619e+001, -2.55000470702606e+002, -2.75734810522121e+002,
1.62680971165662e+002, -8.77271503993161e+001, -7.26224338366502e+001,
8.02533927116236e+001 }

};

double output_bias[1]={ -8.78297705012941e+001 };

```

```

double max_input[4]={ 90000000000e+002, 7.640000000000000e+002,
400000000000e+002, 600000000000e+001 };

double min_input[4]={ 8.700000000000000e+002, 700000000000e+002,
500000000000e+001, 2.500000000000000e+001 };

double max_target[1]={ 1.150000000000000e+003 };

double min_target[1]={ 000000000000e+000 };

double input[4];
double hidden[16];
double output[1];

void ScaleInputs(double* input, double minimum, double maximum, int size)
{
    double delta;
    long i;
    for(i=0; i<size; i++)
    {
        delta = (maximum-minimum)/(max_input[i]-min_input[i]);
        input[i] = minimum - delta*min_input[i]+ delta*input[i];
    }
}

void UnscaleTargets(double* output, double minimum, double maximum, int
size)
{
    double delta;
    long i;
    for(i=0; i<size; i++)

```

```

{
    delta = (maximum-minimum)/(max_target[i]-min_target[i]);
    output[i] = (output[i] - minimum + delta*min_target[i])/delta;
}
}
double logistic(double x)
{
    if(x > 100.0) x = 1.0;
    else if (x < -100.0) x = 0.0;
    else x = 1.0/(1.0+exp(-x));
    return x;
}
void ComputeFeedForwardSignals(double* MAT_INOUT,double*
V_IN,double* V_OUT, double* V_BIAS,int size1,int size2,int layer)
{
    int row,col;
    for(row=0;row < size2; row++)
    {
        V_OUT[row]=0.0;
        for(col=0;col<size1;col++)V_OUT[row]+=(*(MAT_INOUT+(row*size1)+col)*V_I
N[col]);
        V_OUT[row]+=V_BIAS[row];
        if(layer==0) V_OUT[row] = tanh(V_OUT[row]);
        if(layer==1) V_OUT[row] = logistic(V_OUT[row]);
    }
}

```

```

}
void RunNeuralNet_Regression ()
{
ComputeFeedForwardSignals((double*)input_hidden_weights,input,hidden,hi
dden_bias,4, 16,0);
ComputeFeedForwardSignals((double*)hidden_output_wts,hidden,output,out
put_bias,16, 1,1);
}
int main()
{
int i=0;
int keyin=1;
while(1)
{
printf("\nEnter values for Continuous inputs\n");
printf("Cont. Input-0(Temp.): ");
scanf("%lg",&input[0]);
printf("Cont. Input-1(P (torr)): ");
scanf("%lg",&input[1]);
printf("Cont. Input-2(gas flow rate): ");
scanf("%lg",&input[2]);
printf("Cont. Input-3(time (min)): ");
scanf("%lg",&input[3]);
ScaleInputs(input,0,1,4);
RunNeuralNet_Regression();
}
}

```

```

        UnscaleTargets(output,0,1,1);
        printf("\nPredicted Output of length = %.14e",output[0]);
        printf("\n\nPress any key to make another prediction or enter 0 to quit
the program.\n");
        keyin=getch();
        if(keyin==48)break;
    }
    return 0;
}

```

XML Document

```

<?xml version="1.0" encoding="UTF-8"?>
<PMML version="3.0"><Header copyright="Copyright (c) StatSoft, Inc. All
Rights Reserved."><Application name="STATISTICA Automated Neural
Networks (SANN)" version="2.0"/></Header><DataDictionary
numberOfFields="5"><DataField name="length"
optype="continuous"/><DataField name="Temp."
optype="continuous"/><DataField name="P (torr)"
optype="continuous"/><DataField name="gas flow rate"
optype="continuous"/><DataField name="time (min)"
optype="continuous"/></DataDictionary><NeuralNetwork modelName="CVD
VA-SWNTs in Workb_MLP 4-16-1"
functionName="regression"><MiningSchema><MiningField name="length"
usageType="predicted"/><MiningField name="Temp." lowValue="87000"
highValue="90000"/><MiningField name="P (torr)" lowValue="70000"
highValue="76400"/><MiningField name="gas flow rate" lowValue="5000"
highValue="40000"/><MiningField name="time (min)" lowValue="2500"
highValue="6000"/></MiningSchema><NeuralInputs
numberOfInputs="4"><NeuralInput id="0"><DerivedField><NormContinuous

```

```

field="Temp."><LinearNorm orig="8.700000000000000e+002"
norm="000"/><LinearNorm orig="90000000000e+002"
norm="100"/></NormContinuous></DerivedField></NeuralInput><NeuralInput
id="1"><DerivedField><NormContinuous field="P (torr)"><LinearNorm
orig="70000000000e+002" norm="000"/><LinearNorm
orig="7.640000000000000e+002"
norm="100"/></NormContinuous></DerivedField></NeuralInput><NeuralInput
id="2"><DerivedField><NormContinuous field="gas flow rate"><LinearNorm
orig="50000000000e+001" norm="000"/><LinearNorm orig="40000000000e+002"
norm="100"/></NormContinuous></DerivedField></NeuralInput><NeuralInput
id="3"><DerivedField><NormContinuous field="time (min)"><LinearNorm
orig="2.500000000000000e+001" norm="000"/><LinearNorm
orig="60000000000e+001"
norm="100"/></NormContinuous></DerivedField></NeuralInput></NeuralInput
s><NeuralLayer numberOfNeurons="16" activationFunction="tanh"><Neuron
id="4" bias="1.35327813428559e+001"><Con from="0"
weight="6.88538167880656e+001"/><Con from="1"
weight="5.19705031137239e+001"/><Con from="2" weight="1.96349725020864e-
001"/><Con from="3" weight="-3.96837035101177e+001"/></Neuron><Neuron
id="5" bias="1.41134751024459e+001"><Con from="0" weight="-
9.41151995629373e+001"/><Con from="1" weight="-
1.13003504340434e+002"/><Con from="2"
weight="3.81656846849003e+001"/><Con from="3"
weight="5.23240862449531e+001"/></Neuron><Neuron id="6"
bias="1.76482123707594e+001"><Con from="0"
weight="4.01810908021807e+001"/><Con from="1" weight="-
9.18610797701283e+001"/><Con from="2" weight="-
1.04453192467511e+001"/><Con from="3"
weight="5.36469081765266e+001"/></Neuron><Neuron id="7" bias="-
2.41673416249054e+001"><Con from="0" weight="-
1.56383045945218e+001"/><Con from="1" weight="-
9.06987638452360e+001"/><Con from="2" weight="-
1.01933995373302e+000"/><Con from="3"

```

weight="8.40483484092657e+001"/></Neuron><Neuron id="8" bias="-
1.59566330977438e+000"><Con from="0"
weight="5.22265263772885e+001"/><Con from="1"
weight="8.89616582166964e+001"/><Con from="2" weight="-
3.93660084263335e+001"/><Con from="3" weight="-
4.43438171715207e+001"/></Neuron><Neuron id="9" bias="-
1.00669497804693e+001"><Con from="0"
weight="1.42040275574771e+001"/><Con from="1"
weight="1.84972652282273e+001"/><Con from="2"
weight="3.96386196954803e+000"/><Con from="3" weight="-
7.87681671339185e+000"/></Neuron><Neuron id="10"
bias="3.08661961534460e+001"><Con from="0"
weight="3.36355319990229e+001"/><Con from="1" weight="-
1.25864192194514e+002"/><Con from="2" weight="-
4.65829507148270e+001"/><Con from="3"
weight="6.53305874680016e+001"/></Neuron><Neuron id="11"
bias="6.60304331325891e+001"><Con from="0" weight="-
7.52932016934223e+001"/><Con from="1"
weight="5.83281611885973e+001"/><Con from="2"
weight="3.30854101777050e+000"/><Con from="3" weight="-
1.31102191213292e+001"/></Neuron><Neuron id="12"
bias="8.84922792181880e+000"><Con from="0"
weight="1.02433398178607e+001"/><Con from="1"
weight="1.33528450578865e+002"/><Con from="2" weight="9.86575161041711e-
001"/><Con from="3" weight="-1.26542861376054e+002"/></Neuron><Neuron
id="13" bias="1.11914973077307e+001"><Con from="0" weight="-
5.45262588816080e+001"/><Con from="1" weight="-
8.60668501080394e+000"/><Con from="2" weight="-
3.21967335331254e+001"/><Con from="3"
weight="5.00334975291107e+001"/></Neuron><Neuron id="14"
bias="7.33639561516985e+000"><Con from="0" weight="-
3.36133417636788e+000"/><Con from="1" weight="-
1.27130873750613e+002"/><Con from="2" weight="-

2.28795241300012e+001"/><Con from="3" weight="-
 5.93673720091773e+000"/></Neuron><Neuron id="15" bias="-
 3.20387893627937e+001"><Con from="0" weight="-
 4.94871677241414e+000"/><Con from="1"
 weight="1.75006370691987e+001"/><Con from="2"
 weight="4.70229690719144e+000"/><Con from="3"
 weight="1.61215658839238e+001"/></Neuron><Neuron id="16"
 bias="7.09087687782888e+001"><Con from="0" weight="-
 7.82230091690304e+001"/><Con from="1" weight="-
 1.54029768119110e+001"/><Con from="2" weight="-
 1.27426390300539e+002"/><Con from="3"
 weight="1.61760741125225e+000"/></Neuron><Neuron id="17"
 bias="1.49338018849561e+001"><Con from="0"
 weight="3.45486568045511e+001"/><Con from="1"
 weight="6.27126567698776e+001"/><Con from="2" weight="-
 9.12086705919135e+001"/><Con from="3"
 weight="4.75735499149714e+000"/></Neuron><Neuron id="18"
 bias="1.45155945812972e+001"><Con from="0"
 weight="3.55321485300413e+001"/><Con from="1" weight="-
 6.05696311234928e+000"/><Con from="2" weight="-
 1.46376742164126e+001"/><Con from="3" weight="-
 3.04507464104846e+001"/></Neuron><Neuron id="19"
 bias="6.17382693600943e+001"><Con from="0" weight="-
 3.21699982266888e+001"/><Con from="1"
 weight="1.19627496082985e+002"/><Con from="2" weight="-
 7.65554470841906e+001"/><Con from="3" weight="-
 1.42725907753947e+002"/></Neuron></NeuralLayer><NeuralLayer
 numberOfNeurons="1" activationFunction="logistic"><Neuron id="20" bias="-
 8.78297705012941e+001"><Con from="4" weight="-
 1.83866503181541e+002"/><Con from="5" weight="-
 9.08345298647669e+001"/><Con from="6"
 weight="7.35533974495154e+001"/><Con from="7"
 weight="4.73836303200020e+001"/><Con from="8"

```
weight="4.87935957704203e+001"/><Con from="9" weight="-
5.98846120080697e+001"/><Con from="10"
weight="8.34668938379424e+001"/><Con from="11" weight="-
9.83377480284121e+001"/><Con from="12"
weight="1.23223156059255e+002"/><Con from="13" weight="-
8.15416774789619e+001"/><Con from="14" weight="-
2.55000470702606e+002"/><Con from="15" weight="-
2.75734810522121e+002"/><Con from="16"
weight="1.62680971165662e+002"/><Con from="17" weight="-
8.77271503993161e+001"/><Con from="18" weight="-
7.26224338366502e+001"/><Con from="19"
weight="8.02533927116236e+001"/></Neuron></NeuralLayer><NeuralOutputs
numberOfOutputs="1"><NeuralOutput outputNeuron="20"><DerivedField
optype="continuous"><NormContinuous field="length"><LinearNorm
orig="00000000000e+000" norm="00000000000e+000"/><LinearNorm
orig="1.15000000000000e+003"
norm="10000000000e+000"/></NormContinuous></DerivedField></NeuralOutp
ut></NeuralOutputs></NeuralNetwork></PMML>
```

Appendix D

Experimental Data

Temp	Flow	Time	Press	Length
880	150	60	700	0
880	150	5	700	325
880	150	60	700	325
880	150	60	700	325
880	150	60	700	325
880	150	60	700	325
880	150	60	700	325
880	150	60	700	325
880	150	30	700	325
880	150	30	700	325
880	150	30	700	325
880	150	30	700	325
880	150	30	700	325
880	150	30	700	325
880	150	60	700	325
880	50	5	700	325
880	20	5	700	325
880	150	60	700	500
880	150	60	700	500
880	150	60	700	500
880	150	60	700	500
880	150	60	700	500
880	150	60	700	500
880	150	60	700	500
880	150	60	700	500

880	150	60	700	500
880	150	60	700	500
880	150	5	700	500
880	150	30	700	500
880	150	30	700	500
880	150	30	700	500
880	150	30	700	500
880	150	30	700	500
880	150	30	700	500
880	150	30	700	500
880	150	30	700	500
880	150	30	700	500
880	150	30	700	500
880	150	60	700	650
880	150	90	700	650
880	150	20	700	675
880	150	60	700	1000

DOE data

Flow	Time	Length
20	50	325
20	32.50000	325
20	600	503.7915
85	50	628.0037
85	32.50000	357.7051
85	600	640.5887
150	50	675
150	32.50000	429.475
150	600	649.8988

XML Document

```
<?xml version="1.0" encoding="UTF-8"?>
<-PMML version="3.0"><-Header copyright="Copyright (c) StatSoft, Inc. All
Rights Reserved."><Application version="2.0" name="STATISTICA Automated
Neural Networks (SANN)"/></Header><DataDictionary
numberOfFields="3"><DataField name="Length"
optype="continuous"/><DataField name="Flow"
optype="continuous"/><DataField name="Time"
optype="continuous"/></DataDictionary><NeuralNetwork
functionName="regression" modelName="Monte Carlo Data -- Replication 12
(recent) in nonparamet_MLP 2-6-1"><MiningSchema><MiningField
name="Length" usageType="predicted"/><MiningField name="Flow"
highValue="15000" lowValue="2000"/><MiningField name="Time"
highValue="9000" lowValue="500"/></MiningSchema><NeuralInputs
numberOfInputs="2"><NeuralInput id="0"><DerivedField><NormContinuous
field="Flow"><LinearNorm norm="000"
orig="20000000000e+001"/><LinearNorm norm="100"
orig="1.5000000000000000e+002"/></NormContinuous></DerivedField></NeuralIn
put><NeuralInput id="1"><DerivedField><NormContinuous
field="Time"><LinearNorm norm="000"
orig="50000000000e+000"/><LinearNorm norm="100"
orig="90000000000e+001"/></NormContinuous></DerivedField></NeuralInput>
</NeuralInputs><NeuralLayer activationFunction="logistic"
numberOfNeurons="6"><Neuron id="2" bias="-2.34605521309488e+000"><Con
weight="-8.43053970865299e-001" from="0"/><Con weight="-
2.31405662902162e+000" from="1"/></Neuron><Neuron id="3" bias="-
4.02665223356582e-001"><Con weight="-8.31149712079690e-003"
from="0"/><Con weight="-3.13040212864502e-001" from="1"/></Neuron>-
<Neuron id="4" bias="-2.45349983538043e-002"><Con weight="-
```

```
1.46958441487193e-001" from="0"/><Con weight="2.21153869088144e+000"
from="1"/></Neuron><Neuron id="5" bias="-1.77086489918581e-001"><Con
weight="-4.27712184823327e-001" from="0"/><Con
weight="1.41015887585967e+000" from="1"/></Neuron><Neuron id="6"
bias="2.14377123761839e-001"><Con weight="-3.41038575786699e-001"
from="0"/><Con weight="4.11123928698177e+000" from="1"/></Neuron>-
<Neuron id="7" bias="-1.16892250788823e+000"><Con weight="-
3.29827505060424e+000" from="0"/><Con weight="1.50765983953288e+001"
from="1"/></Neuron></NeuralLayer><NeuralLayer
activationFunction="identity" numberOfNeurons="1"><Neuron id="8" bias="-
3.41668192093133e+000"><Con weight="2.63281674121808e+000"
from="2"/><Con weight="2.42953493133018e+000" from="3"/><Con
weight="2.21252553836957e+000" from="4"/><Con weight="1.81199062188609e-
001" from="5"/><Con weight="3.66986350798838e+000" from="6"/><Con
weight="-2.10447746169748e+000" from="7"/></Neuron></NeuralLayer>-
<NeuralOutputs numberOfOutputs="1"><NeuralOutput outputNeuron="8">-
<DerivedField optype="continuous"><NormContinuous
field="Length"><LinearNorm norm="00000000000e+000"
orig="00000000000e+000"/><LinearNorm norm="10000000000e+000"
orig="6.75000000000000e+002"/></NormContinuous></DerivedField></NeuralO
utput></NeuralOutputs></NeuralNetwork></PMML>
```

Appendix E

First Run		Second Run	
Time	Pressure	Time	Pressure
1	708	1	711
2	700	2	709
3	700	3	705
4	699	4	702
5	700	5	699
6	700	6	698
7	700	7	697
8	701	8	700
9	702	9	703
10	709	10	707
11	710	11	712
12	711	12	722
13	713	13	702
14	714	14	692
15	716	15	693
16	717	16	704
17	717	17	709
18	713	18	710
19	710	19	715

20	702	20	720
21	697	21	714
22	695	22	692
23	697	23	683
24	697	24	682
25	700	25	685
26	702	26	699
27	704	27	708
28	708	28	717
29	709	29	713
30	705	30	701
<u>AVERAGE</u>	<u>705.2</u>	<u>AVERAGE</u>	<u>703.467</u>